# POLITECNICO DI MILANO

SCUOLA DI INGEGNERIA INDUSTRIALE E DELL'INFORMAZIONE
CORSO DI LAUREA MAGISTRALE IN INGEGNERIA BIOMEDICA

**EFFECTS OF BRONCHOPULMONARY DYSPLASIA ON RESPIRATORY CONTROL, MECHANICS AND ENERGETICS IN PRETERM NEWBORNS**

Relatore: Prof. Raffaele Dellacà
Correlatore: Ing. Chiara Veneroni

Tesi di Laurea Magistrale di:
Giulia Pagani *matr.* 854894

**Anno Accademico 2017-2018**

# Index of contents

# Index of figures

# Index of tables

# Summary

Preterm birth, defined as childbirth occurring before the 37th week of gestation, is an important health problem across the globe. As estimated by Beck at Al. in 2005 the 9.5% of births were preterm. [1] Nowadays, approximately 15 million infants are delivered preterm each year and the respiratory complications due to interrupted lung development in the womb are the leading cause for neonatal mortality and morbidity, responsible for 1 million deaths in 2015. [2]

More than three quarters of premature infants can be saved with feasible, cost-effective care; however, the criticality of a preterm birth is also associated to long-term adverse consequences for health, resulting in neurophysiological sequels and financial implication for health-care systems.

Preterm infants are frequently affected by respiratory disease caused by the structural immaturity of their respiratory system, the lack of surfactant and the thickness of the alveolar-capillary membrane that prevent the gas exchange from occurring correctly. All these anomalies result in a minimal pulmonary functionality that can lead to the development of a chronic lung disease called Bronchopulmonary Dysplasia (BPD).

BDP affects approximately 25% of very preterm infants presenting at least one of the main risk factors that include a gestational age lower than 32 weeks, low birth weight, mechanical ventilation and early administration of oxygen. BPD is associated with arrested alveolarization resulting in impaired pulmonary gas exchange.

The current NICHD definition of BPD is based on the oxygen requirement of the infant and the respiratory support at the 28th day after birth. However, this can depend on specific oxygenation targets and protocol of the clinical centres and can lead to incorrect conclusions on the severity of the respiratory disfunction and, consequently, to the initiation of harmful treatments. BPD is also a multifactorial disease that has different origins and different characteristic signs, according to which it can develop in various pathological conditions that require distinct therapies.

Identifying a method for evaluating in a more objective and accurate manner the respiratory impairment in early life is fundamental to choose more specific and appropriate treatments, independently from the daily patient situation and differences in the SpO2 target range in neonatal

units. Because of different severity and phenotypes of this pathology, the assessment of several physiological factors is required.

A more detailed evaluation of the patient clinical conditions and the complete awareness of the disease could benefit from the instant access to physiologic measures, such as the lung volumes and the mechanical properties of the respiratory system, leading to the identification of personalized treatments and to a more effective intervention given the extreme heterogeneity of prematurity cases and the lack of standard strategy for their therapy.

Specifically, this work is focused on the development of accurate methods to characterize the functional alterations in breathing control and respiratory mechanics in infants with bronchopulmonary dysplasia and determine their relationship with the development and severity of the disease by means of a measurement system exploitable at bedside in NICU clinical practice.

The prospect of this approach is the achievement of a detailed phenotyping of the disease that could ease the introduction of personalized treatments, tailored to specific clinical cases.

The mechanisms of control of breathing has been studied applying a Detrended Fluctuation Analysis (DFA) to the series of inter-breath-intervals (IBI), tidal volumes ($V_T$) and end-expiratory lung volumes (EELV). The breathing patter has been described using the paradoxic motion indexes and the percentage contributions of rib cage and abdomen to $V_T$. The static and dynamic compliances of lung and chest wall have been computed to describe the mechanical properties of the respiratory system. Finally, the work of breathing has been determined as a measure of the respiratory effort.

In order to measure these parameters and reach the goal of the study, it is necessary to acquire the values of flow, volume and pressures implementing a system that can be easily used by the clinician and that provides accurate measurements in real-time. A specific set-up for the acquisition and elaboration of the respiratory signals has been developed and tested in-vitro.

The in-vitro tests underlined that both the tidal volume measured by means of respiratory inductive plethysmography (RIP) after calibration and the esophageal pressure obtained through a catheter inserted into the esophagus were accurate enough to allow a proper assessment of respiratory variability and mechanics.

The developed and tested set up has been then used in-vivo within a clinical study performed in the NICU of the King Edward Memorial Hospital in Perth (WA), where 14 preterm infants have been studied. A specific protocol has been defined to measure the parameters of interest and compare the values obtained in healthy infants with the one collected from the BPD patients.

Tidal volume, paradoxic motion and thoraco-abdominal asynchrony indexes and other breathing pattern parameters have been computed breath-by-breath and averaged for each infant.

The correlation properties of the main breathing pattern parameters have been quantified computing the scaling exponent $\alpha$. Lung and chest wall compliance and work of breathing have been

computed constructing the P-V curves and loop and considering changes in the pressure exerted on the considered structure.

This in-vivo study allowed the comparison of infant without BPD and infants with different BPD severity.

The tidal volumes measured for each infant show a statistically significant difference between healthy patients and patients with BPD, having mean values equal to 6.75 ± 1.02 mL and 4.61 ± 1.04 mL, respectively.

The main breathing pattern parameters significantly differ between the two groups of patients: both the inspiratory and expiratory times decrease in presence of BPD, while, the respiratory rate increases with the severity of the disease. In infants without and with BPD, $T_i$ is equal to 0.45 ± 0.012 s and 0.40 ± 0.010 s, $T_e$ is equal to 0.61 ± 0.058 s and 0.48 ± 0.060 s and RR is 63.07 ± 3.46 and 73.17 ± 3.49 breaths/min, respectively. The thoraco-abdominal asynchrony and paradoxic motion indexes (IAI, EAI and LBI), however, present similar values for both the groups and the mean values do not show a statistically meaningful difference to distinguish between them. The analysis of the breathing pattern variability shows that EELV and $V_t$ time series in presence of BPD are characterized by a stronger long-range correlation, while, IBI exhibits a lower value of $\alpha$ in infants with chronic lung disease. The values of $\alpha$ show a regular tendency in presence of BPD, even if the difference between the two categories is not statistically significant.

The effects of the BPD on the respiratory mechanics have been investigated calculating both the static and dynamic compliance. The measurement of a total system compliance by an occlusion technique was simple to perform and gave reproducible and reliable results.

The static compliance of the total respiratory system, indeed, differs in a statistically significant way between the healthy and sick infants presenting mean values of 1.36 ± 0.50 mL/cmH2O*kg and 0.47 ± 0.36 mL/cmH2O*kg. In contrast, there is a meaningless difference in the values of $\mathrm{C_{CW_{stat}}}$ and $\mathrm{C_{L_{stat}}}$ obtained as averages in each group. Despite the absence of a statistically significant difference in these mechanical properties between the groups, the values of both the chest wall and lung compliance show a trend with the level of severity of BPD.

On the other hand, the dynamic compliance of the lung in infants with BPD (0.37 ± 0.13 mL/cmH2O*kg) is consistently different (p=0.039) from that obtained in patients without BPD (0.63 ± 0.20 mL/cmH2O*kg).

Finally, statistically different WOB indices have been found considering both its elastic and resistive components: the elastic WOB is equal to 4.24 ± 1.15 without BPD and 7.25 ± 2.22 with BPD, while, the total resistive WOB is 8.37 ± 2.06 in the first case and 13.80 ± 4.22 in the second one. These differences between the two classes of patients are present also considering the partition between

inspiratory and expiratory resistive work. These outcomes could be very useful for the clinician to evaluate the breathing efforts of critically ill patients and to optimize the type of respiratory support for a particular disease condition.

Thus, it is possible to conclude that the developed system represents a useful tool for monitoring the effects of BPD on respiratory control mechanics and energetics in preterm newborns with different level of severity of the disease and may be used in the clinical practice to customize the treatment.

# Sommario

La nascita pretermine, definite come il parto che avviene prima della 37esima settimana di gestazione, è un importante problema per la sanità di tutto il mondo. Come stimato da Beck et al., nel 2005 il 9.5% delle nascite è avvenuto prematuramente. Attualmente, circa 15 milioni di neonati vengono partoriti pretermine ogni anno e le complicazioni respiratorie dovute all'interruzione dello sviluppo polmonare nell'utero materno sono la principale cause di mortalità e mobilità neonatale, responsabili di un milione di decessi nel 2015. Più di tre quarti dei neonati prematuri possono essere salvati con cure facilmente accessibili, tuttavia, la criticità di una nascita prematura è anche associata a conseguenze avverse a lungo termine per la salute, risultanti da cause neurofisiologiche e complicazioni finanziarie per il sistema sanitario. I neonati prematuri sono spesso affetti da complicazioni respiratorie causate dalla immaturità strutturale del loro apparato respiratorio, la mancanza di surfattante e lo spessore notevolmente ridotto della membrana alveolo-capillare, che impedisce allo scambio di gas di avvenire in maniera corretta. Tutte queste anomalie sfociano in una scarsa funzionalità polmonare che può portare allo sviluppo di malattie di malattie polmonari croniche, tra cui la displasia broncopolmonare. La BPD colpisce approssimatamene il 25 % dei neonati molto prematuri che presentano almeno uno dei principali fattori di rischio che includono: un tempo di gestazione inferiore alle 32 settimane, un basso peso alla nascita, la necessità di ventilazione meccanica e la precoce somministrazione di ossigeno.

La BPD è associata con l'arresto del processo di formazione degli alveoli che porta ad alterato ed inefficiente scambio di gas polmonari.

La recente definizione di BPD proposta dall'istituto di ricerca NICHD si basa sul fabbisogno di ossigeno del bambino e sul supporto respiratorio che egli necessita al 28esimo giorno dopo la nascita. Tuttavia, tali drivers possono dipendere da specifici target di ossigeno e dal protocollo clinico utilizzato nei diversi centri e possono condurre a diagnosi errate sulla gravità della disfunzione respiratoria e, di conseguenza, all'avvio di trattamenti che possono rivelarsi dannosi per il paziente.

Inoltre, la BPD è una malattia multifattoriale che può avere diverse origini e differenti segni caratteristici, a seconda dei quali può svilupparsi in diverse condizioni patologiche che richiedono differenti terapie.

Identificare un metodo per valutare in modo più obiettivo e accurato la patologia respiratoria sin dai primi giorni di vita è fondamentale per scegliere trattamenti più specifici e appropriati, indipendentemente da una limitata situazione quotidiana del paziente e dalle differenze nei differenti target di SpO2 applicati nelle unità di terapia intensiva neonatale. A causa dei vari livelli di severità e fenotipi di questa patologia è richiesta la valutazione di numerosi fattori fisiologici. Una più dettagliata valutazione delle condizioni cliniche del paziente e una completa consapevolezza della patologia possono trarre vantaggio da un accesso istantaneo alle misure fisiologiche di interesse, come i volumi polmonari e le proprietà meccaniche del sistema respiratorio, portando all'identificazione di trattamenti personalizzati e ad un intervento più efficace data la estrema eterogeneità dei casi di prematurità e la mancanza di strategie standard per il loro trattamento.

Nello specifico, questo lavoro si concentra sullo sviluppo di metodi accurati per caratterizzare le alterazioni funzionali del controllo e della meccanica respiratori in neonati con BPD. La prospettiva di questo approccio è il raggiungimento di una fenotipizzazione dettagliata della malattia, che potrebbe facilitare l'introduzione di trattamenti personalizzati adatti a casi clinici specifici. I meccanismi di controllo respiratorio sono stati studiati applicando il metodo della Detrended Fluctuation Analysis (DFA) alla serie temporale di intervalli inter-respiro (IBI), volume tidale e volume di fine espirazione (EELV). Il pattern respiratorio è stato descritto utilizzando gli indici per identificare i respiri paradosso e i contributi percentuali della gabbia toracica e dell'addome al volume tidale. Le compliance statiche e dinamiche del polmone e della gabbia toracica sono state calcolate per descriver le proprietà meccaniche del sistema respiratorio. Infine, il lavoro respiratorio è stato determinato come misura dello sforzo.

Al fine di misurare questi parametri e raggiungere l'obiettivo di questo studio, è stato necessario acquisire i valori di flusso, volume e pressioni implementando un sistema che possa essere facilmente utilizzato dal medico e che ottenga misure accurate in tempo reale. È stato quindi sviluppato e testato in-vitro un set-up per l'acquisizione ed elaborazione dei segnali respiratori.

I test in-vitro hanno sottolineato che sia il volume misurato mediante pletismografia respiratoria induttiva (RIP) e in seguito calibrato che la pressione esofagea ottenuta mediante l'utilizzo di un catetere inserito nell'esofago risultano sufficientemente accurati da consentire una corretta valutazione della variabilità e della meccanica respiratoria.

Il set-up sviluppato è stato utilizzato in-vivo in uno studio clinico condotto presso l'Unità di Terapia Intensiva Neonatale del King Edward Memorial Hospital di Perth (WA), dove sono stati studiati 14 neonati pretermine. Un protocollo specifico è stato definito per misurare i parametri di interesse e confrontare i valori ottenuti in neonati sani con quelli di pazienti affetti da BPD. Il volume tidale, gli indici di asincronia toraco-addominale e altri parametri dell'andamento respiratorio sono calcolati per ciascun respiro e mediati in ogni neonato.

Le proprietà di correlazione dei principali parametri respiratori sono state quantificate calcolando il fattore di scala $\alpha$. Le compliance del polmone e della gabbia toracica e il lavoro respiratorio sono stati calcolati costruendo le curve e il ciclo pressione-volume e considerando i cambiamenti di pressione esercitata sulla struttura considerata.

I test in-vivo hanno permesso di confrontare neonati sani e neonati con BPD a diversi stadi. I valori di volume tidale misurati per ogni neonato mostrano una differenza statisticamente significativa tra pazienti sani e non, riportando rispettivamente valori medi di 6.75 ± 1.02 mL and 4.61 ± 1.04 mL.

Anche i principali parametri dell'andamento respiratorio differiscono significativamente: i tempi inspiratori ed espiratori sono più brevi in presenza di BPD, mentre la frequenza respiratoria aumenta con l'aumentare dello stadio della patologia.

Nei pazienti sani e in quelli affetti da BPD, $T_i$ assume rispettivamente un valore pari a 0.45 ± 0.012s e 0.40 ± 0.010s, $T_e$ equivale a 0.61 ± 0.058s contro ai 0.48 ± 0.060s e la frequenza respiratoria rispettivamente 63.07 ± 3.46 73.17 ± 3.49 respiri/min.

Per quanto riguarda gli indici di asincronia toraco-addominale e di movimento paradosso, essi presentano valori simili in entrambi i gruppi, con valori medi che non mostrano una differenza statisticamente significativa per distinguere i due gruppi di pazienti.

L'analisi di variabilità del segnale respiratorio mostra come le serie dei valori di volume tidale e volume di fine espirazione (EELV) possiedano una forte correlazione temporale a lunga durata, gli intervalli inter-respiro (IBI), invece, mostrano un valore basso di $\alpha$ nei neonati con patologie croniche. I valori di $\alpha$ mostrano una tendenza regolare in presenza di BPD, anche se la differenza tra le due categorie non è statisticamente significativa.

Gli effetti della BPD sulla meccanica respiratoria sono stati investigati calcolando sia le compliance statiche che quelle dinamiche. La misura della compliance del sistema respiratorio totale tramite una tecnica di occlusione ha permesso di ottenere risultati riproducibili e affidabili.

La compliance statica del sistema respiratorio totale, infatti, differisce in maniera statisticamente significativa tra i pazienti sani e quelli patologici con valori rispettivamente di 1.36 ± 0.50 mL/cmH2O*kg e 0.47 ± 0.36 mL/cmH2O*kg. D'altro canto, non esiste differenza statisticamente significativa per quanto riguarda I parametri di $\mathrm{C_{CW_{stat}}}$ e $\mathrm{C_{L_{stat}}}$, mediati per ogni gruppo.

Nonostante ciò, questi ultimi valori mostrano una tendenza inversamente proporzionale al crescere dello stadio di BPD.

La compliance dinamica del polmone, invece, risultata essere un parametro consistente ($p=0.039$) per classificare la popolazione studiata con una media di $0.63 \pm 0.20$ mL/cmH2O*kg in pazienti sani e $0.37 \pm 0.13$ mL/cmH2O*kg per pazienti affetti da BPD.

Sono stati ottenuti valori di lavoro respiratorio statisticamente significativi, considerando sia le componenti elastiche che quelle resistive: il lavoro elastico è uguale a $4.24 \pm 1.15$ in assenza di BPD e $7.25 \pm 2.22$ in caso di BPD, mentre il lavoro resistivo è uguale a $8.37 \pm 2.06$ nel primo caso e $13.80 \pm 4.22$ nel secondo.

Queste differenze tra le due classi di pazienti sono presenti anche considerando la partizione tra lavoro resistivo inspiratorio ed espiratorio. Questi risultati potranno essere di grande utilità nella pratica clinica per la valutazione degli sforzi respiratori in pazienti critici e per l'ottimizzazione delle modalità di supporto respiratorio a seconda della particolare condizione patologica.

Pertanto, si può concludere che il sistema sviluppato rappresenti uno strumento utile per monitorare gli effetti della BPD sui meccanismi di controllo, l'energetica e la meccanica respiratoria in pazienti nati pretermine affetti da differenti stadi della patologia e possa, inoltre, essere utilizzato nella pratica clinica per personalizzare il trattamento.

# Introduction

The respiratory system is the set of organs and tissues capable of assimilating the inspired air oxygen and, at the same time, expelling the carbon-dioxide produced by the cellular activity and representing a waste product. The whole exchange process between the external environment and the body is called ventilation that includes the pulmonary gas transfer from alveoli to lung capillaries, the gas transport through the circulation system and the tissues and the peripheral gas exchange between tissue capillaries and organs cells.

The respiration process in adult is very different compared to the infants' one, as the development of the lungs takes time to be completely achieved, reaching its ripening in the late childhood.

Many preterm infants may have difficulty breathing on their own when they are born, they run out of strengths and may stop breathing having apnoea. This is a risk that can lead to the development of disabilities that will affect them for their entire lives, to an extent that depends on the quality of care they receive during and around birth and the days that follow. Indeed, birth represents a critical event associated with dramatic changes in the lung that have to be carefully monitored: the lungs have to be filled with air after the absorption of the fetal fluid which maintained the lungs in a distended state, the gas-exchanging surface area has to adequately widen to allow the pulmonary blood flow to greatly increase and carry oxygen to the peripheral tissues and the surfactant system has to prevent the collapse of the lungs by decreasing the alveolar surface tension. In the case that birth occurs prematurely, the development of the lungs doesn't fully accomplish inside the utero and their structure results to be incomplete and immature for air life, mostly because of the insufficiency of surfactant production and the thickness of alveolar-capillary membrane that prevents the gas exchange from occurring correctly causing the maldistribution of oxygen supply to the peripheral units. [3]

Due to the combination of all these factors preterm infants are at a very high risk of contracting respiratory system pathologies and, therefore, almost the fifteen percent of them require care in specialized Intensive Care Units for Neonates (NICUs). The choice of a correct ventilatory therapy for a preterm new-born is a crucial task from the first moment of life since its lungs are highly vulnerable to injury and an inappropriate intervention can worsen patient conditions.

Several studies have suggested that a less invasive treatment that avoid excessive oxygen and strain may decrease the incidence and severity of chronic pathologies, guaranteeing a ventilation that is not only supportive but also protective of pulmonary function and structure. However, the wide heterogeneity of clinical cases in the NICUs makes it difficult to settle a standard strategy for the therapy of preterm new-borns. So far, there is little knowledge about optimal target levels and threshold for harmful stress that can be applied to the lung tissue to implement protective ventilation strategies. Therefore, nowadays, increasing importance is given to the need of personalized treatments that can be achieved with the tailoring of ventilation parameters to the patient demand, based on the bedside assessment of infant lung mechanics and respiratory function measurements. Moreover, continuously adapting the treatment and optimizing it according to the condition of the infant could overcome the dramatic changes that occur in the first weeks of life because of the growth of the lungs and the development of the pathology. Even if the assessment of lung function in infants is still a challenge in clinical practice, new techniques and approaches have been developed to ensure the availability at bedside of parameters that reflect lung mechanics and to identify the ones that could lead the choice of the correct ventilatory treatment.

The focus of this work is on Bronchopulmonary Dysplasia and on the importance to achieve a wider knowledge of this disease to treat it more efficiently. The Bronchopulmonary Dysplasia is the most frequent lung morbidity diagnosed among survivors of preterm infants, it is a multifactorial disease caused by an impaired alveolar-capillary maturation both during the fetal and neonatal life. One of the main problem in describing BPD is the inadequacy of the current definitions, for their inability of capturing the severity and the different clinical phenotypes of the disease itself. Actual definitions take into account the patients oxygen requirements and the respiratory support at specific time point only, without defining the disease by its pathophysiology. In a recent study Poindexter and colleagues [4] compared the three commonly used definitions of BPD in a multicentre study on extremely preterm infants and concluded that a contemporary and more accurate definition of BPD is needed.

In fact, BPD diagnosis can depend on specific oxygenation targets and protocols of specific clinical centres leading to incorrect conclusions on the severity of the respiratory disfunction and, consequently, to the initiation of harmful treatments. As BPD is a multifactorial disease that has different origins and different characteristic signs, it can develop in various pathological conditions that requires distinct therapies. Identifying a method for evaluating more objectively and accurately the respiratory impairment in early life is fundamental to choose more specific and appropriate treatments, independently from the daily patient situation and the differences in the SpO2 target range in neonatal units. Because of different severity and phenotypes of this pathology, the assessment of several physiological factors is required.

This study is part of the research carried out at the King Edward Memorial Hospital that aims to develop a bed-side approach able to provide useful information for the evaluation of patients with Bronchopulmonary dysplasia. In particular, lung and chest wall mechanics, work of breathing and indirect measurements of control of breathing have been studied in this work.

The knowledge of the mechanical properties of the respiratory system could be helpful to have a deeper insight of a multifactorial pathology like bronchopulmonary dysplasia. The assessment of respiratory mechanics, together with other parameters such as the oxygen requirements and breathing pattern indexes, can offer an objective evaluation of the disease starting from the initial phase of the pathology and considering its various aspects. This kind of comprehensive approach could allow to determine different phenotype of the pathology itself that could drive an individual therapeutic approach.

Considering the critical condition of premature pathological infants and their incapacity to actively respond to respiratory manoeuvre, it is important to provide the clinicians with direct information regarding the respiratory dysfunctions by means of a simple technique that does not require the patient collaboration.

Therefore, the work of this thesis aims to develop accurate methods to evaluate and characterize the functional alterations in breathing control and respiratory mechanics in infants with bronchopulmonary dysplasia that can be easily applied in the clinical NICU environment to tailor the treatments.

# Chapter 1 Respiratory System in Preterm Infants

# 1.1 The Respiratory System

## 1.1.1 Anatomy, Physiology and Functions of the Respiratory System

Animal cells' life depends on the supply of oxygen to get energy from the substances taken with food. The main function of the respiratory system is to preserve the physiological conditions that ensure the gases exchange between the lung and the blood in the pulmonary circulation, which means, settle the pressure gradient that drive the diffusive transfer of respiratory gases. Then, respiration is the act of taking oxygen from the external environment, during inhalation, and removing carbon dioxide, which is a waste product of cellular function, during expiration. The first step is the pulmonary ventilation that is achieved by filling and emptying rhythmically the lungs, whose movements reflect the ones of the chest wall due to the respiratory muscles action. This process is followed by the external respiration during which the gas passes from the alveoli to the pulmonary capillaries to be transported through the systemic circulation to the tissues. The last step is the gas exchange between tissues capillaries to the cells, that is called internal respiration.

The perfusion of oxygen in the organism is essential to perform its vital function, so a correctly developed and well-functioning system is required for a healthy life as an impairment in the oxygenation process can lead to respiratory failure and cause severe damages.

In addition to the pressures balance, a very large surface of contact between air and blood needs to be maintained to achieve a proper gas exchange. This is guaranteed by an architectural design of the respiratory system, characterized by a fractal geometry to exploit the limited space of the chest cavity and a well-organized system of airways and blood vessels, which efficiently reaches all the points on the gas exchange surface.

The functional components of the respiratory system are:

- The neurological control centre which drives the respiratory muscles to contract or release;
- The chemical and stretch receptors located in the airways and sensitive to changes in O2 and CO2 blood concentrations which stimulate the respiratory centre;
- The respiratory muscles, among which the most important is the diaphragm, which allow the expansion and reduction of the space into the thorax cavity;
- The airways through which the air moves within the alveoli to exchange oxygen and carbon dioxide with the blood;
- The lung tissues able to sustain the elastic recoil forces that promote expiration;

- The chest wall that with its compliant properties facilitate the expansion of the thorax during inspiration.

A summary of the process is shown in the scheme presented in figure 1.1.

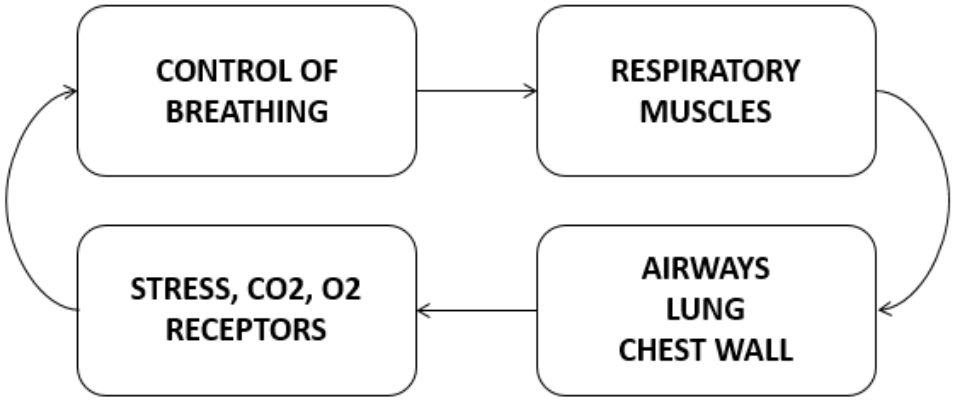


*Figure 1.1: Closed-loop feedback for the control of breathing*

*Airways and lung*

The airways can be divided into upper airways tract and lower airways tract. The upper ventilatory system is composed by the nose and the nasal cavity through which air is breathed in and filtered to remove pollutants and harmful substances, the pharynx that contains the intersection with the oesophagus and the larynx whose opening has a special flap of cartilage, called epiglottis, that opens to allow ait to pass through but closes to prevent food from moving into the airways. The upper tract is important to moisten the incoming air and warm it up until body temperature. The lower ventilatory system, or tracheobronchial tree, consists of the portion of the larynx below the vocal fold, the trachea that branches off into one main-stem bronchus for each lung and the bronchi that successively branch off many times throughout the lungs reducing their diameter into smaller sections called bronchioles that eventually form tiny thin-walled specialized sacs known as alveoli where gas exchange takes place.

The lungs can be considered a part of the lower respiratory system and can be described separately as paired, cone-shaped organs located in the thoracic cavity and protected from physical damages by the rib cage. They are covered by a membrane that folds in on itself to form a two-layered protective barrier called pleurae. The pleurae encase a cavity that contains the pleural fluid used to preserve the lungs from the friction experienced during breathing.

At the base of the lungs there is a sheet of skeletal muscle called diaphragm that, controlled by the sympathetic nervous system, is the main responsible for the breathing rhythmic activity.

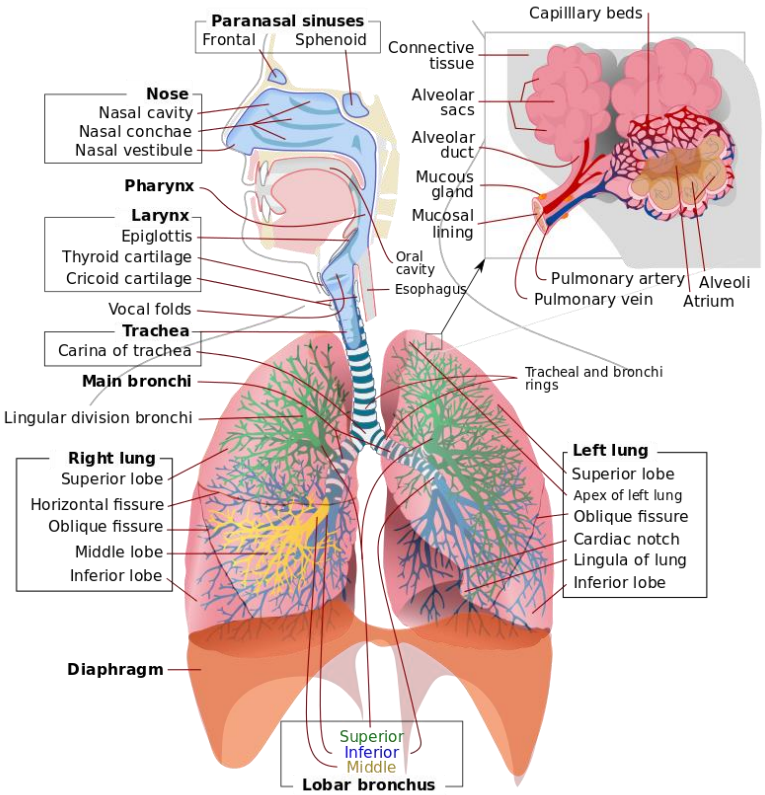


*Figure 1.2: Anatomy of the human respiratory system*

Going down the respiratory structure deeper into the lungs and passing from a bronchial generation to the following one, the diameter of the single airways decreases while their number raises. The latter overcomes the calibre reduction resulting in the increase of the total cross-sectional area approaching the alveoli. As a fluid dynamics consequence, the velocity of the flow is reduced to near-zero in the alveoli and the airways resistance drops.

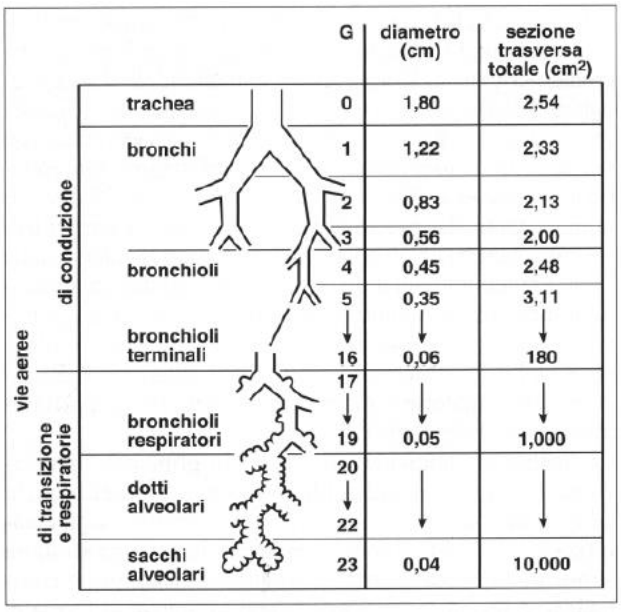


*Figure 1.3: Diameter and area of the total airways cross-section as a function of the bronchial generation.*

According to their function, the different parts of the respiratory system can also be divided into conducting and respiratory zone. The conducting zone conducts gases into and out of the lungs, filtering and humidifying breathed air, and offers a low resistance pathway for the airflow to equally distribute it into the peripheral units. The respiratory zone is the site of oxygen and carbon dioxide exchange with the blood and includes alveolar ducts, which are transitional elements, and alveoli.

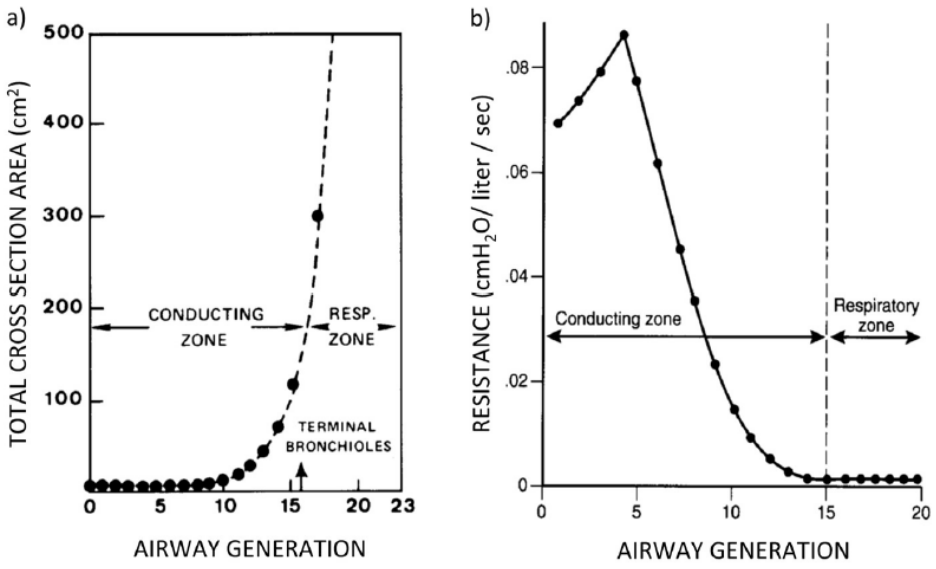


*Figure 1.4: a) Total cross-section area as a function of the airway generation. b) Resistance variation in different airway generations.*

The alveolus is the primary functional unit of the lung where the exchange of oxygen and carbon dioxide takes place between inspired air and blood. They have the shape of a hollow cavity covered with a dense grid of elastic and collagen fibres.

This structure allows them to stretch and enlarge during the inspiration and to recoil during expiration. Each alveolus is covered by a whole network of little blood vessels, called capillaries. Inside the alveoli the blood is separated from the inspired air by a thin layer of endothelium through which oxygen can easily diffuse into the bloodstream and carbon dioxide can combine with air to be breathed out.

The thickness of the alveolar-capillary membrane enables an effective gas diffusion that is guaranteed by a complex balance of factors which results in a minimal volume of hydration of the extracellular compartment. In fact, the alveolar stability depends on the interaction between different forces that affect the hydraulic pressure of the liquid phase of the pulmonary interstitium (Pip), which reflects the level of hydration of the extracellular matrix. The Pip is the result of the sum of the Starling forces, the forces exerted by the elastic connective parenchyma, the action of the lymphatic pump and the surface tension at the alveolus-air interface that tend to collapse the alveolus.

To prevent collapse, the alveolar surface is provided with a duplex lining layer constituted by two different types of epithelial cells: type I and type II alveolar cells. The type II pneumocyte cells synthesize and secrete the pulmonary surfactant that forms an underlying watery protein-containing hypo phase and an overlying thin film of phospholipids which cover the whole air-liquid interface. This substance enables to lower the surface tension in the small alveoli, preventing their collapse during expiration, and, at the same time, to avoid the excessive growth of the larger ones, during inhalation.

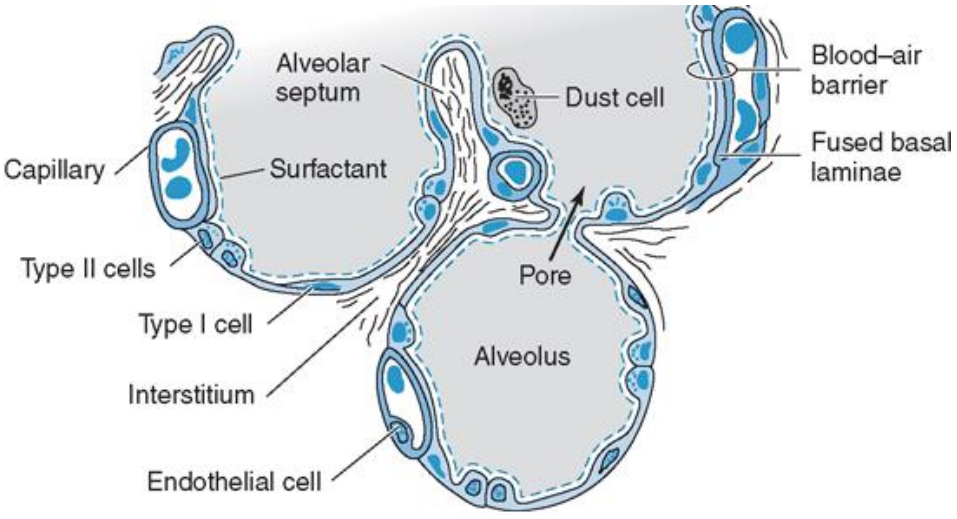


*Figure 1.5: Air-liquid interface in the alveoli*

In fact, at the air-liquid interface in the alveoli, the liquid has a surface tension that gives rise to a pressure directed towards the inner part of the cavity.

This pressure can be determined by the Young-Laplace equation:

$$P_\gamma = \frac{2\gamma}{r} \tag{1}$$

This equation suggests that the smaller is the radius, the higher is the pressure difference across the thin surface that separates the two static fluids. This pressure increases also with an increasing surface tension that, however, can be reduced to nearly zero thanks to the biophysical properties of the surfactant film, ensuring a well-distributed flow of air in each alveolus. Moreover, surfactant reduces lung recoil pressure together with the work of breathing and increases pulmonary compliance, which reflects the capability of the lung to change its volume when a specific pressure is applied.

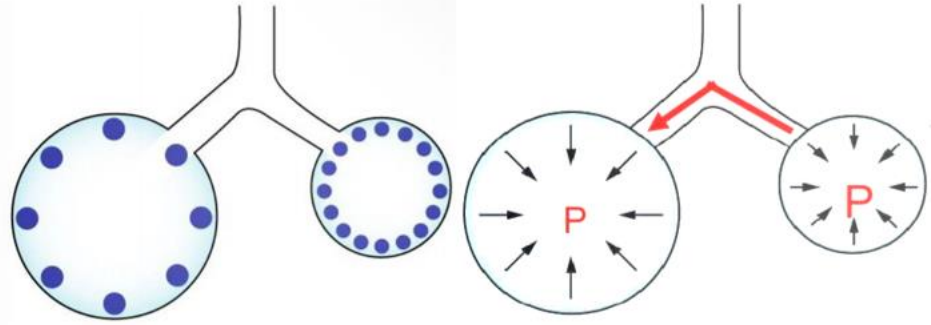


*Figure 1.6: Surfactant (left) and stress (right) distribution on the alveoli surface*

*Definition of Lung Volumes and Pressures*

The expansion or decrease of the lung volume is due to the up and down movement of the diagraph which increase or reduce the longitudinal axe of the rib cage together with the elevation of the ribs, that changes the antero-posterior diameter of the thorax.

The spirometry is the most common test to evaluate the functionality of the respiratory system as it is a non-invasive diagnostic device, standardized and easily reproducible. It allows to monitor tidal ventilation and changes in lung volumes under different breathing conditions.

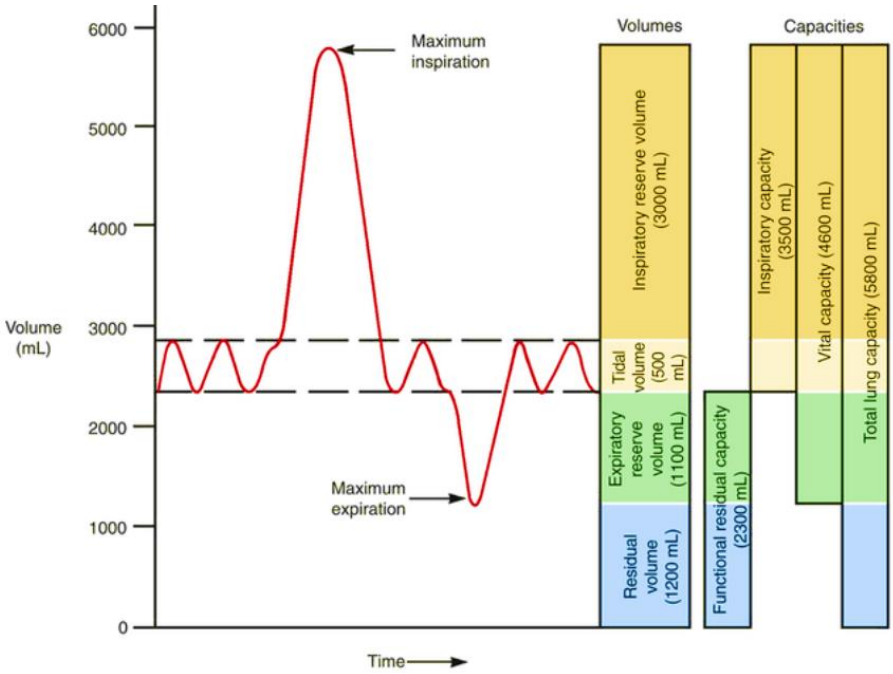


*Figure 1.7: Volume trace over time during spontaneous breaths and a maximal inspiration and expiration*

From the spirometer trace different lung volumes can be defined. In this work the following volumes will be used:

- *RESIDUAL VOLUME*: is the volume of air remaining in the lungs after a maximal-effort expiration.
- *TOTAL LUNG CAPACITY*: is the volume in the lung after a maximal inspiratory effort.
- *TIDAL VOLUME*: is the volume of air inhaled or exhaled with each breath.
- *FUNCTIONAL RESIDUAL CAPACITY*: is the amount of air in the lung at the end of a spontaneous expiration when all ventilatory muscles are completely relaxed, also known as the resting level.

These changes in lung volumes are the result of the air flow in and out the respiratory system. This convective flow occurs thanks to pressure gradients, which means pressure differences between two points that cause air to move from the point at higher pressure to the one of lower pressure. If the pressure difference between two points is equal to zero, no airflow is present. Thus, air flows in or out the lungs thanks to a pressure gradient established between open air and alveolar space by the dimensional variation of the thoracic cavity resulting from the contraction and relaxation of the chest muscles.

The airway opening pressure ($P_{ao}$) is the pressure measured at the mouth and is always equal to atmospheric pressure during spontaneous breathing. The pressure at the body surface is also equal to 0 mmHg. The alveolar pressure ($P_{alv}$) is the pressure within the alveoli and can be zero when airflow is absent. The pleural pressure ($P_{pl}$) is the pressure within the pleural space that in normal breathing conditions is negative.

The most important pressure gradients can be defined as follow:

- *TRANSPULMONARY PRESSURE* ($P_L$): is the difference between alveolar and intrapleural pressures. When there is no airflow, it is equal to the sub-atmospheric pressure $P_{pl}$ that counterbalances the elastic recoil force that tends to collapse the lung. This gradient is responsible of the alveoli inflation, breathing consists of the increase or decrease of $P_L$.
- *TRANSTHORACIC PRESSURE* ($P_W$): is the difference between the intrapleural pressure and the body surface pressure. When there is no airflow, it is equal to the outward recoil force of the thoracic wall.
- *TRANSDIAPHRAGMATIC PRESSURE* ($P_{di}$): is the difference between the esophageal pressure and the gastric pressure. It's a measure of the work done by the respiratory muscle to contract and expand the system to guarantee the gas exchange.
- *RESPIRATORY SYSTEM PRESSURE* ($P_{rs}$): is the difference between the alveolar pressure and the airways opening pressure. $P_{rs}$ is the total pressure to which the respiratory system is exposed and can be calculated as the sum of the pressure drop in the airways plus the pressures exerted on the lungs. No airflow exists at the end of inspiration or at the end of expiration because $P_{alv}$ is equal to $P_{ao}$ and, thus, $P_{rs}$ is zero at both these two points in the breathing cycle. The magnitude of this pressure gradient reflects both the airways frictional resistance to the airflow and the elastic components of the lungs and chest wall.

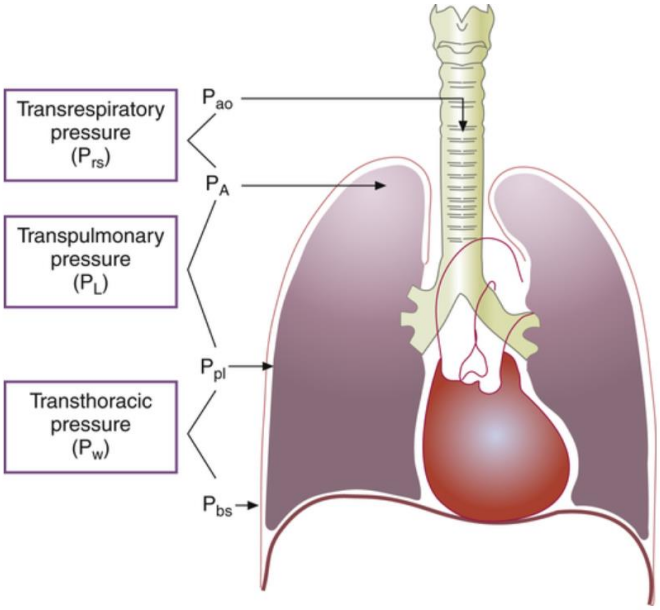


*Figure 1.8: Pressure gradients involve in ventilation*

The understanding of the interactions between the gas flow, the lung volume and the pressures acting on the respiratory system is fundamental to determine the impact of the ventilatory support on the patient.

## 1.1.2 Control of Breathing and Respiratory Muscles

The mechanisms of respiratory control provide the motor pathway responsible for the automatic rhythm that assures the ordered contraction of the muscles involved in ventilation and responds to the metabolic need and to the variation of the mechanical conditions.

*Neurological control and receptors*

Rhythmic ventilation is an automatic process controlled by the central nervous system.

Basic respiratory rhythm is generated by the activity of a neural network, composed by groups of cells located in the brainstem, specifically in the medulla oblongata in which numerous small nuclei of respiratory neurons oscillate their firing rate according to ionic current generated by changes in membrane potential in response to both excitatory and inhibitory neurotransmitters released from nearby neurons. Indeed, basic rhythm is subject to modulation by both conscious and reflex actions. The medullary pattern generator is subject to influences from other areas of the central nervous system and from chemoreceptors and mechanoreceptors that make the system a feedback loop. The parasympathetic (vagal) stimulation of the respiratory activity is attributed to afferent pathways present in the upper airways and lungs. Among these peripheric control centres, the stretch receptors mediate the Hering-Breuer reflex, which consists in inhibiting the inspiration and activating the expiration in response to pulmonary distension. The HB reflex contributes to setting the balance between tidal volume and respiratory rate to attain a given minute volume. Superimposed on this tonic control additional protective reflexes can be recruited to protect the lungs and airways with responses such as cough and sneeze when necessary.

The chemical control ensures the adaptation of respiratory activity to the metabolic demand of the organism, increasing the ventilatory response in case of a decrease in oxygen concentration, an increase in carbon dioxide or decrease in pH. In normal individuals, the respiratory minute volume is set to closely regulate arterial carbon dioxide tension at approximately 5.3kPa [5], predominantly via a negative feedback reflex involving the central chemoreceptors, while a separate group of chemoreceptors, the arterial chemoreceptors, are responsible for avoiding hypoxia. Combined hypercarbia and hypoxia is a very powerful stimulus to breathe as the two inputs interact in a synergic manner.

The motor receptors are important when in changing position the activity of the muscles results to be insufficient to generate the force required to exchange gases.

*Respiratory muscles*

The respiratory muscles are skeletal muscles from both the morphological and functional point of view. Their task is to displace the chest wall rhythmically in order to pump gas in and out the lungs. The respiratory muscles include the neck muscles, the intercostal muscles, the abdominal muscles and the diaphragm.

The action of the neck muscles is to counterbalance the force exerted by the diaphragm on the upper rib cage. In normal subjects under resting conditions these muscles are inactive, being recruited only when ventilation increases substantially or when the inspiratory muscles are abnormally loaded. The intercostal muscles are two thin layers of muscle fibres occupying each of the intercostal spaces. When an intercostal muscle contracts in one interspace, it pulls the upper rib down and the lower rib up. The wall of the abdomen is mainly made up of four abdominal muscles: the rectus abdominis, the external and internal obliques and the transverse abdominis. The action of these muscles is essential during both inspiration and expiration. Indeed, as they contract, they pull the abdominal wall inward producing an increase in abdominal pressure that causes the diaphragm to move cranially into the thoracic cavity. This motion, in turns, results in an increase in pleural pressure and an increase in lung volume. They also pull the lower ribs caudally deflating the cage. The diaphragm is the dome-shaped sheet of muscle and tendon primarily used for respiration. As the diaphragm contracts during inspiration its muscle fibre shortens, and the axial length of the apposed diaphragm diminishes so that the dome of the diaphragm descends sliding on costal insertions. The height of the zone of apposition, the portion of muscle directly connected to the inner part of the lower rib cage, in normal subjects decreases by about 1.5 cm during quiet inspiration. This descend of the dome has the effect of generating a fall in the pleural pressure that leads the thoracic cavity to expand.

The airways have been fully descripted in the previous chapter (1.1.1) from the oral and nose cavity to the lungs, while both the lung and chest will be described focusing on their mechanical properties in the following section.

### 1.1.3 Mechanical Properties and Models of the Respiratory System

The forces acting on the respiratory system can be schematically represented in a model constituted by a non-rigid airway, that applies a resistance to the gas flow, a viscoelastic deformable chamber and a deformable element surrounding the lungs and representing the chest wall that, thanks to the respiratory muscles, allows the breathing movements. The gap between the lung unit and the chest wall represents the liquid filled inter-pleural space.

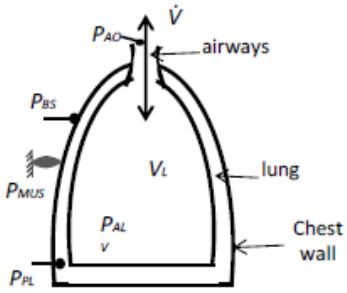


*Figure 1.9: Schematic representation of the forces acting on the respiratory system*

The mechanical behaviour of the respiratory system can be described using an equivalent electrical model composed by four elements: airways, lung, chest wall and respiratory muscles.

Each of these elements in turn can be represented by a very simple electric circuit characterized by a resistance, a capacitance, and an inductance in parallel representing respectively the resistance, compliance and inertance of the considered element. The values of the different mechanical parameters can be obtained by measuring pressure differences and changes in volume across the various subsystems.

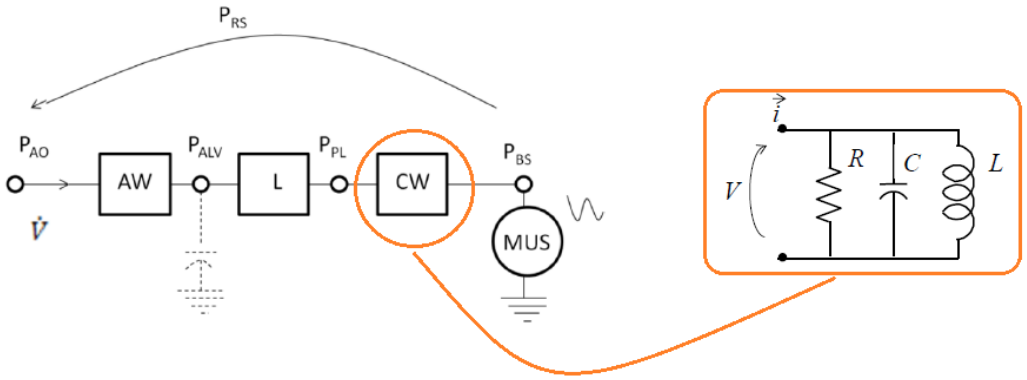


*Figure 1.10: Electrical model of the respiratory system*

The first block (AW) represents the airways resistance, the second block (L) represents the resistance and the static compliance of the lungs and the third one (CW) represents the same parameters of the chest wall.

In this model, the volume corresponds to the electric charge and thus the derivative, the electric current is the flow of air, driven by the electric potential that stands for the pressure.

The compression and expansion of the gas, during rapid changes in volume, can produce a difference between the instantaneous rate of volume change in the lung and the volume flow of gas at the mouth. However, in normal tidal breathing, this difference can be neglected and the flow at the air opening can be taken as a good approximation for $\dot{V}_L$.

The respiratory muscles are represented as a voltage generator as they are responsible of the change in the pleural pressure throughout the chest wall. Because of compression and expansion of gas, a capacitor is inserted between the airways and the lung.

For small amplitude flows and low frequency breathing, such as during resting conditions, the mechanics of the respiratory system can be adequately described by a linear approximation through a set of equations that define the relationship between the pressures acting on the different elements, the volumes and the gas flow through them.

$$P_{AO} - P_{ALV} = R_{AW} * \dot{V} \tag{2}$$

$$P_{ALV} - P_{PL} = \frac{1}{C_L} * V_L \tag{3}$$

$$\Delta P_{MUS} + (P_{PL} - P_{BS}) = \frac{1}{C_{CW}} * V_L \tag{4}$$

The parameters of the equations describe the mechanical properties of the respiratory system that are evaluated in the pulmonary function tests.

The resistance to lung inflation can be categorized as elastic resistance and frictional resistance. Frictional resistance is applied only under dynamic condition, that is, when gas is moving through the airways. Elastic resistance, instead, is present under both dynamic and static conditions, that is, when there is no air movement. The lungs and the chest wall have equal but opposite recoil forces. The lung tends to recoil inward, away from the chest wall, while the thorax tends to recoil outwards. When no air is moving these two oppositely directed forces exactly balance each other, creating a negative sub atmospheric pressure in the space between the two structures. Either the static and dynamic characteristics of the lung and chest wall system influence the work of breathing and the distribution of the inspired air in the lung. Hence, understanding lung-chest wall mechanics is essential in treating patient needing respiratory therapy.

#### 1.1.3.1 Static Lung and Chest Wall Mechanics

***Volume-Pressure Curve of the Lungs***

The elastic properties of the lungs can be obtained by measuring the transpulmonary pressure required to inflate the lung until certain volumes under static conditions. Indeed, combining the equations (2) and (3), the transpulmonary pressure ($P_L$) can be defined as following:

$$P_L = P_{AO} - P_{PL} = \frac{1}{C_L} * V_L + R_{AW} * \dot{V} \tag{5}$$

When the flow is zero, it is reduced to a function of the volume only. Pressure measurements can be taken several times at various lung volumes to construct a pressure-volume (P-V) curve. This curve describes the relationship between the lung's distending pressures and the volumes reached at different level of lung expansion.

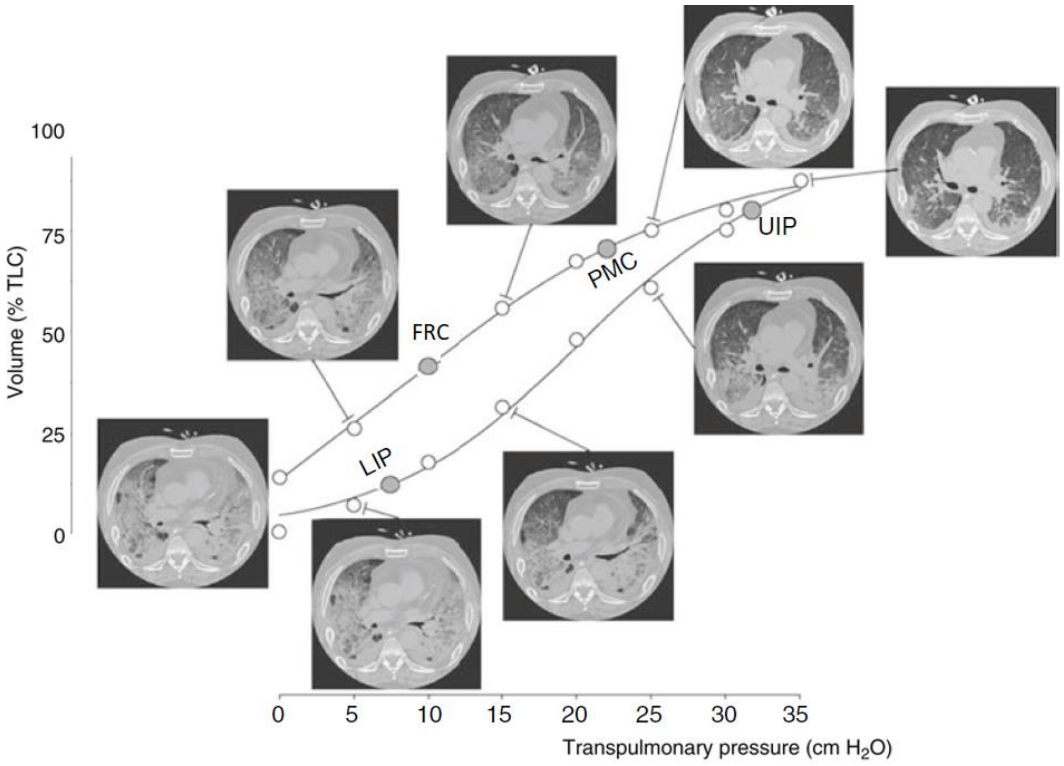


*Figure 1.11: Pressure-Volume curve of the isolated lung*

Over the normal physiological range of tidal breathing the elastic structure of the lungs expands in response to increasing pressure according to Hooke's Law, which means, it enlarges of a quantity directly proportional to the amount of force applied. As the lung volume increases, the recoil forces increase. This linear relationship is maintained up to the elastic limit, beyond which lung rupture is liable to happen.

The slope of the P-V curve corresponds to the static compliance of the lung and expresses its distensibility when flows and all derivatives of volume are zero: the steeper the slope, the greater the tendency of the lung to distend.

$$C_L = \frac{\Delta V_L}{\Delta P_L} = \frac{\Delta V_L}{\Delta(P_{ao} - P_{pl})} \tag{6}$$

The pressure exerted on the lung ($P_L$) is the difference between $P_{alv}$ and $P_{pl}$. The alveolar pressure is measured at the mouth, as under static condition it is equal to $P_{ao}$. The intrapleural pressure can be measured using an esophageal catheter or balloon, as described in the following chapter.

However, the resulting curve obtained on the entire range of pressure values is non-linear with a sigmoid shape and can be divided in three different zones. At low lung volumes and pressures the compliance is low because of the need of a high critical pressure to open the terminal alveoli. The central region of the curve is bounded by lower inflection point (LIP) and an upper inflection point (UIP) and correspond to the $V_T$ range in which the curve is relatively linear and the compliance increases. This is the zone of the normal tidal breathing where a small change in pressure gives rise

to a large change in volume. At the upper end the slope of the curve flattens again as the lung becomes stiffer to oppose to further volume increase.

The non-linearity of the curve is caused by the fact that the lung parenchyma is composed by collagen and elastic fibres that are not uniform springs. Elastic fibres are easily stretched, whereas collagen fibres are more resistant to deformation.

The inspiratory curve is constructed incrementing in a stepwise fashion the transpulmonary pressure, hence, inflating the lung from RV to TLC. At each step the volume is held until all airflow ceases and the pressure is recorded. To obtain the expiratory curve, the lung is slowly deflated in the same stepwise way.

The curve during inflation follows a different pathway than the deflation curve. The lung volume at each given distending pressure is larger during expiration than during inspiration. This phenomenon is called hysteresis and is attributable to the viscoelasticity of the lung tissues. In other terms, the pressure required to keep the lungs inflated during deflation is less than the force needed during inflation. This is related to the fact that, during inflation, the lung dissipate energy in the alveolar recruitment to overcome the molecular adhesive forces of surface tension that are not present during expiration when alveoli are already open.

Changes in the elastic properties of the lungs can modify the characteristics of the curve. The shape of the P-V curve provides useful information of the health lung conditions allowing to identify severe lung injuries. [6]

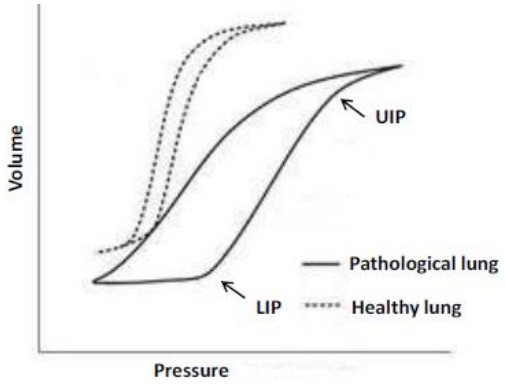


*Figure 1.12: Comparison of the P-V curve of a pathological lung with a healthy one*

***Volume-Pressure Curve of the Chest Wall***

The same curve can be constructed also for the chest wall. The compliance of the chest wall defines the relationship between the transthoracic pressure $P_W$ and the volume in the chest cavity:

$$C_{CW} = \frac{\Delta V_L}{\Delta P_W} = \frac{\Delta V_L}{\Delta(P_{pl} - P_{bs})} \quad (7)$$

Since the pressure at the body surface $P_{bs}$ is, by definition, equal to atmospheric pressure (0 mm Hg), the transthoracic pressure corresponds to the pleural pressure $P_{pl}$.

Thus, the partitioning of the total respiratory system compliance into lung and chest wall components requires a measurement of the pleural pressure, usually estimated using an esophageal balloon or catheter.

Indeed, as the lung and chest wall recoil in opposite directions, the pressure between the pleural membranes decreases. No true space exists between the visceral and the parietal pleurae, that means, the idea of measuring $P_{pl}$ placing a tube within these membranes would be too invasive and dangerous in clinical practice. For clinical and research purposes changes in $P_{pl}$ may be estimated from the esophageal pressure ($P_{es}$) because of the close apposition of the flaccid oesophagus to the pleural space. The thin-walled oesophagus has little muscle tone and easily transmits $P_{pl}$ changes to the tip of the catheter.

The chest cavity has a large volume when there is no transthoracic pressure. This is the result of the natural tendency of the chest wall to spring outward. Consequently, in order to reduce the chest cavity volume, progressively large negative intrapleural pressures must be generated. However, the outward springing tendency of the chest wall is limited, and, above a certain threshold, greater chest cavity volumes can only be achieved by applying positive intrapleural pressures.

Therefore, as shown in figure 1.14, at extremely large volumes the chest cavity begins to resist further expansion and tends to recoil toward smaller volumes.

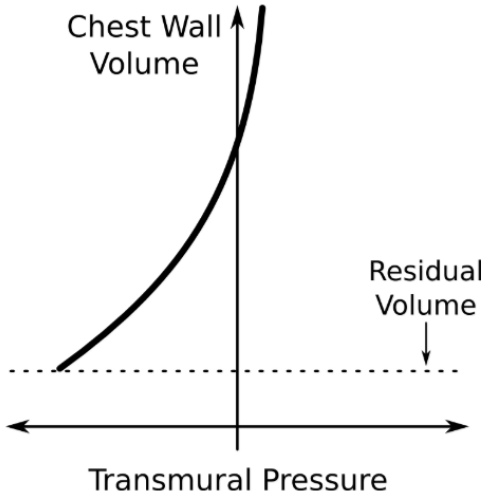


*Figure 1.13: Pressure-volume curve of the chest wall*

Several studies have demonstrated that in some cases the chest wall has a significant influence on the total respiratory system P-V curve. This method of correcting the respiratory system P-V curve for the effect of the chest wall can be used to obtain precise pressure settings for the lung during mechanical ventilation. [7]

***Volume-Pressure Curve of the Respiratory System***

Since the lung volume is determined by the interaction between lung and chest wall, the sum of the static curves of these structures results in a pressure-volume curve that describes the elastic behaviour of the whole respiratory system.

The compliance of the whole respiratory system can be computed as follow:

$$C_{rs} = \frac{\Delta V_L}{\Delta P_{rs}} = \frac{\Delta V_L}{\Delta(P_{ao} - P_{bs})} \tag{8}$$

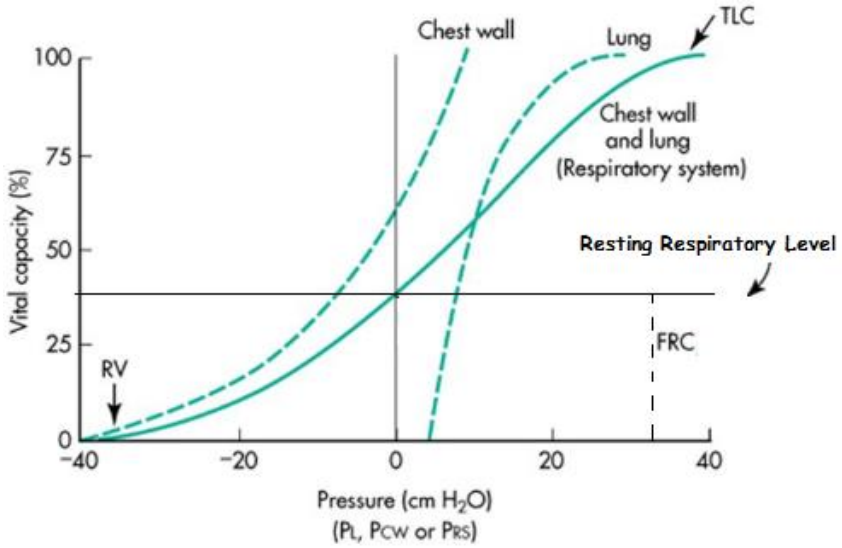


*Figure 1.14: The static P-V curve of the total respiratory system*

While in the lung curve the pressure is always positive, the chest wall curve has negative pressure at low volumes and becomes positive when the volume is increased over the 75% of the vital capacity. The point in which the global P-V curve crosses the zero-pressure point corresponds to the FRC, the total pressure of lung and rib cage becomes sub-atmospheric below this resting volume. Contraction of the lung-chest wall unit below the FRC requires negative transmural pressures, meaning that without any applied forces the unit would expand (inhalation). Expansion of the lung-chest wall unit beyond the FRC requires positive transmural pressures, meaning that without any forces applied the unit would collapse (exhalation). At zero pressure, the lung is at its minimal volume, which is lower than residual volume, the minimal volume reached by the chest wall only.[8]

### 1.1.3.2 Dynamic Lung and Chest Wall Mechanics

The electrical model described above doesn't take into account the force exerted by the respiratory muscles to overcome the elastic recoil of the lung and chest wall, the viscous friction of air flowing through the airways and the forces caused by the viscoelastic properties of the tissues that act

during breathing. A mechanical model better illustrates the balance of forces describes by the following equation, known as the equation of motion of the respiratory system:

$$P_{ao} + P_{MUS} = \frac{V}{C_{rs}} + \dot{V}R_{rs} + \ddot{V}I_{rs} \quad (9)$$

In this equation $P_{MUS}$ is the pressure generated by the respiratory muscles, while, $V$, $\dot{V}$and $\ddot{V}$ are the volume of the lung above end-expiratory volume and its time derivatives, flow, and acceleration. The parameters of this simple linear system are the dynamic compliance ($C_{rs}$), resistance ($R_{rs}$) and inertance ($I_{rs}$).

*Compliance*

The compliance relates the pressure to the volume and it's a measure of the elastic recoil of the lung and the chest wall. The dynamic compliance is normally lower than the static one. The compliance of the lung depends on its size in a proportional way: the bigger the lung, the higher the compliance. For this reason, compliance is greater in adults than in infants, as adults' lungs accept more volume for a given pressure. To correct for lung size and describe the elastic properties of the lung tissues in a more accurate way, the compliance per unit of lung volume or per kilograms is normally used.
The mathematical reciprocal of compliance is elastance (E), defined as the change in pressure required to produce a unit change of volume. The more elastic the lung, the less its elastance and the higher its compliance.
If no respiratory muscles forces are present, the lung and chest wall can be considered as aligned in series. Indeed, the pressure applied to the airway is first transmitted to the lung and then, only a reduced amount of pressure, is transmitted to the chest wall. Therefore, the pressure acting to distend the respiratory system is the sum of the pressures needed to inflate the lung and enlarge the chest wall. Thus, the elastance of the respiratory system ($E_{rs}$) can be defined as the sum of the lung elastance ($E_L$) and chest wall elastance ($E_{CW}$):

$$E_{rs} = E_L + E_{CW} \quad (10)$$

Then, the compliance of the total respiratory system ($C_{rs}$) is the sum of the reciprocals of the lung and chest wall compliance:

$$\frac{1}{C_{rs}} = \frac{1}{C_L} + \frac{1}{C_{CW}} \quad (11)$$

*Resistance*

Resistance represents the opposition to the flow due to frictional forces and is defined as the pressure gradient required to move gas through the airway at a constant flow rate.

$$\mathrm{R} = \frac{\Delta P}{\dot{V}} \tag{12}$$

The resistance of the respiratory system is the sum of a viscous component given by the lung tissue during breathing and a resistance generated within the airways because of the relative movements between the gas molecules and the airway walls.

R depends not only on the length and the diameter of the conducting airways, but also on the viscosity and density of the gas, on the flow rate and on the kind of flow, that can be laminar or turbulent. When both the flow regimes are present the relationship between pressure and flow is expressed by the *Rohrer's equation*:

$$\Delta P = K_1\dot{V} + K_2\dot{V}^2 \tag{13}$$

When flow is fully turbulent only the second part of the equation has to be considered, while when flow is fully laminar a linear equation can be used.

In a cylindrical rigid tube with length much greater than its radius, if the flow is steady and laminar and the fluid is ideal, resistance can be defined by Poiseuille's Law:

$$K_1 = \frac{128\mu L}{\pi I D^4} \tag{14}$$

$K_2$, instead, is linearly related to the density of the gas $(\rho)$and its viscosity $(\mu)$:

$$K_2 = \frac{L\mu\rho}{r^5} \tag{15}$$

Thus, human lung can be modelled as a multiple tube system whose resistance depends on the total cross-sectional area of all tubes. Although the individual bronchi decrease in diameter as they extend towards periphery, the cross-sectional area of the airway increases dramatically.

*Inertance*

Inertance of the respiratory system is a measure of the tendency of the respiratory system to resist changes in flow. It is the analogue of the electric inductance. At frequencies normally reached during spontaneous and mechanical ventilation inertance is usually negligible. The pressure caused by the inertance is in the opposite direction to that generated by the elastance. Therefore, inertial forces tend to balance the impedance to the flow provided by the stiffness of the respiratory system.

# 1.2 Infant Respiratory System

## 1.2.1 Differences between Adults and Infants

Many physiological and anatomical differences exist between infant and adult respiratory systems that make newborns less able to cope with the stress acting on their immature lungs. The functional unit of breathing is the alveoli. The alveolar development starts approximately at the 7$^{th}$ month of

intrauterine life. The increase in alveolar number and the maturation of the elastic fibres requires years to be completed and to reach the adult shape.

The airways in the lungs of a newborn are relatively large in comparison with those of an adult but in absolute terms they have a small diameter and even a modest reduction in the airway radius results in a marked increase in resistance to airflow.

Indeed, in infants, viscous resistance is much higher than in adults in which peripheral large cross-sectional area contributes minimally to the total airways resistance. Conversely, the small peripheral airways provide a great contribution to the total pulmonary resistance in the infant lung, making risky any disease that causes a decrease in the peripheral resistance.

The relatively elevated resistance in infants is due not only to the smaller size but also to the higher tissue density and higher collapsibility of the airways. In fact, the larynx, trachea and bronchi are considerably more compliant while the activity of the muscles responsible for maintaining upper airway patency is decreased as the elastic reoil provided by the alveoli. Thus, during forced respiratory efforts, both dynamic inspiratory collapse of the upper airways and dynamic expiratory collapse of the lower airways can occur, according to the position of the airways obstruction.

Although in absolute terms airways resistance is elevated in infants, the resistance normalized to the lung volume is lower than in adults because new-borns bronchial tree is shorter and the inspiratory flow velocities are lower.

The chest wall is highly compliant in infants because the ribs are still not ossified, the cartilage is thinner, and the muscular tone is lower due to incomplete mineralization of the bones.

Moreover, the infant's ribs are aligned horizontally providing the intercostal muscles with less space to move in the anteroposterior direction and, then, limiting the elevation of the ribs and producing a lower intrathoracic volume during inspiration than in adults. In addition, the more horizontal insertion of the infant's diaphragm induces an inward distortion of the lower ribs rather than moving upward during inspiration. For all these reasons the respiratory pump is poorly effective in infants even because of the histochemical properties of the respiratory muscles.

Indeed, new-borns are poorly equipped to sustain high workloads having low muscle mass and a low percentage of fatigue-resistant type I muscle fibres compared to adults. To endure the work of breathing and avoid respiratory failure, the diaphragm must be provided with a continuous supply of oxygen. Maturational changes in the respiratory musculature occur with increased mass and a progressive increase in 'slow-twitch' type I fibres.

In the adult half of the total impedance of the respiratory system is due to the chest wall, so about half of the force generated by the respiratory muscles is dissipated in moving it. From this point of view the highly compliant chest wall of the infant appears advantageous.

As previously discuss, the two pressure generators in the respiratory system are the diaphragm and the intercostal muscles. Inspiratory action of either one of them has an expiratory recoil action on the other.

The magnitude of this motion depends on the relative compliances of lung and chest wall because the diaphragm acts on these in parallel and splits its displacement proportionally. The ratio of the passive compliance of the chest wall to the passive compliance of the lung in preterm infants is very high (approximately 5:1) and result in a division of the displacement of the diaphragm inadequate for ventilation.

Moreover, the high compliance of the chest wall reduces the outward elastic recoil in infants resulting in a relaxation volume of the respiratory system that is lower than in adults. Consequently, the new-borns, especially the premature ones, have a low FRC that makes the infant more predisposed to alveolar instability and terminal airways occlusion. The dynamic end-expiratory volume is substantially above the passively determined elastic equilibrium volume and the resting FRC is close to the closing volume of the lung, that is the volume at which lung regions cease to ventilate because of the closure of the airways leading to them. Therefore, infants have to constantly re-establish lung volumes through active and energy-consuming mechanisms like a high respiratory rate with insufficient time to exhale to the elastic equilibrium volume and a laryngeal contraction during expiration to increase the airflow resistance.

The compliance of the lung, instead, is related to lung volume: the smaller the lung, the lower the compliance. For this reason, in clinical studies and comparisons between patients it is more accurate to use the specific compliance that is normalized to FRC. The latter is nearly identical in term infants and adults, whereas in premature infants it remains low due to the presence of unabsorbed fetal lung fluid and failure to achieve a normal FRC.

Finally, the infants breathing pattern is irregular with considerable breath-to-breath variability and periodic breathing at times. All these differences are particularly evident and marked for preterm newborns, who thus are more prone to respiratory failure.

### 1.2.2 Fetal Lung Development and Preterm Birth

The formation of the lungs begins at about 4 to 5 weeks of gestation with the appearance of lung bud in embryo and achieves its end into late childhood. The development of the lung can be divided into two phases: structural growth and functional maturation. Fetal breathing movements begin as early as 10 weeks of gestation and the breathing of amniotic fluid in and out is essential for the stimulation of lung development.

During organogenesis, the lung surface area expands, the thickness of the alveolar epithelium decreases and a close interaction with an extensive capillary network is established to assure an efficient gas exchange. Lung growth proceeds through gestation with a progressive branching of the airways and the final development of alveolar spaces in the last trimester.

In the last functional phase, the development of the surfactant system is required to ensure the stability of the lung huge surface area. It reaches maturity by approximately 36 weeks of GA decreasing surface tension within the alveoli and preventing their collapse during exhalation. Lung keeps on growing after birth and each of the structural lung components continues to remodel during the first years of life. Airways, alveoli, and blood vessels increase in number as well as in size. This development process results in an organ with an extremely large surface area (50-100 m2) capable of exchanging gases through a very thin membrane.

Also, the structure of the rib cage and the respiratory muscles undergo modification to reach their complete maturity.

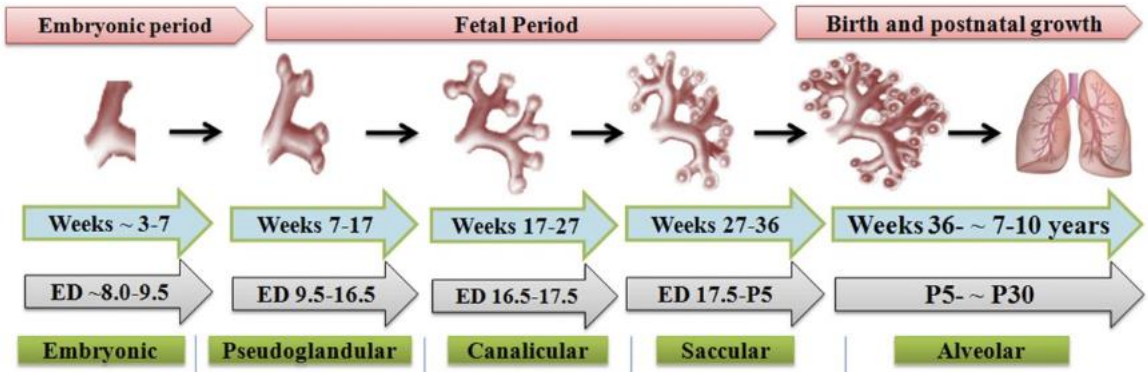


*Figure 1.15: Phases of human lung development*

Birth is not the end of the development of the respiratory system but represents a critical event associated with dramatic changes in the lung function. During fetal life, indeed, lung is filled with liquid and receive only a small amount of cardiac output. When the responsibility for the gas exchange passes from the placenta to the lung, the fetal lung fluid needs to be absorbed, the lungs must be filled with air, the pulmonary blood flow has to greatly increase, and the surfactant system has to make the lungs remain expanded.

Many factors can influence the physiological organogenesis, following pathogenic pathways both during intrauterine growth and first months of life, bringing to different types of lung injuries. Incomplete growth of lung structure and premature birth lead to respiratory compromises or insufficiency.

A birth is defined “preterm” when occurs before the 37$^{th}$ complete week of gestation. It therefore can involve a wide range of gestational age associated with very different problems. The risk of acute neonatal illness decreases with gestational age, reflecting the fragility and immaturity of the brain,

lungs and immune system. In general, more immature preterm infants require more life support. The complications of preterm birth arise from immature organ systems that are not yet prepared to support life in the extrauterine environment where straining active breathing and a full cardiac output are required.

The preterm respiratory system is characterized by an incomplete structural development that involves the lack of surfactant, a reduced alveolar stability and a thickened alveolar-capillary membrane that impairs gas exchange. This results in a lower capacity of fetal liquid reabsorption, low specific lung volumes and increased tissue stiffness, that means low lung compliance value. [9]

Moreover, if the birth occurs extremely preterm (around the $27^{th}$ week of gestation) the vascularization of the mesenchyme is still at its early stage, the differentiation of alveolar epithelium cells in type I and II is still immature and the air -blood barrier has just begun to shrink.

Even if the birth is between 27 and 37 weeks of gestation, the lung is not already correctly developed presenting simplified distal pulmonary acini with reduced number of alveoli and abnormal capillary morphology that alter the pulmonary functionality and lead the infant to breath using terminal bronchioles and primitive air sac. After delivery, the central control of breathing adapts to air conditions and the breathing pattern generally becomes more regular and continuous, but the still immature regulatory system can lead to brief episodes of apnoea. A considerable amount of maturation of the breathing control system occurs in the last few weeks of gestation, which explains the high prevalence of apnoea in infants born prematurely. None of these stages of development is compatible with an autonomic ventilation and in most cases requires some form of ventilatory support.

Hence, the undeveloped premature lung and its postnatal completion of growth, together with the surfactant-deficit, renders the preterm infants vulnerable to suffer from respiratory failure and contract pulmonary disease (RDS). To treat this condition and save lungs from collapse, mechanical ventilation and surfactant administration are required. However, although assisted ventilation is indispensable for the survival of these patients, if it is not administrated properly, it can exacerbate the pre-existing lung injury leading to ventilator induced lung injury (VILI). An inadequate therapy or a wrong choice of the ventilator control parameters may cause the development of a chronic lung pathology called Bronchopulmonary Dysplasia (BPD), which is characterized as an arrest of lung development with significant long-term effects during childhood and adolescence.

## 1.3 Bronchopulmonary Dysplasia

Bronchopulmonary dysplasia (BPD) is the most common chronic lung disease that affects preterm infants at birth and one of the most severe long-term complications of prematurity with

longstanding consequences involving multiple organ systems including adverse effects on pulmonary function and neurodevelopment outcome. Infants with BPD have significant pulmonary morbidity during both childhood and adolescence presenting more chest deformities and asthma than other children. [10]

BPD is a multifactorial pathology which takes its origin from an impaired alveolar-capillary maturation during fetal and neonatal life. Different interdependent causal factors that play a role in the abnormal growth of the premature lung are associated with BPD.

In addition to premature birth and consequently immature lung development, the main risk factors include prenatal and postnatal infections, supplementary oxygen therapy and mechanical ventilator support (VILI). [11]

A strong correlation has been found especially between BPD and days of mechanical ventilation and oxygen therapy. Other factors, such as intrauterine infections and genetic predisposition may contribute to the pathogenesis of this disorder.

### 1.3.1 Epidemiology

In 1967 Northway et al. [12] recognized a distinct and recurrent pattern of serial changes in the chest radiographs of preterm new-borns who survived long enough to develop a form of chronic lung disease. Indeed, preterm infants ventilated for severe respiratory distress syndrome (RDS) showed airway injury and parenchymal fibrosis caused by aggressive mechanical ventilation and high concentration of oxygen. Over the years, the development of better ventilators and the progress in perinatal care units have dramatically improved the survival rate of extremely preterm infants, however, BPD remains the most common adverse outcome for infants who survived.

In the early 90', with the availability of surfactant treatments the mortality of extremely low birth weight (BW) infants decreased further and BPD became the major pulmonary complication of prematurity, despite the increased emphasis given to tailoring ventilation therapies to suit at best patient-specific needs. In 1999 a new definition of BPD was proposed, that was no longer related to ventilator induced injuries but rather associated to alveolar and vascular development.

Its incidence depends on different factors, such as the medical centre and the diagnostic criteria applied. BPD is nowadays uncommon in infants weighting more than 1200g or with a gestational age greater than 30 weeks. However, some very low birth weight infants who initially have minimal or no lung disease but who develop increasing oxygen and ventilatory need can evolve in a chronic pathology. According to the last definition of BPD, the average rate of incidence in infants with BW below 1200g is 30%. [13]

Similarly, if we take into account the gestational age, the incidence of BPD in surviving preterm infants with less than or equal to 28 weeks GA is approximately 40% over the last few decades. The rate of incidence among infants born before 32 weeks GA varies significantly according to the care centre and the country. The incidence of severe BPD is inversely correlated with GA and remains about 16% for all infants born below the 32$^{th}$ week.

In a study carried out by Stoll et al. BPD was found to affect the 68% of the extremely preterm newborns (22-28 GA weeks) involved in the study. [13]

## 1.3.2 Pathophysiology

The characteristics of BPD have evolved over the years allowing to distinguish between 'old BPD' and 'new BPD'. This reflects the distinct embryologic differences in pulmonary development, the changes in treatment strategies and the improvement in technological and pharmacological solutions. The 'old' or 'classic' BPD corresponds to the disease described by Northway in 1967, occurring mainly in relatively large premature newborns (30-34 week of GA). [12]

This BPD defines the progression from acute respiratory failure with diffuse parenchymal lung disease and low lung volume (RDS) to a chronic disease characterized by extensive heterogenous fibrotic and cystic lesions, area of severe hyperinflation and distal lung inflammation.

As the practice of neonatology evolved, exogenous surfactant improved lung compliance and reduced oxygen requirements, whereas ventilators became more sophisticated and less invasive. These innovations enabled less aggressive methods of ventilation and reduced damages to airways and resultant fibrosis, changing the phenotype of BPD. As a result, the survival rate improved for more immature infants, establishing an inverse relationship between the severity of BPD and gestational age.

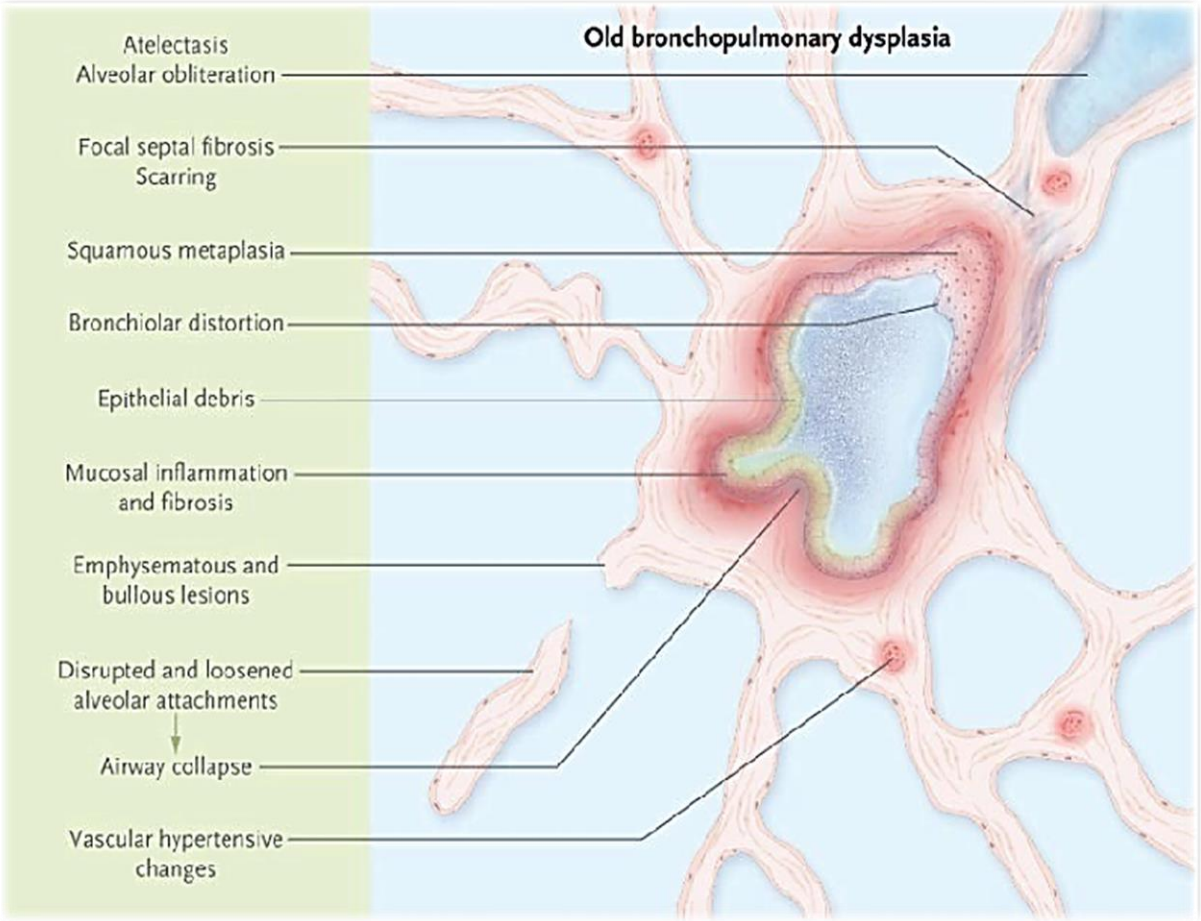


*Figure 1.16: Nonhomogeneous airway and parenchymal disease in old BPD*

As neonatal centres started working on the refinement of their management of respiratory diseases, a reduction of the clinical presentation of 'old' BPD in the older preterm infants has been noticed but a different form of CLD has been introduced that may not be associated only with absence of surfactant, high oxygen exposure or lung damage related to ventilation. Indeed, even though the reduction of volutrauma and the administration of surfactant significantly decreased BPD, chronic changes in respiratory function of newborns experiencing intrauterine infection, hypoplasia and meconium aspiration appeared. This pathological entity is characterized by respiratory insufficiency, impaired vascular development, and impaired pulmonary function in the first years of life but less heterogeneous lung injury. In this way, this new pathology, defined 'new' BPD, includes a decrease in the alveolar number, a simplification of distal lung septation and abnormalities in the growth of the pulmonary microvasculature that lead to a dysmorphic pattern of vascular organization and an unbalanced distribution of capillaries. Moreover, the pulmonary capillaries appeared to be abnormally dilated and frequently located within thickened alveolar septa, rather than immediately adjacent to the alveolar epithelium reducing gas exchange efficiency.

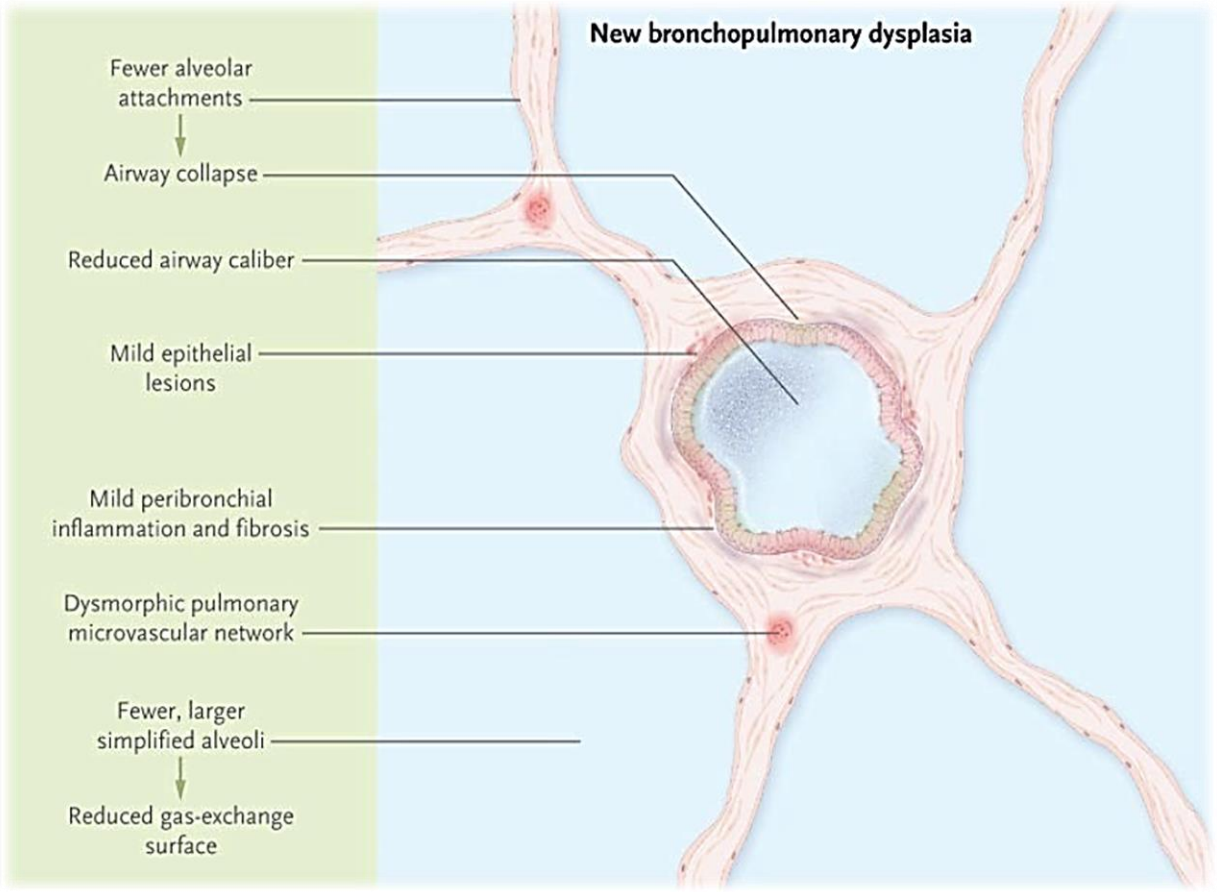


*Figure 1.17: Main pathological features of new BPD*

These alteration result in important functional consequences, such as reduced tidal lung volume, compromised ventilation distribution and changes in pulmonary mechanics, predominantly an increase in airway resistance and a decrease in lung compliance. The measurement of this resistance, however, is not a sensitive test for lower airway disfunction. Plethysmography measurements of lung volumes in 'new' BPD infants demonstrate that functional residual capacity (FRC) and residual volume (RV) are reduced because of a significant obstructive airway disease with air trapping. Inflammation and fibrosis are usually milder than in 'old' BPD. [14]

Despite being delivered several weeks before alveolarization begins, infants at risk for new bronchopulmonary dysplasia often have only mild respiratory distress syndrome at birth. However, at this early stage, even minimal exposure to injurious factors may affect the normal process of pulmonary growth and alveolar maturation. With the advances of clinical care, most preterm infants with 'new' BPD tend to have a milder disease, although a small but important subgroup of ventilator dependent infants with severe BPD persists.

*Table 1-1: Main features and differences between 'old' and 'new' BPD*

| OLD BPD | NEW BPD |
|---|---|
| Larger preterm infants | Extremely premature infants |
| High ventilation and oxygen needs | Modest ventilation and oxygen needs |
| Severe large airway injury<br>Inflammation | Minimal large airway injury<br>Inflammation less prominent |
| Extensive small airway disease with alternating areas of over inflation | Minimal small airway disease |
| Parenchymal fibrosis | No fibrosis |
| Interstitial and alveolar oedema | Decreased septation<br>Arrested alveolarization (hypoplasia) |
| Pulmonary artery muscularization | Fewer and abnormal pulmonary vascularization resulting in increased airway resistance |

The pathologic features of this chronic disease result from the combination of multiple pathogenic factors that concur to pulmonary deterioration. A study conducted from the Newborn and Infant Chronic Lung Disease Program at the Children's Hospital of Philadelphia and involving 200 premature infants allows to define three major phenotypical variants of the disease:

- Severe lung parenchyma disease
- Pulmonary vascular disease
- Sever airway disease

## 1.3.3 Prevention and Management

Bronchopulmonary dysplasia is a multisystem disorder that affects not only the lungs and is likely to remain a lifelong condition although decreasing in severity with growth. The BPD prevention address a variety of aspects including both ventilation strategies, saturation target and medical therapy. The use of non-invasive ventilation techniques has been proved to reduce the risk of BPD.

Less invasive surfactant administration is usually preferred to mechanical ventilation and early nasal CPAP is a recommended alternative to routine intubation. Nowadays, most guidelines suggest that a reasonable and safe saturation target is between 90 and 94%, although there is still a high level of uncertainty on the ideal saturation point.

In the population with established BPD, the management of the disease is focus on providing an adequate support facilitating an effective ventilation to promote lung maturation while avoiding further lung damage. When non-invasive respiratory support modalities fail, mechanical ventilation through endotracheal tube needs to be considered. A study reported by the BPD Collaborative group states that 28% of infants with sever BPD were on invasive MV at a mean PMA of 47 weeks. [15]

Supplemental oxygen is the most commonly used therapy since it helps to promote growth of the immature lung when an oxygen saturation above 90% is maintained.

Infants with respiratory distress syndrome exposed to higher level of given oxygen to reach higher levels of saturation have been found to have more persistent lung disease.

Considering that the initial respiratory course of many sick infants is mild, they are firstly managed with nasal CPAP that is replaced by invasive mechanical ventilation in case of poor respiratory effort. Besides, these patients initially require no or very little supplemental oxygen. However, during the first weeks after birth the pathological condition of many ELBW infants gradually gets wore, requiring both increasing inspired oxygen concentrations and respiratory support. The transition between the early respiratory status to either recovery or the development of BPD is often prolonged and extremely variable.

The use of positive-pressure ventilation (CPAP) is one of the factors closely related with the pathogenesis of BPD. For this reason, it is essential to use the minimal setting necessary to maintain gas exchange. Currently, a great interest is given to the developing of tailored ventilation strategies based on the lung physiopathology of each infant to obtain the most performing therapy. These strategies have to reflect the lung mechanics characteristic of a BPD situation, that means, obstructed airways, high resistance, low lung compliance and reduced FRC. Consequently, chronic respiratory support strategies require higher tidal volume than those used with early lung protective strategies during the acute phases of the disease. The variability of resistance and compliance over time make preferable the use of volume-targeted or pressure-regulated and volume-controlled ventilation to ensure delivery of adequate tidal volume with the least pressure. To ensure gas exchange and the emptying of slower compartments in infants with heterogenous lung disease and maldistributed ventilation, it is suggested to use a low rate and a long inspiratory time strategy. In contrast, if the lung disease is uniform and homogenous with a generalized alveolar simplification, respiratory insufficiency is due to a decrease in the alveolar surface are and it is better to operate with faster rate and shorter inspiration time.

To achieve an optimal lung volume, the level of PEEP has to be established individually for each patient and changed as the disease progresses. The appropriate level of PEEP, that increases FRC, reduces work of breathing and improves perfusion, must be determined looking at the mechanical characteristics of the lung to obtain the best compliance and the lowest resistance.

High Frequency Oscillatory Ventilation (HFOV) is not recommended in infants with established BPD because of its active exaltation and relatively high I:E ratio that may cause further air trapping and exacerbate respiratory failure. In a pilot trial, conducted by Plavka et al., High Frequency Jet Ventilation (HFJV) used with optimal lung volume strategy turned out to improve gas exchange and facilitate weaning from mechanical ventilation in extremely immature infants with evolving chronic lung disease. [16]

## 1.3.4 Definition

As stated before, bronchopulmonary dysplasia is the most common lung morbidity diagnosed among premature infants, however, definition and classification of this pathology are still difficult tasks and most prediction models for BPD have limited utility for clinical use. The pathophysiology of BPD is complex and may differ substantially between infants with different intrauterine and postnatal history.

Northway and colleagues described BPD in 1967 as a ventilation and oxygen related lung injury in relatively mature preterm infants. [12]

Subsequent research has shown that the majority of infants who developed BPD were always more immature whose lung can be acutely injured by either oxygen or mechanical ventilation resulting in inhibition of alveolar and vascular development

In 1979, Tooley suggested that oxygen use at 28 days of age might better identify preterm infants with BPD. [17]

With increasing survival of more immature infants, in 1988, Shannon and colleagues proposed that the best predictor of abnormal pulmonary outcomes for very low birth weight premature infants was the clinical use of oxygen at 36 weeks postmenstrual age (PMA). [18]

After clinical variation in oxygen administration, a workshop was supported by the National Institute of Child Health and Human Development (NICHD) together with the (NHLBI) and the Office of Rare Diseases (ORD) to review the definition of BPD and to identify the best indicators of clinical outcomes in infants with BPD. Jobe and colleagues proposed the current definition of BPD as the requirement of supplemental oxygen for at least 28 days after birth. Furthermore, this study introduces a severity-based diagnostic criteria for BPD based on the assessment of respiratory support at 36 weeks PMA. [19]

In an attempt to find a better definition, Ehrenkranz analysing the NICHD Neonatal Network data base for all infants with birth weights under 1 kg and GA under 32 weeks, found out that oxygen administration for the first 28 days after birth and at 36 weeks PMA resulted in the highest sensitivity, specificity and percent of infants correctly classified with respect to predicted oxygen need at discharge.[20]

Nowadays, BPD is mainly common in very low birth weight infants who initially have minimal or no lung disease but develop increasing oxygen and ventilatory needs over the first weeks of life.

*Table 1-2: Definition and severity grades of BPD*

| *Gestational Age* | *< 32 weeks* | *> 32 weeks* |
|---|---|---|
| *Time point of assessment* | 36 wk PMA or discharge to home | > 28 days but < 56 days postnatal age or discharge to home |
| | Treatment with oxygen (FIO2 > 21%) for at least 28 days + | |
| *Mild BPD* | Room air at 36 wk PMA or discharge | Room air by 56 days postnatal age or discharge |
| *Moderate BPD* | FIO2 ≤ 30% at 36 wk PMA or discharge | FIO2 ≤ 30% at 56 days postnatal age or discharge |
| *Severe BPD* | FIO2 ≥ 30% with or without positive pressure (NCPAP) at 36 wk PMA or discharge | FIO2 ≥ 30% with or without and positive pressure (NCPAP) at 56 days postnatal age or discharge |

***Limits of current definition***

One of the main problem in describing BPD is the inadequacy of the current definitions for the inability of capturing the severity and the different clinical phenotypes of the disease itself.

Actual definitions take into account the patients oxygen requirement and the respiratory support at a specific time point only without defining the disease by its pathophysiology.

Evolution in management practices related to respiratory support, such as use of high-flow nasal cannula, limits the application of existing definitions and may result in misclassification. As a result, the definitions reported above may not accurately capture the current pulmonary pathology of BPD. Indeed, recent changes in the variable use of non-invasive respiratory support with nasal catheters with high flow rate across a range of FIO2 around 0.21 or very low flow rate with high oxygen concentration may compromise the categorization of BPD.

Existing definitions of bronchopulmonary dysplasia fail to adequately classify infants. The NICHD/NHLBI workshop definition, that is the one considered in the following study, is not fully accurate at present, as infants on high-flow nasal cannula cannot be classified and those on low flow with 100% FIO2 should arguably not be classified as severe BPD.

Moreover, these definitions have the limitation that rely on oxygen administration which may vary according to clinical practice among different medical centres. Oxygen level, indeed, is influenced by the medical centre and the specific pharmacological treatment that could reduce the oxygen need even if the disease is severe.

Furthermore, the current definitions of BPD have poor predictive value for longer-term pulmonary outcomes that can also be influenced by nutrition, viral infections, and environmental exposures.

Therefore, a contemporary definition of BPD that encompasses all current clinical practices and correlates with respiratory morbidity in childhood, providing reasonable prediction of later respiratory outcomes, is needed. The aim for a new definition of BPD is to develop a classification based on the pathophysiology and an objective lung function evaluation offering a more accurate assessment for individual patients. For this purpose, an exhaustive and deeper insight of this multifactorial disease that considers all different aspects is required.

From the respiratory point of view, the evaluation of respiratory mechanics together with other parameters, such as oxygen requirements or duration of ventilatory support, can give an objective evaluation of the disease starting from the initial phase of the pathology. Other essential factors that can be investigated are the cardiocirculatory function and the nutritional program of these infants. The echocardiography is indeed a non-invasive method that can characterize the vascular aspect of BPD.

The following research fits in this context with the purpose to enhance the current understanding of BPD leading to the introduction of optimal clinical strategies that can improve the outcomes in this subgroup of sick infants. Specifically, it tries to identify physiological parameters that influence the development and severity of BPD and can be obtained by means of non-invasive techniques.

### 1.3.5 Predictive Models

The development, implementation and validation of prognostic models have a key role in helping clinicians with the objective estimation of the probability of a disease course. These models can be useful for a better understanding and diagnosis of BPD.

In neonatology, several studies have developed clinical predictive models using logistic regression to predict which preterm infants are more likely to contract BPD. The most challenging part of this process is to determine risk factors in a heterogenous population of patients, extracting them from various clinical and respiratory parameters at different postnatal ages. The aim of these models is to predict BPD outcomes by using universally accessible clinical information collected from the first day of life, such as birth weight, gestational age, administered oxygen amount and applied inspiratory positive pressure.

The main problem about these studies is that BPD risk factors have been investigated retrospectively by examining the conditions that have led to a specific diagnosis conditioning the outcome of the prediction.

In conclusion, the use of estimators and models to early identify infants at greatest risk of affecting chronic lung disease may allow a targeted approach to reduce long-term consequences of BPD.

# 1.4 Assessing Lung Function in Preterm New-borns

The availableness of physiologic parameters at bedside, such as lung volumes, respiratory mechanics, work of breathing and their variability over time, has a key role in evaluating lung function and, then, in optimizing the management of critical clinical situation to minimize ventilator-associated lung injury. The increasing importance given to respiratory mechanical parameters to assess the severity of a disease and the structures involved in the respiratory impairment has led to the development of different measurement techniques for clinical and resource purposes. Different measurements can be combined in order to have a better understanding of the respiratory condition and a continuous follow-up of different parameters is useful to assess both the effect of therapeutic interventions and the readiness to wean off respiratory support.

## 1.4.1 Lung Volumes

Tidal volume is a fundamental parameter that we can easily obtain by means of a flowmeter, that measures the mouth flow and allows to obtain lung volume changes by mathematical integration. Breathing frequency, tidal volume and inspiratory/expiratory time can be computed from the volume track. In case of non-invasive ventilation this measure can be affected by air leak from the face mask. Breath by breath changes in end-expiratory lung volume can be used to monitor the alveoli recruitment phenomenon.

The evolution of volume in time can also be obtained by with two other techniques: the respiratory inductive plethysmography (RIP) and the opto-electronic plethysmography (OEP).

RIP uses two compliant belts displaced around the rib cage and the abdomen to measure the local cross-sectional area. The calibrated sum of the changes in these two sections yields an estimation of the volume changes in the thoracic cavity.

OEP is based on the high accuracy and high temporal resolution 3D localization of retroreflective passive markers positioned on the infant thoraco-abdominal wall. Starting from the position of these markers the chest wall surface is reconstructed and the chest wall volume is computed using the Gauss' theorem. These two techniques provide also a measure of the degree of thoraco-abdominal asynchrony during ventilation to evaluate the maturation and efficiency of this process.

The assessment of absolute lung volume, however, is necessary as the correct lung ventilation and gas exchange relays on the establishment of an adequate lung volume and its maintain during the respiratory cycle. FRC measures can be provided by the gas dilution (washout) technique. This technique consists in recording the wash-in and washout of a specific gas during tidal breathing and calculating the FRC knowing the volume and the initial and final concertation of the indicator gas.

When the stress and strain are not homogenously distributed in the lung, because of an obstructed or collapsed area, the measure of the lung volumes is not enough to avoid mechanical ruptures caused by greater tension and distortion development in some regions.

## 1.4.2 Breathing Variability

New-borns and premature infants are prone to develop unstable respiratory patterns characterized by periods of insufficient breathing or apnoea, suggesting important developmental differences in control of breathing during early postnatal life. [21]

It's known that the respiratory rhythm is generated in the central nervous system by a group of respiratory neurons that form a neural oscillator and drive the respiratory muscles.

Respiratory system involves many non-linear feedback mechanisms and a network of subsystems that interact with each other to drive this respiratory generator within different time scale and gain. The immaturity of these brain stem rhythm generators and of the central and peripheral chemoreceptors may be the major cause of apnoea in infants. Indeed, the increased incidence of significant apnoea in preterm infants and infants with chronic lung disease suggests that control of breathing is affected by both maturation and disease. [22]

In the studies on physiological control systems, increasingly attention has been given to the mechanisms that determine how these systems regulate their output in order to maintain a stable homeostatic internal environment. External fluctuations acting on the feedback loops within the control system often result in significant variabilities of the output.

Although the relationship between the maturation of respiratory-related central and peripheral neural network and breathing pattern is difficult to interpret, the analysis of the fluctuations in physiological control parameters provides an evaluation of the overall properties of the complex respiratory system.

Moreover, variability in the respiratory system has been found to have an important role in the cell activity as it affects surfactant secretion, be related to the maturation of the breathing control in infants and be modified by RDS and assisted ventilation in new-borns.

Specifically, the analysis of fluctuations in respiratory pattern properties can be used to gain insight into neuro-respiratory regulation and complex chronic disease and give rise to a specific temporal clinical phenotype. Indeed, measures of variability can be exploit in the management of preterm infants to evaluate if the natural variability is maintained during mechanical ventilation and it might be useful to identify a ventilation strategy that preserve the natural values of variability and promote the development of the control of breathing and a successful weaning.

Both lower and excessive variability have been associated with pathological conditions that results respectively in reduced adaptability of the system or loss of control. [23]

The variability analysis is based on quantifying the short- and long- term temporal history of tidal breathing and other lung function parameters to monitor the temporal behaviour of the disease, assess its severity and evaluate the impact of external treatments. For this analysis, time series obtained from different respiratory signals can be considered. The tidal-flow waveform contains information about breathing regulation as well as mechanical properties of the thoraco-pulmonary system. However, the fact that the complex dynamics of breathing in infants is usually arbitrary and instantaneous in changing rather than being based on an understanding of respiratory brain stem function, makes it hard to identify a physiologically justifiable parameter to describe the control of breathing in new-borns for clinical purposes.

For instance, the time interval between breaths (IBI) has been found to be an important measure presenting both stochastic and deterministic dynamic characteristics that can be used to analysed irregular breathing pattern in neonates. Moreover, the study of the correlation between variations in different parameters may provide additional information. Not only different parameters but also different time scale can be considered depending on the phenomena of interest.

Bravi et al. [24] reported an overview of different variability analysis techniques that have been proposed to describe the time series under study in the attempt to untangle the information hidden within biological signal variability. However, to date just some of them have been applied to the study of the breathing pattern of new-borns. The most common are the statistical techniques that allow to describe the stochastic properties of data and to determine the statistical self-affinity of respiratory signals. In the informational domain, entropy measurements have been applied to the study of changes in irregularity of tidal volume and respiratory rate with age and size among preterm infants. Recently, new technique in the invariant domain have been introduced as in several studies the fetal irregular breathing pattern appeared similar to a fractal process [25]. While the breathing pattern of healthy term infants is fractal, the one of preterm infants presents lower memory that tend to increase with postnatal age. Indeed, certain disease states may be accompanied by alteration in the scale-invariant correlation property allowing to detect respiratory pathologies.

Between these techniques the Detrended fluctuation analysis (DFA) has the advantages of non-requiring the stationarity of the data and distinguishing between intrinsic fluctuation generated by a complex system and those caused by external stimuli acting on the system (see chapter 2.2.3).

### 1.4.3 Pulmonary Mechanics

Monitoring the changes in the mechanical properties of the respiratory system allows to identify structural modifications that reflect different pathologies, providing further insights of the disease and a guidance in the choice of therapy. Different techniques have been developed to estimate resistance and compliance.

The mechanical properties of the lung can be described through simultaneous measurement of lung volume and trans pulmonary pressure. To compute the trans pulmonary pressure, the measurement of the pleural pressure is required, considering that it can be estimated by the esophageal pressure obtained by means of esophageal manometry. The changes in flow, volume and pressure are analysed throughout the entire respiratory cycle using the multiple linear regression (MLR), aiming to the calculation of different mechanical parameters according to a specific linear model.

Other techniques, such as single and multiple occlusion technique can be performed at the end of a tidal expiration to compute resistance and compliance through the analysis of other parameters that can be extracted from different graphs, such as the volume-flow loop and the PV curve, obtained plotting the volume above FRC remaining in the lung at the time of the occlusion against the corresponding pressure. However, these techniques are not reliable on infants, as they are based on the hypothesis that the EELV is stable. A great importance has also been given to the Forced Oscillation technique (FOT), during which a sinusoidal pressure stimulus is applied at the airway opening and the response of the system in terms of flow and chest wall motion is measured. This technique is easier to use in new-borns with respiratory diseases.

### 1.4.4 Work of Breathing

The work of breathing in infants is the energy expended to inhale and exhale gas flowing against pressure. It can be subdivided into elastic and resistive work. The elastic work, stored as potential energy, is required to overcome the lung elastic recoil and the alveolar surface tension and to move the chest wall. The resistive work is required to overcome frictional forces between tissues and gas molecules due to viscosity. The work of breathing can increase because of a decrease in the compliance or an increase in the airways resistance.

The WOB in infants is three times that of an adult, even if the weight-corrected WOB is the same, and in pathological conditions it can be difficult for a new-born to sustain. Thus, monitoring its values may be advantageous for the clinician to better adjust the ventilator settings or to choose the appropriate treatment that optimizes respiratory muscles loading and decreases the effort.

However, the use of work of breathing to affect direct patient care during mechanical ventilation has been limited by the invasive nature of these measurements, which require the estimation of $P_{pl}$ changes by esophageal pressure.

Moreover, the work of breathing is influenced by the respiratory and flow rate and it can be minimised by optimising some determinants. The elastic work decreases with increased respiratory rate, while respiratory work decreases with decreased respiratory rate. The respiratory rate at which the optimal work of breathing occurs depends on the size and weight of the subject.

# Chapter 2 Experimental Set-Up and Data Analysis

This study aims to provide methods for evaluating the relative contribution of different factors to the respiratory impairment experienced by preterm infants with BPD, that can be applied to obtain a better definition of BPD and a classification of its severity according to the relevance of these components.

Lung and chest wall compliances have been measured as their values and ratio can distinguish between healthy and sick infants providing important guidance for clinicians for follow-up. The assessment of these compliances and their role in evolving BPD can result in a better definition of the respiratory disease and, thus, in more successful clinical outcomes. To understand and differentially diagnose the most common respiratory chronic disease in preterm infants, also the work of breathing has an important role being a measure of the labour exerted by the infant to get enough oxygen to survive. Finally, the breathing variability has been study to understand if and how BPD affects the functioning of the neurological control system of respiration.

In this chapter, the developed methods and techniques for characterizing the functional alterations of the respiratory system in infants with bronchopulmonary dysplasia are described.

Specifically, we aimed to measure:

1. The breathing pattern and its variability that provides indirect information about the development of the control of breathing;
2. The mechanical properties of both lung and chest wall and the work of breathing to obtain information about the impairment of the respiratory system.

The measuring system should meet specific requirements due to the purpose of studying at bedside preterm infants that are admitted in the neonatal intensive care unit, namely it must be composed by certified devices and suitable to be exploited in that unit. The developed methods must:

- be easy to be used by clinicians;
- avoid any interference with clinical practice and instrumentation already present in NICU;
- minimize the interaction with the user;
- minimize the time duration of the measurement;
- display the essential parameters;
- ensure adequate accuracy of the measurements in several conditions of application.

In order to assess breathing pattern properties among which its variability and the long-term correlation of its main parameters, the changes in volume over time have been acquired using Respiratory Inductive Plethysmography (RIP), which is a tool used in NICU for non-invasive measurement of pulmonary function testing. RIP obtains tidal breathing measurements via thoraco-abdominal motion analysis performed on volume signals collected at the chest wall and abdomen.

The analysis of thoracoabdominal motion determined with RIP allows to examine also the chest wall and abdominal asynchrony and apply the DFA to compute indexes of variability and gain information on the control system.

Moreover, the estimation of lung mechanics and work of breathing requires the measurement of the pressure involved in ventilation, namely $P_{ao}$ and $P_{es}$, simultaneously to the recording of lung volume trace, together with the definition of the chest wall relaxation curve.

The sensors and the protocol employed in this study are described in the following chapter.

# 2.1 Measurement System

## 2.1.1 Hardware

Among different techniques used in literature to evaluate respiratory function (see section 1.4), respiratory inductive plethysmography (RIP) has been chosen in this study to monitor tidal volume and detect changes in end-expiratory lung volume over time because of its non-invasiveness and the possibility of deriving several parameters of breathing pattern and variability. In particular, Detrended fluctuation analysis (DFA) has been selected as the best method to investigate the mechanisms of breathing control because of the advantage to be performed on different signals related to the respiratory system that can be measured non-invasively. The determination of pulmonary and chest wall compliances along with work of breathing requires also reliable measurements of pleural pressure changes simultaneously with tidal flow and volume. in order to measure these mechanical properties and identify the relative contribution of lung and chest wall, measurements of pleural pressure have been obtained through an esophageal catheter, inserted into the oesophagus to measure the pressure swings.

A schematic representation of the set-up used to assess the different parameters of interest is shown in Figure 2.1.

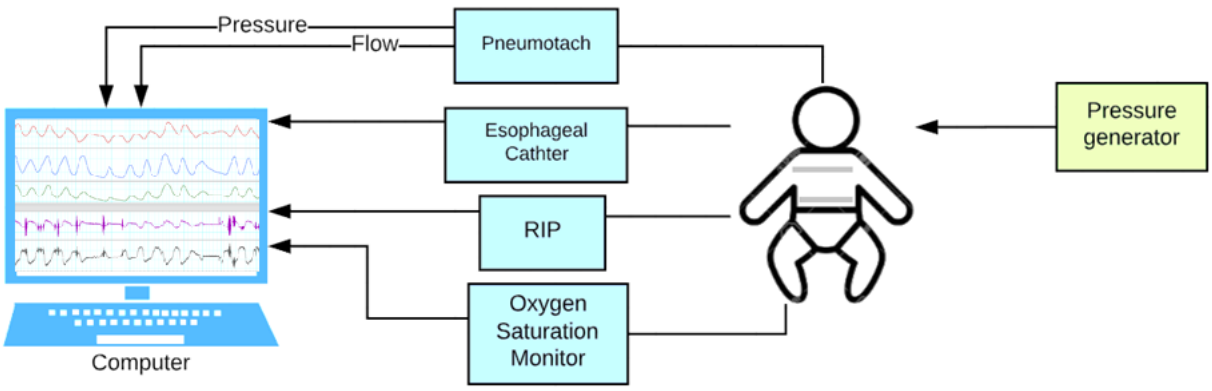


*Figure 2.1: Clinical set-up diagram*

The instrumental setting includes:

- The respiratory inductive plethysmography device composed by the disposable paediatric *NOX RIP belts* (NOX-RIPDP20-0111) attached to *Respitrace 200* (Nims, North Bay Village, FL, USA) sampling the signals at 200Hz;

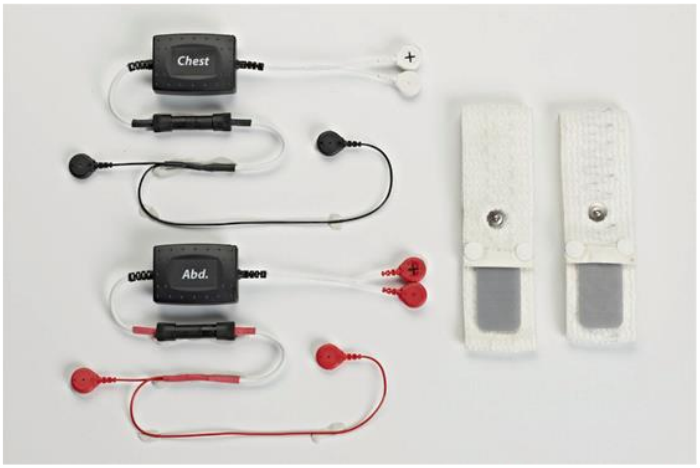


*Figure 2.2: RIP bands and connecting cables*

- The *ultrasonic flowmeter* (Eco Medics AG, Duernton, Switzerland) to measure functional residual capacity;
- The esophageal *Millar Microtip Catheter* (Millar Instruments Inc., Houston, TX, USA) connected to the *Millar Pressure Control Unit* (PCU 2000);


*Figure 2.3: Millar Microtip catheter and control unit*

- A purpose built *pneumotachograph (PNT)* (University of Szeged, Hungary) connected to a differential pressure transducer to measure airways opening flow and pressure;
- The *Neopuff Infant T-piece Resuscitator* (Fisher & Paykel Healthcare, Auckland, NZ) as CPAP device to generate the desired pressure to apply at the infant's airways opening;

*Figure 2.4: Neopuff CPAP device*

- The *SpO2 and HR monitor MasimoSET Radical-7* to constantly check patient conditions;
- The *interface with infant*: the commercial silicon masks readily available in NICU and usually employed for CPAP treatments.

*Figure 2.5: CPAP nasal mask used in the following study*

- A *computer* that permits to import flow, pressure and volume data and show them through a graphical interface in *LabChart*.

All the data acquired through these devices are recorded and converted with a high-performance data acquisition hardware *PowerLab 16/35* (ADInstruments).

From a clinical practice perspective and a real-time understanding of the infant severity situation, the algorithm developed should be integrated in the devices already present in NICU to avoid data exportation for analysis and implement online elaboration. However, to conduct this clinical study, the meddling in the instrumentation already in use have been minimised exploiting the acquisition of accurate pressure and flow data to be analysed offline.

#### 2.1.1.1 Respiratory Inductive Pletysmography

Respiratory Inductive Plethysmography (RIP) is a non-invasive method of evaluating changes in lung volume that can be easily used as a bedside tool in intensive care unit for both ventilated and spontaneously breathing patients. As it is leaks independent, it can accurately measure end-expiratory lung volume and tidal volume. RIP determines changes in lung volume by measuring the changes due to both chest and abdominal volume displacement through two elastic bands places around the rib cage at the nipple line and around the abdomen at the umbilicus line, respectively.

A sinusoidal wire embedded in an elastic self-adherent material is present in each band to measure changes in the cross-sectional area that are the result of volume changes. [26]

The stretch of the bands produces a variation in the electrical self-inductance within the wire causing a variation in the frequency of the sinewave generated by the oscillator connected to the transducers. This frequency change is converted in an analogue voltage waveform.

The signals from the bands are digitized at a sampling rate of 200Hz and stored on computer for visualization and analysis.

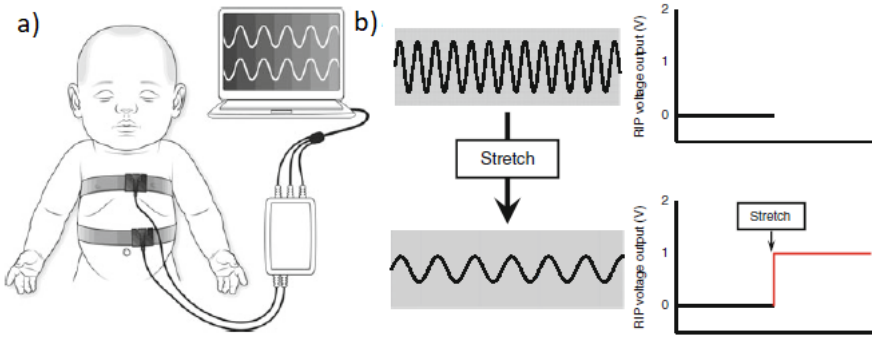


*Figure 2.6: a) RIP equipment b) Relationship between RIP voltage output and stretch of the sinusoidal wire*

### 2.1.1.2 Esophageal Manometry

Measurements of driving pressure are required for calculation of pulmonary mechanics and work of breathing. In spontaneously breathing infants, this driving pressure is the difference between pressure at the airway opening $P_{ao}$ and that in the pleural space $P_{pl}$, in other words the transpulmonary pressure:

$$P_{tp} = P_{ao} - P_{pl} \tag{16}$$

Whereas $P_{ao}$ is usually readily accessible, $P_{pl}$ is not. In animals, $P_{pl}$ can be measured directly using invasive techniques. For clinical and research purposes, instead, changes in $P_{pl}$ may be estimated from esophageal pressure $P_{es}$ because the body of the esophagus is a flaccid passive structure able to transmit pressure from the adjacent pleural space.

The most common techniques to measure esophageal pressure in infants are the esophageal balloon manometry, the use of a liquid- or air- filled catheter ad the use of small transducers placed in the esophagus. In this study, a double-tip catheter pressure transducer has been used thanks to the fact that its measurements of $P_{es}$ have been proved to accurately reflect the changes in pleural pressure and be independent on the position of the tip and the chest wall distortion.[27]

## 2.1.2 Software

Infant multiple breath washout (MBW) testing serves as a primary outcome in clinical study to evaluate the functional residual capacity. In this study, MBW measurements have been performed with an ultrasonic flowmeter and elaborated through the *WBreath* software (V3.19.6.0. Ndd Medizintechnik, Zurich, Switzerland).

To obtain accurate outcomes in the computation of the respiratory parameters under investigation, it is important that flow, pressure and volume signals are acquired correctly. An instantaneous feedback from the clinician is achieved through a Graphical User Interface built in *LabChart*, that allow to visualize, control and storage the data. *LabChart* is a data analysis software created by ADInstruments that provide a platform for many recording devices to work together, allowing to acquire biological signals from multiple sources simultaneously and apply advanced calculations during the unfolding of the experiment. This software displays the waveforms and enables to select portions of the traces to count the number of breaths occurred and determine the baseline and the maximum and minimum values reached by the signal of interest.

The signals acquired and visualized in the graphic *Labchart* interface are:

- *RIP_RC*: the volume acquired from the rib cage band;
- *RIP_AB*: the volume acquired from the abdomen band;
- *RIP_SUM*: the sum of the previous contributions to the volume;
- $Pga$: the gastric pressure measured with the catheter;
- $Pes$: the esophageal pressure measured with the catheter;
- $Pga - Pes$: the sum of the previous signals;
- $SpO2$: the haemoglobin oxygen saturation;
- $O2$: the concentration of oxygen in the blood;
- $Co2$: the concentration of carbon dioxide in the blood;
- *Pressure*: the pressure at the airway opening;
- *Flow*: the flow of gas at the airway opening.

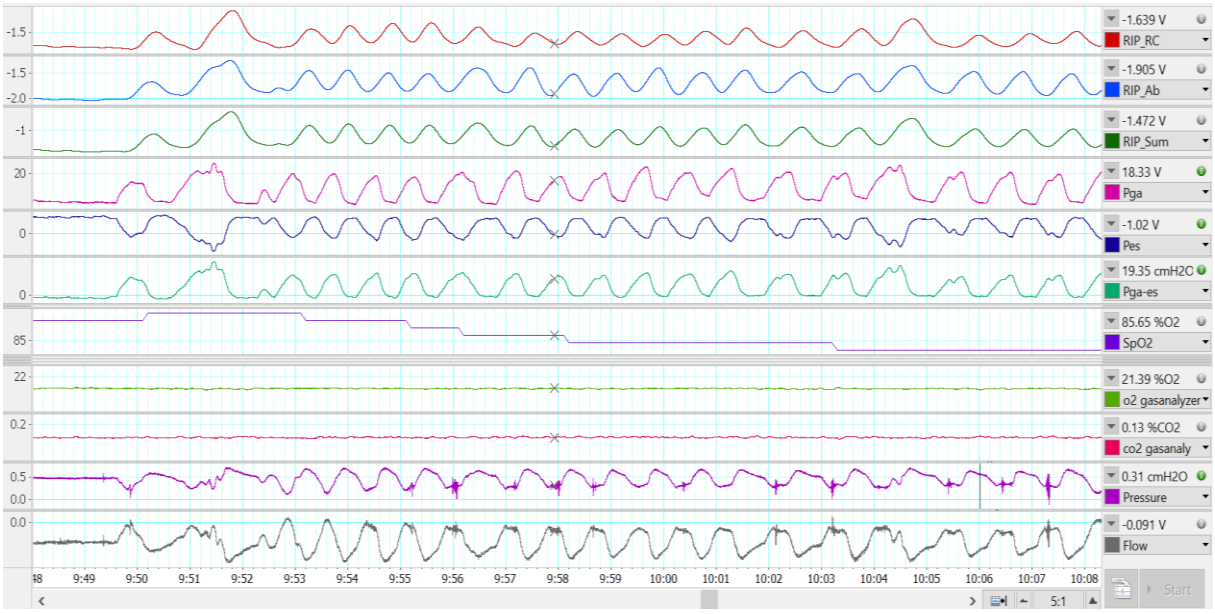


*Figure 2.7: Graphic Interface in Labchart*

## 2.2 Data analysis and parameters calculation

The computation of the respiratory parameters selected to comprehend BPD, classify the patient population and customize the treatments requires a preliminary calibration and processing of the acquired signals from which they are extracted. The elaboration of the original data supplied by the above described devices has been conducted in *MATLAB*, a multi-paradigm numerical computing environment and proprietary programming language developed by Mathworks.

Particularly, for this study a specific step-by-step procedure has been conducted for each infant, that has been fed just before the measurements. Respiratory inductive plethysmography bands are fitted around the chest and abdomen. The esophageal catheter is positioned in the lower oesophagus for the estimation of the pleural pressure. Air leaks are constantly detected through the graphic interface and the infant's mouth is gently kept close if necessary. Heart rate and oxygen saturation are continuously monitored on the bedside monitor. Fraction of inspired oxygen (FiO2) is recorded at the start of the study and is adjusted when necessary to maintain oxygen saturation between 90% and 96%. Esophageal pressure, flow and volume data are used to obtain breathing pattern, lung and chest wall mechanics and energetics parameters as well as to calibrate the RIP.

### 2.2.1 Volume Calibration

The change in total thoracic volume can be determined from the combination of the volume displacement in each separate compartment and is a reliable measure of the lung volume.

Therefore, it is assumed that the tidal volume ($V_T$) can be estimated as the weighted sum of the rib cage (RC) and abdominal (AB) inductance signals:

$$V_T = \alpha RC + \beta AB \tag{17}$$

Where $\alpha$ and $\beta$ are the proportionality coefficients between RC and AB amplifiers.

Various calibration methods have been experimented to estimate these coefficients. The most common are the qualitative diagnostic calibration (QDC) algorithm [28] and the least mean squares technique [26]. QDC is based on equations of the isovolume maneuverer calibration (ISOCAL) and is carried out during a 5-minute series of breaths at the start of the RIP recording. However, in this study it has been decided to perform an offline LMS calibration of the RIP digitized signals. This technique is based on the mathematical relation between flow and volume that permits to obtain a volume signal through the electronic integration of a flow signal with respect to time. The reference respiratory flow has been simultaneously recorded by pneumotachograph (PNT) with the flowmeter and a differential transducer attached to the face mask during a brief period of spontaneous breathing. The pneumotachograph was calibrated with consecutive injections of 20 ml air by means of an appropriate syringe. A series of 30 leak-free and regular breaths has been manually selected for the integration of the air flow to calculate the tidal volume. These breaths have been then matched with the corresponding RIP breaths to calibrate the latter. Indeed, Simultaneous PNT and RIP signals have been analysed trough a specific algorithm implemented in MATLAB. A least squares method based on the tidal volume has been used over the 30-cycle reference period to estimate $\alpha$ and $\beta$ coefficients, allowing to obtain a RIP volume signal $V_{RIP}$ by combination of RC and AB signals in comparison to the integrated recorded flow signal $V_{PNT}$:

$$V_{RIP} = \beta(\alpha RC + AB) \tag{18}$$

The calibration algorithm computes the optimal coefficients that minimize an error defined as the difference between the tidal volume calculated from $V_{PNT}$ signal and the one from $V_{RIP}$:

$$err = \overline{(V_{T_{RIP}} - V_{T_{PNT}})^2} \tag{19}$$

The accuracy of the RIP bands is dependent on a reliable calibration of the contribution of each band to the summed signal. The reliability of the calibration is best when measurements are immediately preceded by calibration and tend to deteriorate with time. RIP calibration accuracy decreases significantly with the severity of lung disease and after body movements. Indeed, calibration and signal stability are better maintained if the patient position doesn't change and the band location remains constant.

## 2.2.2 Breathing Pattern and Thoraco-Abdominal Asynchrony

Apart from a direct measure of the tidal volume, RIP allows the potential to assess the respiratory effort and pattern over time, leading to the computation of mechanical properties, work of breathing and thoraco-abdominal asynchrony in the studied infants.

During normal tidal breathing, indeed, diaphragm contraction leads inspiration followed quickly by chest wall muscle activity and in healthy conditions the RC and AB cross-sectional areas increase and decrease in synchrony. However, in presence of a respiratory disease, an excessive negative intrapleural pressure is required generating excessive AB excursions to compensate for the inward motion of RC during inspiration. This result in paradoxical or asynchronous motion between the RC and AB compartments, characterized by a lag of AB motion behind RC. As pathology develops, there is an increasing amount of thoracoabdominal asynchrony (TAA), resulting from worsening respiratory muscle fatigue. The degree of asynchrony significantly relates to pulmonary resistance and weighted-corrected compliance and is a useful approach in assessing the severity of the respiratory problem.

RIP can determine the level of synchrony between the two bands evaluating the phase shift between the rib cage and abdominal tidal signals, that can be quantified by the phase angle expressed as:

$$sin\theta = m/s \tag{20}$$

Where *m* is the length of the midpoint of the RC excursion and *s* is the maximal AB excursion.

During normal breathing, this phase angle is less than 20°, increasing as TAA worsens.

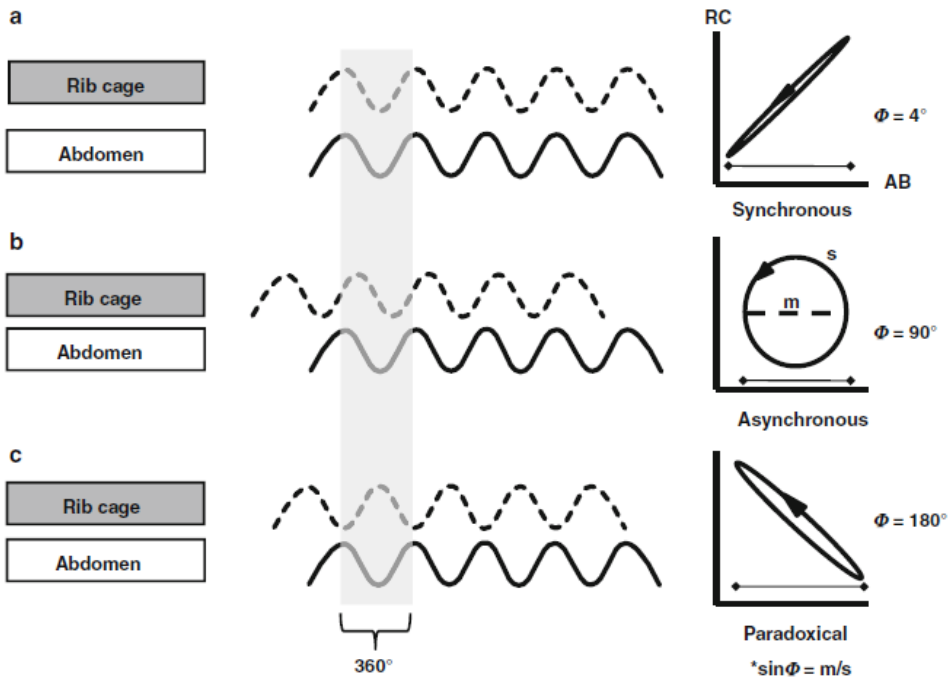


*Figure 2.8: RIP waveform and phase angle measurement from RC-AB curve to illustrate synchronous (a), asynchronous (b) and paradoxical (c) pattern of thoraco-abdominal motion.*

In addition to theta, other coordination indices have been computed. The inspiratory and expiratory time and the respiratory rate (RR) have been obtained multiplying the sampling frequency (200 Hz) by the numbers of samples composing each breath. The duty cycle has also been expressed as the percentage of the time involved in inspiration in each breath. The RC and AB inspiratory and expiratory asynchrony indices (IAI and EAI respectively), representing the percent time paradoxical to $V_T$, are a series of indices that quantify the extent to which the RC or AB compartments are paradoxical to $V_T$ during inspiration and expiration. Computations of these indices are done by comparing the algebraical signs of the derivative of either RC or AB and the calibrated sum signal. Specifically, they are calculated by a pairwise comparison of the slopes of the RC, AB and CW volume signal for each breath. The accumulated value of time spent in paradoxical motion is then divided by the inspiratory total time of breath and expressed as a percentage. Paradoxic motion as a percentage of the time of inspiratory and expiratory compartmental excursions for each breath is indicated when RC or AB compartments move in an opposite direction and detected by a negative product between the slopes. Then, IAI and EAI are defined as the fractions of inspiratory or expiratory time during which the abdomen and the rib cage move in opposite directions. We have also computed for each infant, the percentage contribution of the rib cage (%RC) and the abdomen (%AB) to the chest wall $V_T$ .

The last index that has been considered during thus study is the Labored Breathing Index (LBI), based on the efficiency ratio computed as amount of power at the source (RC+AB) divided by the amount delivered (SUM). It is defined as the sum of the integrals of absolute values of the derivatives of rip cage and abdominal volume signals divided by the integral of the derivative of the sum signal over the duration of inspiration. When RC and AB signals are in phase, the ratio is equal to one, when they are out of phase with each other the ratio exceeds unity. Thus, LBI increases with thoraco-abdominal asynchrony and work of breathing.

## 2.2.3 Detrended Fluctuation Analysis

In this study, we quantified the variability and the long-range correlation properties of resting breathing pattern and lung volumes using the Detrended fluctuation analysis (DFA), a technique which can detect intrinsic correlation properties embedded in non-stationary time series. Since many physiological variables associated with breathing exhibit significant breath-to-breath variability, we decided to analyse three of them: the tidal volume $V_T$, the inter-breath interval (IBI) and the end-expiratory volume (EELV) time series.

First, from the trace of $V_{CW}$ acquired with the RIP, all the end-expiratory and end-inspiratory points have been identified to compute all the breathing pattern parameters for each breath and to build

a time series for each of these parameters. Then, these time series have been analysed by the DFA as suggested by Peng et al. [29]

Each time series containing N data point is first integrated:

$$y(k) = \sum_{i=1}^{k} (x(i) - \bar{x}) \tag{21}$$

Where $x(i)$ is the i-th value of time series and $\bar{x}$ is the corresponding average of the time series. Next the integrated time series $y(k)$ is divided into non-overlapping windows of equal length (n). In each window, a linear regression line $y_n(k)$ is fit to the data point, representing the local trend in that box. The integrated time series is then Detrended by subtracting the local trend, $y_n(k)$, from the data in each window. The root-mean square fluctuation of this integrated and Detrended time series is computed as follows:

$$F(n) = \sqrt{\frac{1}{N} \sum_{k=1}^{N} (y(k) - y_n(k))^2} \tag{22}$$

This computation is repeated over all time scales, that means for different n, and plotted as a function of n on a log-log plot, to provide a relationship between $F(n)$ and the window size.

A linear increase of $F(n)$ indicates the presence of scaling and the fluctuation is said to follow a power-law functional form:

$$F(n) = An^{\alpha} \tag{23}$$

Where $\alpha$ is the scaling exponent corresponding to the slope of the line relating $F(n)$ and n in the double-log graph and A is the amplitude of the power-law fluctuation function.

According to the value assumed by $\alpha$ different correlation properties can be established for each signal, carrying useful information on the functioning of the examined respiratory control system (section 1.1.2). For a random walk, that is an uncorrelated time series, $\alpha$ is equal to 0.5. For a positively correlated signal, $\alpha$ is between 0.5 and 1, indicating persistent long-range power-law correlations. In contrast, $\alpha$ between 0 and 0.5 is proper of anticorrelated signals, characterized by a power-law correlation such that large and small values of the time series are likely to alternate. If $F(n)$ follows a power law over at least an order of magnitude time scale with an $\alpha$ different from 0.5, the corresponding variable is said to exhibit long-range correlations or scale-invariant behaviour. For $\alpha > 1$, correlations exist but cease to be of a power-law form. For example, $\alpha$=1 corresponds to 1/f noise and $\alpha$=1.5 corresponds to Brownian noise.

### 2.2.4 Pressure Calibration

The calibration of the pressure catheter needs to be performed before each test by simultaneously exposing the transducers at a specific pressure difference and adjusting the amplifiers to obtain the correct output. The tip catheter transducer may be calibrated by immersion to different depths in a graduated column of water. To obtain a linear output over the range of experimented pressures, a 3 points calibration has to be performed. The accuracy of the esophageal manometry system can be tested through an occlusion test. This test can be conducted occluding the airways at their opening. Indeed, it assumes that, during airway occlusion, both alveolar volume change and gas flow in the airways are minimal, so that pressure changes should equilibrate throughout the respiratory system, causing tidal pressure swings in the airways to be almost equal to the pleural pressure ones. Results can be obtained, comparing $\Delta P_{es}$ with changes in pressure at the airway opening while the infant makes respiratory efforts against the obstruction. Although absolute $P_{pl}$ differs from alveolar pressure by static elastic recoil pressure of the lung, under conditions of no flow, $\Delta P_{pl}$ is transmitted to the alveoli and can be measured directly at the airway opening. Hence, the recorded $\Delta P_{es}$ should be of similar magnitude as $\Delta P_{ao}$ measured at the airway opening, indicating that pleural pressure changes are well transmitted to the esophagus. Factors influencing the $\Delta P_{es}/\Delta P_{ao}$ ratio during the occlusion test include patient position, catheter position and lung volumes. These factors should be checked continuously to ensure the best concordance between swings in the pressures. Cardiac contractions can also distort $P_{es}$ signal creating artefact. Esophageal contraction due to peristalsis is sometimes present but can be easily detected as a large increase in pressure that brings to discard the surrounding tract of the signal during data analysis, until the baseline is re-established. [30]

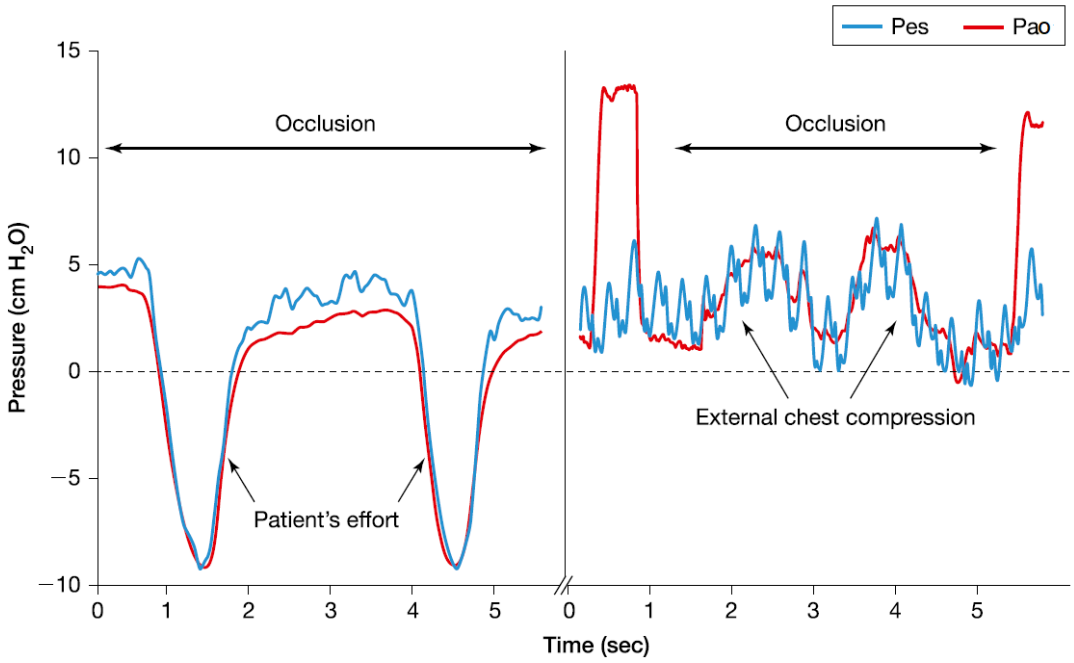


*Figure 2.9: Occlusion test in a spontaneously breathing patient (left) and in a paralyzed patient (right). Pao axis is shifted to obtain overlap of the two signals.*

Once that the catheter is inserted into the esophagus, it is advanced until the lower tip is in the stomach and it's positioning is checked looking at the positive pressure deflections with each inspiration that must be opposite to the negative deflections produced by the upper catheter in the esophagus. Once that the correct position is reached, it is fixed in place.

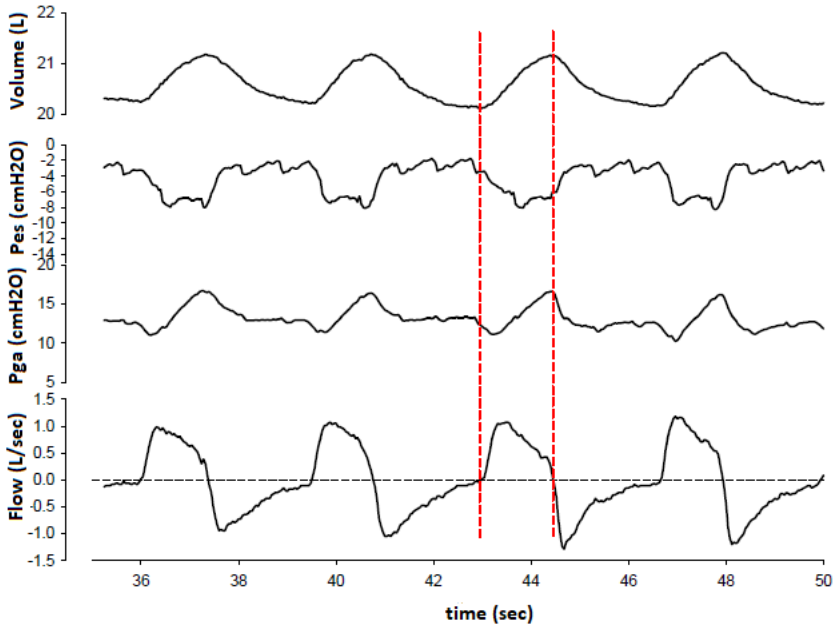


*Figure 2.10: Recorded section of spontaneous breathing pattern: Pga and Pes are out of phase indicating that the esophageal catheter is correctly positioned.*

## 2.2.5 Static Compliances Computation

The measurement of the passive properties of the respiratory system requires the relaxation of the respiratory muscles. This can be achieved applying a brief end-expiratory occlusion delaying expiration for a few hundred milliseconds and then making measurements during the following passive expiration. The airway occlusion technique for assessing passive respiratory mechanics are based on the ability to invoke Hering-Breuer inflation reflex (HBIR) that temporally inhibit respiratory drive.

To apply this occlusion the Neopuff is attached to the side of the PNT opposite to the face mask. Supplemental oxygen may be supplied through the CPAP device if the infant has an increased oxygen requirement. Different values of positive pressure are applied at the airway openings through the mask provided rapid equilibration that can be reached during period of no flow. The relaxation pressure at the airway opening $(P_{ao})$ represents alveolar pressure, which in turns represents the summed elastic recoil pressure of the lung and chest wall during periods of muscle relaxation. This pressure can be related to changes in volume in order to calculate the compliance of the respiratory system. In this study, apneas are performed several times at different points of expiration, relying on the multiple-breath occlusion technique (MOT). Specifically, the pressure values apply to reach apneas are:

- $P_{ao} = 5\ cmH2O$;
- $P_{ao} = 10\ cmH2O$;
- $P_{ao} = 15\ cmH2O$;

When the HBIR is invoked, respiratory muscles relax and $P_{ao}$ increases to a plateau. The time passed pressure trace will present a series of plateau that represent the elastic recoil pressure at the moment of the occlusion. At the same time, $P_{es}$ increases in parallel with $P_{ao}$. After occlusion release, $P_{ao}$ decrease to zero and $P_{es}$ falls in parallel with it. The corresponding volume above functional residual capacity remaining in the lung at the time of occlusion is simultaneously acquired by RIP, allowing to construct the P-V curve. The slope of this curve, computed by linear regression, correspond to the static compliances of the total respiratory system and the chest wall, depending on whether $P_{ao}$ or $P_{es}$, respectively, is plotted on the graph.

In this study, the static compliances of both the respiratory system and the chest wall have been computed considering only the slope passing through the points corresponding to the airway occlusion at 5 and 10 cmH2O, as it is the range of pressure normally maintained during spontaneous breathing.

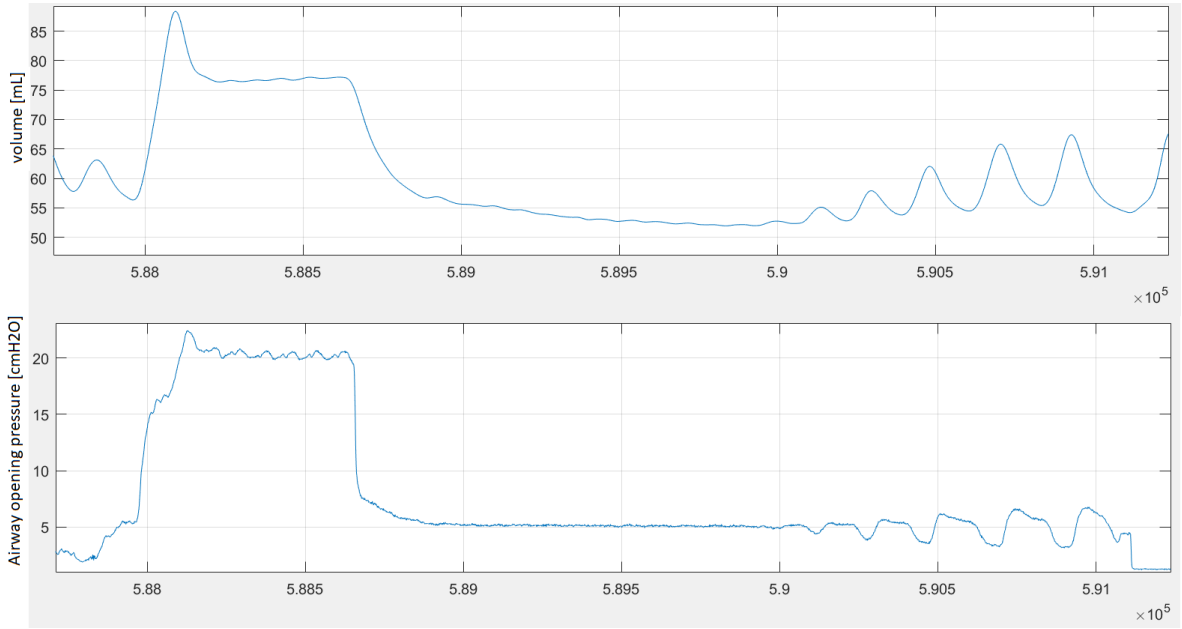


*Figure 2.11: Breathing pattern of volume and airways opening pressure during airway occlusion at 5 cmH2O*

As shown in figure 2.11, before each apnea a pressure of 20 cmH2O is applied to reach the total lung capacity, that is necessary for the correction of the volume absolute values.

## 2.2.6 Work of Breathing

In this study the respiratory muscle effort is assessed by calculating the work of breathing. Indeed, measuring WOB is a useful approach to estimate the energy dissipated or consumed by the respiratory muscles.

The work of breathing can be calculated from $P_{es}$ and volume recordings both in spontaneously and ventilated patients. In a spontaneously breathing patient, the measurement of the most significant and dynamic component of WOB requires an estimate of $\Delta P_{pl}$ needed to generate a change in volume. The work performed during each respiratory cycle represents the pressure applied to yield a change in volume and can be expressed as the area enclosed in a P-V loop:

$$WOB = \int_{t0}^{Ti} PV\, dt \tag{24}$$

When respiratory muscles contract, displacement occurs, and mechanical work is product. Muscle contractions can be characterized depending upon where this work is performed.

The work of breathing is related to pressure differences, generated by inspiratory muscles to overcome both resistive forces in the airways and elastic forces of the lung parenchyma and chest wall. To quantitate work performed in distending the lungs alone (excluding the chest wall), the relevant trans-structural pressure is transpulmonary pressure $P_L$, which is equal to the difference between $P_{alv}$ and the pressure in the pleural space:

$$P_L = P_{alv} - P_{pl} = P_{ao} - P_{pl} = P_{ao} - P_{es} \quad (25)$$

During spontaneous breathing $P_{ao}$ is equal to zero and, thus, inspiratory work can be calculated from the $P_{es}$ and the volume recordings alone. If a positive pressure is given to assist the patient, $P_{ao}$ is not zero and has to be considered in the calculation of work.

WOB is calculated looking at the Campbell diagram that illustrates the dynamic relationship between pleural pressure developed by the inspiratory muscles and lung volume. Th elastic and resistive components of the work can be obtained by comparing the difference between esophageal pressure during the patient's effort and under passive conditions, represented by the static volume-pressure curve of the relaxed chest wall.

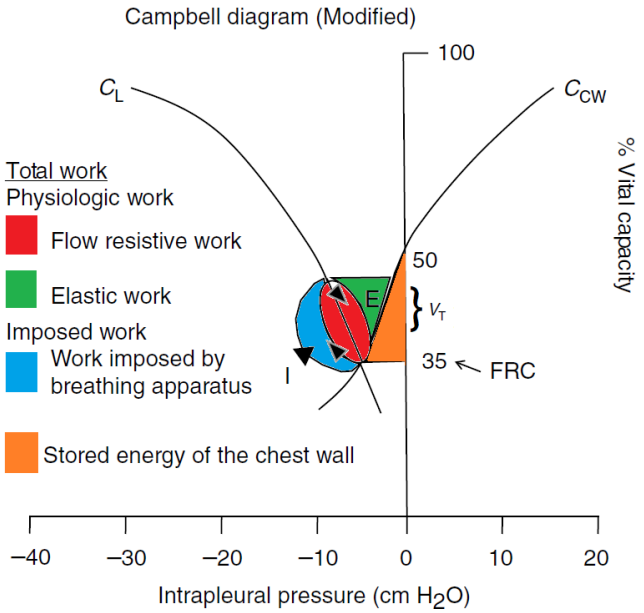


*Figure 2.12: Modified version of the Campbell diagram to represent the total work of breathing to inlcude the workload introduced by the ventilator.*

The red loop in the picture corresponds to a breathing cycle, the inspiration begins at the FRC with an esophageal pressure equal to -5 cmH2O. it continues with a progressive reduction of $P_{pl}$ associating with an increase in volume till the point in which the expiration starts.

In order to clinically apply measurements of WOB, not only the resistive and elastic components have been differentiated but also the elastic contribution of the lung and chest wall.

Total resistive work on the lungs is obtained by integrating the area subtended by $P_{es}$ and lung volume during a single breath. This resistive work is partitioned into its inspiratory and expiratory components represented by the lower and upper half of the inner pressure-volume loop respectively and splatted by the dynamic pulmonary compliance line. Normally, the expiratory work is performed passively at the expense of the elastic energy stored in deformed tissues during inspiration.

The elastic work, instead, is identified in the diagram as the triangular-shaped area subtended by the lung and chest wall static compliance curves previously obtained.

The work on the lung and on the chest wall for spontaneously breathing patient are calculated according to the following formulas:

$$WOB_L = (P_{ee} - P_{es}) \times \frac{dV}{dt} \tag{26}$$

$$WOB_{CW} = \frac{1}{2} \times V_T^2 \times C_{CW} \tag{27}$$

where $P_{ee}$ is the end-expiratory esophageal pressure.

Although the correct computation of WOB requires the measurement of the lung elastic recoil and chest wall relaxation curves, the elasticity of the chest wall results sometimes difficult to measure, because of the unparalysed muscles that generate artefact in the $P_{es}$ signal.

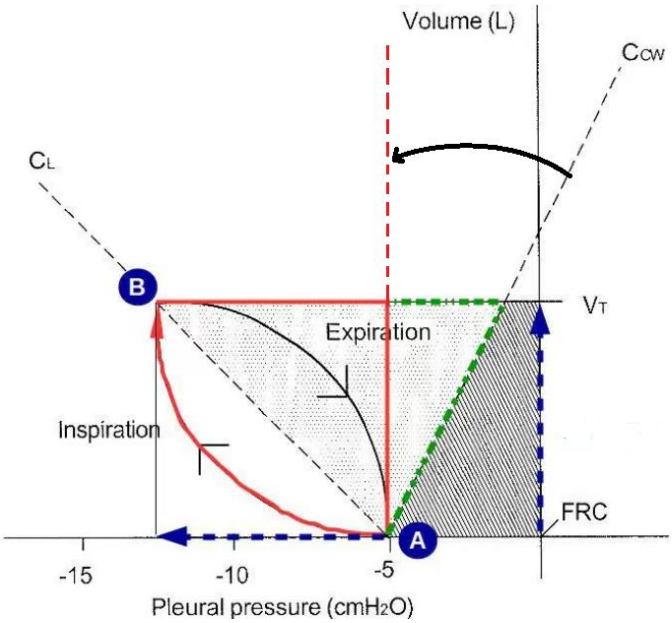


*Figure 2.13: Representation of the simplifications applied to the diagram to facilitate the computation of WOB.*

Therefore, in this work, the WOB is calculated assuming some hypothesis:

1) A constant value of lung compliance is considered over the breathing cycle;
2) The changes in total respiratory system pressure-volume curve around the operating lung volumes are mainly determined by the lung;
3) The end-expiratory lung volume does not change significantly during the recordings;
4) The contribution of the chest wall to the WOB can be neglected shifting the chest wall compliance curve vertically in correspondence of the end-expiration point of the loop, as it is showed in figure 2.13.

# Chapter 3 In-Vitro Studies

The accuracy of the volume and pressure signals acquired using the methods previously described needs to be sufficient for the computation of the considered parameters. In fact, even small variations in volume and pressure could lead to the introduction of errors in measurements and have great impact on the results. Moreover, during clinical practice, different factors can affect the accuracy of the measurements. Therefore, in-vitro experiments have been conducted to evaluate the performances of the applied methods and verify the resulting accuracy of the measured parameters. In this chapter, the outcomes of these in-vitro studies are reported.

# 3.1 Evaluation of RIP Measurements

## 3.1.1 Accuracy of the Tidal Volume Measurements

The reliability of the tidal volume determined by the respiratory inductive plethysmography has been tested placing the bands around a balloon blown up to reach a diameter close to the cross-section of a new-born thorax. The characteristic sinusoidal breathing signal has been recreated over-inflating and deflating the balloon first with a 10mL calibrated syringe and then a with 20mL one. The acquired signal from the RC and AB bands have been summed and the resulting trace has been calibrated imposing to the first three breaths a change in volume equal to 10 and 20 according to the syringe in use. The repeatability of the obtained tidal volumes has been statistically measured using the coefficient of variation (CV), also known as relative standard deviation (RSD), that is a standardized measure of the dispersion of a data series around the mean. The outcomes are presented in the Table 3-1:

*Table 3-1: Coefficients of variation of the RIP tidal volume*

| | **Mean $V_t \pm$ SD** | **CV [%]** |
|---|---|---|
| 10 mL | 10.72 ± 0.38 | 3.5 |
| 20 mL | 20.51 ± 0.78 | 3.8 |

From these values we can state that the amplitude of the tidal volume measured through the *Respitrace* system is highly accurate and the system can be used to get precise estimations of the amplitude changes in the volume signal acquired during the experiments in-vivo. However, this analysis gives no evidence on the accuracy of the absolute values of volume expressed by the calibrated signals from the bands. For this evaluation, an analysis of the drift in the RIP traces is required.

## 3.1.2 Evaluation of the Bands Drift

To evaluate the accuracy of the absolute values from the RIP, the stability of the end-expiratory lung volumes experienced at each breath has been assessed. Firstly, the bands have been placed on the balloon and both RC and AB data have been recorded for three minutes, after all the volume traces have been centred around zero using the default option present in the *Respitrace* software.
The static drift has been computed as the difference between the value showed at the end of the acquisition and the initial one.

| **Drift RC** [units/sec] | **Drift AB** [units/sec] |
|---|---|
| -0.035469 | -0.10437 |

The baseline drift of the RIP signal has revealed a low average increase and decrease in RC and AB signal respectively.
The resulted magnitude of the drifts brings to consider neglectable in this study the instability of the absolute values. Indeed, the experiments conducted in this project require only brief periods of signal acquisition. However, in individual patients, the drift is neither stable nor steadily increasing or decreasing with time, but changes over a wide range.
For this reason, this drift could introduce significant errors in long-term measurements, for which a better control of the baseline should be achieved requiring the application of offline corrections.
A better evaluation of the system is obtained by inflating and deflating the balloon until a fixed end-expiratory volume is reached, guaranteed by full stroke cycles with a 20mL syringe. The baseline drift of the RIP signal was determined by comparing the EELV over a 5-minute period of stable acquisition.
The minimum points of the sinusoidal movements from both RC and AB channels and the summed volume have been stored and their variability investigated computing the coefficient of variation.

*Table 3-2: Evaluation of the RIP drift*

| | **RC** | **AB** | **SUM** |
|---|---|---|---|
| **Mean EELV± SD** | 0.65 ± 0.12 | 1.07 ± 0.05 | 0.92 ± 0.10 |
| **CV [%]** | 18.2 | 4.8 | 11.4 |

As we can see from the results in Table 3-2, the end-expiratory lung volumes remain consistently stable over the short period of the acquisition, presenting coefficients of variation lower than 1% for all the volume recording channels.

To gain a better view of these durability outcomes, the EELV have been plotted over the number of sample giving a visual representation of the volume trend in time.

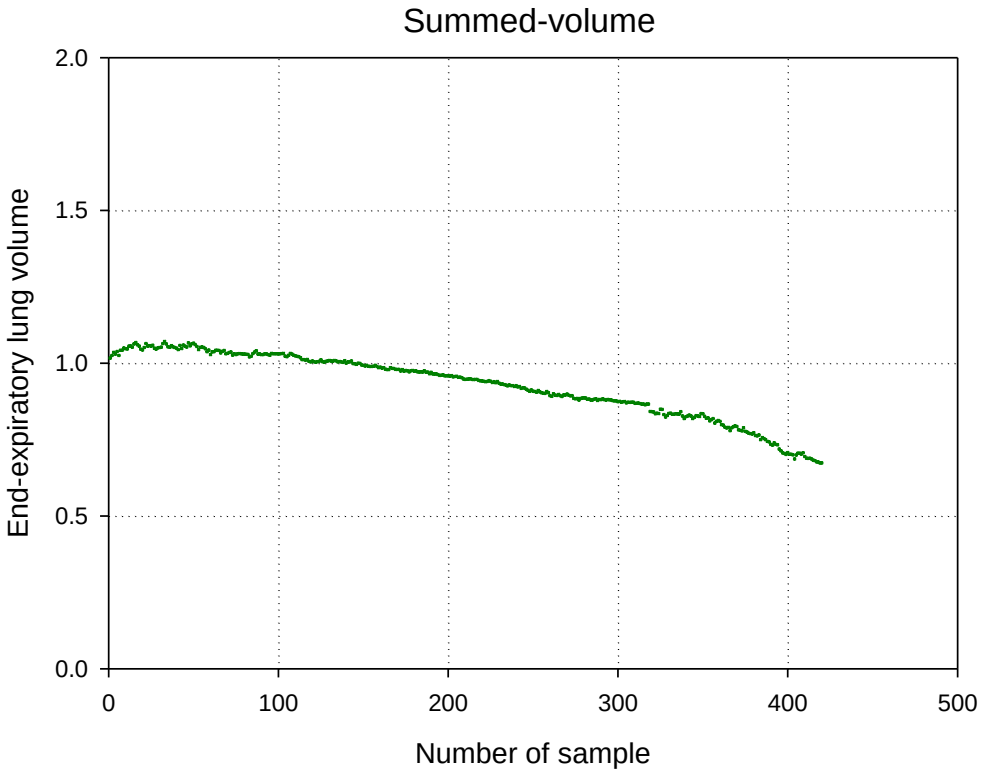


*Figure 3.1: Repeatability of the end-expiratory lung volumes over time*

In controlled conditions, an accurate drift should measure the same value for the entire acquisition period, thus, all the points should align horizontally. Plotting the experimental data, the resulting regression line has a slope close to zero demonstrating a high repeatability of the minimum values. The results are shown in Table 3-3 along with the standard error (SE) of the estimation and the R square.

*Table 3-3: Parameters of the linear regression of the minimum acquired values over time*

| SLOPE | SE | $R^2$ |
|---|---|---|
| 0.65 ± 0.12 | 1.07 ± 0.05 | 0.92 ± 0.10 |

Even if these results show that RIP is consistently precise during quantitative measurements, using the *Respitrace* in-vivo, we have found an unstable baseline drift of the RIP that hinders a higher accuracy of this method. The drift changes rapidly and over a wide range both during the same acquisition process or between different measurement sessions and it is therefore unpredictable for a certain period. However, the short duration of the measurements carried out in this study doesn't require a high long-term accuracy. Nevertheless, to avoid that the calculation of the mechanical properties of the respiratory system could be altered by the drift some precautions have

been taken during the signal processing. Indeed, the absolute values of the volumes corresponding to each apnea have been corrected considering the volume reached when the 20cmH2O pressure is applied at the airway opening favoring the achievement of the total lung capacity. The higher volume reached at 20cmH2O in relation to the prior determined and known FRC, specific for each patient, has been stored and used as reference point. Then, the changes in volumes passing from 20cmH2O to the lower pressure value, have been computed singularly for all the apneas. Finally, these volume Δ have been subtracted to the reference maximum volume to obtain an absolute value for each apnea, unaffected by the drift, that could be used to plot the P-V curve of the respiratory system and the chest wall.

## 3.2 Evaluation of the $P_{es}$ Measurement System

The pressure transducer has been adjusted meticulously in the water column before every measurement through a procedure that exploits a calibration method built into the custom-designed measuring system. The catheter is soaked in the graduated cylinder until the lower tip reaches 6 cm of depth. Since the distance between the two catheter is fixed and equal to 5 cm, if the catheter is kept straight, the higher tip is placed at 1 cm of depth. The signal coming from the two tips of the catheter, the gastric and the esophageal one, and recorded on the computer program is regulated by means of the transducer balance control option to the correct values of pressure, 6 cmH2O and 1 cmH2O respectively. To verify that this calibration remained stable throughout the measurements, the catheter has been immerged deeper and the returned values from the two tips have been analyzed. Moreover, an external known pressure has been applied to be compared with the values from the transducers reported on *Labchart* simultaneously with the generation of the force. The procedure consists in applying five consecutive levels of external pressure at the opening of the water column, namely 0-5-20-5-0 cmH2O and at the same time recording the values measured by the catheter previously calibrated at the depth specified above. The obtained stepwise patterns are showed in the figure 3.2.

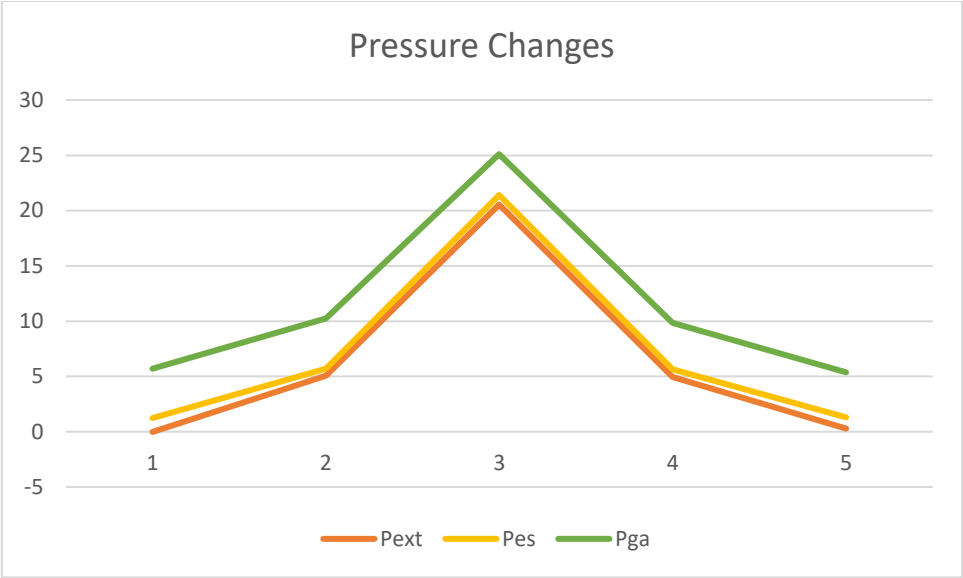


*Figure 3.2: Catheter pressure patterns during the application of an external pressure*

As we expected, the pressure values measured by the esophageal and gastric tips reflect the applied steps in external pressure, maintaining the initially imposed gap and changing linearly with the increasing and decreasing applied force.

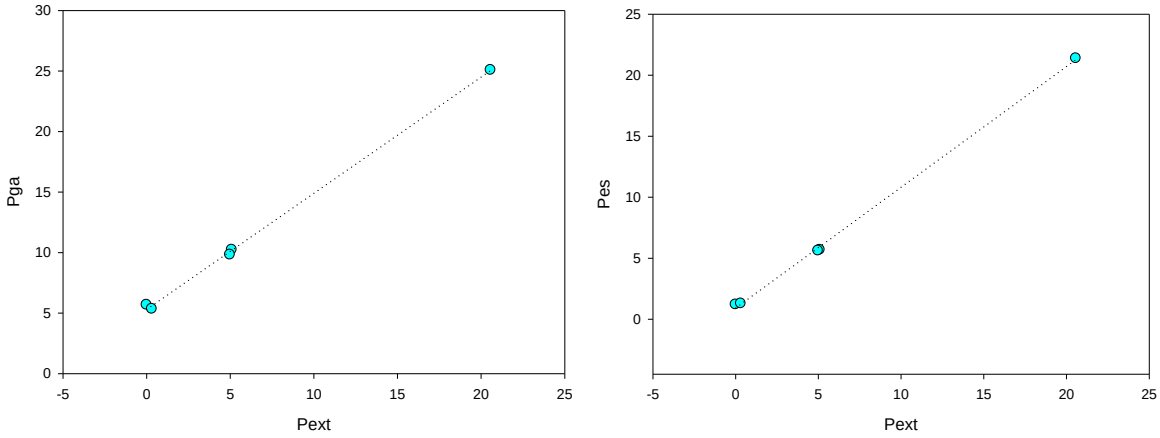


*Figure 3.3: Linear dependency between external pressure and catheter measurements*

The graphs demonstrate an elevated accuracy of the pressure catheter in-vitro, both for the measurement of the gastric and the esophageal pressure. However, this estimation doesn't ensure the achievement of the same positive results once that the catheter is popped into the esophagus. The set calibration of the transducers, indeed, could be compromised by the surface tension acting on the tips during the transferring of the catheter from the water column to the patient's mouth. Moreover, pressure measurements could be affected by a wrong positioning of the tips, infant movements during acquisition and physiological artefacts coming from other internal organs, such as the cardiac artefact.

# Chapter 4 In-Vivo Clinical Studies

Fatigue indices, variability analysis of the breathing pattern, lung mechanics and work of breathing have been used to assess changes in lung function caused by the development of chronic lung diseases. It has been verified whether the analysis of these parameters allow a practical characterization of the disease. Information about control of breathing and mechanical properties of the thoraco-pulmonary system have been obtain and are presented in the following chapter.

## 4.1 Study Protocol

This study is part of a major NHMRC funded clinical research study (PIFCO) being undertaken at the *King Edward Memorial Hospital* in Perth (Western Australia). The following study was conducted in accordance with the National Statement on Ethical Conduct in Human Research and supported by the Human Ethics Committee of the Women and Newborn Health Service. An informed consent was obtained for each infant prior to the study. All the measurements have been performed in the Neonatal Intensive Care Unit (NICU) of KEMH in Perth.

*Aim of the study*

The study aims to measure the breathing pattern variability, the lung mechanics, and the work of breathing to establish a better measure of the severity of lung disease in preterm infants and to understand more about the contribution of these structures development to the respiratory disruption. The clinical study has been conducted on a group of preterm infants at which was assigned a score according to the grade of severity of the bronchopulmonary disease.

*Inclusion criteria*

To be eligible for the study, preterm infants needed to have been born between $28^{+0}$ and $32^{+6}$ weeks gestational age at King Edward Memorial Hospital without diagnosed chronic lung disease or with BPD at different levels of severity who could spontaneously breathe or required a non-invasive respiratory support that didn't obstruct the measurements.

*Exclusion criteria*

Infants with major malformation of the respiratory system, other respiratory disease that might contribute to distress or congenital disease of the central and peripheral nervous system had to be excluded from the study. In case of sickness at the moment of the study or lack of parental consent infants were not studied.

*Experimental protocol*

Patients were study during periods of spontaneous breathing while quite asleep after feeding. Since the aim of this study was to evaluate the functionality and mechanical properties of lung and chest wall, only the pressure acting on the respiratory system was varied, keeping all the other parameter constant at baseline condition for the duration of the acquisition. For patients still dependent on a respiratory support, FiO2 was changed according to the patient's clinical needs.

The pressure sensor is soaked in room-temperature sterile water for 30 minutes prior to use to minimize drift. The flow transducer in the pneumotachograph is calibrated before every measurement using a 20mL syringe and the data are stored on the computer program.

The breathing pattern is measured by placing the RIP elastic bands around the chest of the infant.

The esophageal catheter is inserted into the oesophagus and upper stomach at the beginning of each measurement process.

After the esophageal tube is in place, the infants are observed until they fall asleep and start breathing regularly with minimal variability in tidal volume. Only then, the bands are centred on a zero baseline and the respiratory signals recorded with the pneumotach for approximately 1 minute to obtain the 30 breaths required for the bands calibration.

The recordings are stopped when the infant is moving or shows signs of arousal or agitation.

All the signals of interest are displayed on a monitor to be continuously checked real-time.

Infant's breathing is then interrupted by the induction of apnea of 2/3 seconds following the procedure described in section 2.2.5 to activate the HB reflex.

The number of apnoea obtained for each infant is variable according to the ease of the procedure and the risk conditions evaluated by the clinician. The total duration of this phase is around 20 minutes. Once volume traces have returned to a stable condition, respiratory signals have been acquired during 10 minutes of spontaneous breathing to be used for the analysis of variability.

Data analysis

End-expiratory and end-inspiratory points have been automatically selected and manually checked for artefacts or errors before the computation of the time series of breathing pattern (BP) parameters. Specifically, the chosen BP parameters are tidal volume, inter-breath-interval time and end-expiratory lung-volume that have been computed breath-by-breath over approximately 300 stable breaths in the 10 minutes acquisition.

The statistical properties of these parameters have been quantified using the long-range correlation exponent $\alpha$ obtained by DFA, as described in section 2.2.3. The scaling exponent, its standard deviation and the r-square of the linear fitting have been computed for each considered parameter.

The thoraco-abdominal asynchrony has been analysed using the same traces from which BP parameters have been extracted. TAA indexes have been computed breath-by-breath, considering the time periods between each succeeding EE and EI points previously saved. The construction of the P-V curves and the consequent computation of static compliances required a careful examination of the volume and pressure traces and the manual selection of specific points during the airways occlusion procedures described in section 2.2.5. For each provoked apnea, we have selected a point just before the release of the 20 cmH20 pressure applied at the airways opening and a point in which, during the occlusion, the relaxation pressures and, then, the volume reach a stable condition represented by a plateau. In order to plot the P-V curve and obtain the slope, the values of volume have been corrected subtracting the delta of volume from the total lung capacity reached during the procedure. Portions of pressure signal in which spam or other artefacts were present have been not considered in the computation of the compliance.

In each infant, the P-V loop has been graphed for each breath progressively, plotting in a X-Y plot the values of transpoulmonary pressure ($P_{es} - P_{ao}$ ) and volume experienced between EE and EI in a tract of quiet and spontaneous breathing. The loops for the calculation of WOB have been manually selected to discard the ones distorted or affected by noise.

The dynamic compliance is represented as the slope of the curve crossing the loop and passing through the points EE and EI (see figure 4.9).

*Statistical analysis*

Data have been tested for normality using the Shapiro-Wilk test according to the considered distribution and expressed as mean ± standard deviation.

Calculations (*Sigmaplot 11.0, Systat Software*, Inc.) have been performed to quantify the clinical relevance of the differences in mechanical and variability parameters between healthy and BPD patients. Significance of difference between levels of the disease has been tested using a t-test or by one-way ANOVA on Ranks for repeated measurements. Difference have been considered statistically significant for $p < 0.05$.

*Population*

Fifteen preterm infants have been studied at 36 weeks of GA for a period of 2 hours while they were quietly asleep after having obtained the permission from the parents.

Among the 15 patients that we have enrolled in this study: 9 were not sick and 6 were suffering from chronic lung diseases at different levels of severity. Three of them have been rejected after the measurements because of the impossibility to analyse the data due to the presence of artefacts and errors in the signals that didn't allow to determine the outcomes.

The mean weight at the moment of the study for the cohort is $2.52 \pm 0.4$ kg and the mean gestational age is $36 \pm 0.9$ weeks.

*Table 4-1: Clinical information on the studied infants*

| Patient | Study weight [kg] | BPD score | GA |
|---|---|---|---|
| 1 | 2.21 | 0 | $35^{+2}$ |
| 2 | 2.94 | 0 | $36^{+6}$ |
| 3 | 2.32 | 0 | $36^{+1}$ |
| 4 | 2.30 | 0 | $35^{+4}$ |
| 5 | 2.90 | 0 | $37^{+1}$ |
| 6 | 2.52 | 0 | $36^{+4}$ |
| 7 | 2.92 | 0 | $35^{+3}$ |
| 8 | 2.74 | 0 | $36^{+0}$ |
| 9 | 1.95 | 0 | $37^{+3}$ |
| 10 | 3.03 | 1 | $36^{+6}$ |
| 11 | 2.67 | 2 | $36^{+4}$ |
| 12 | 2.35 | 2 | $35^{+3}$ |
| 13 | 2.70 | 3 | $37^{+2}$ |
| 14 | 2.70 | 3 | $36^{+5}$ |
| 15 | 1.52 | 3 | $36^{+1}$ |

## 4.2 In Vivo Preliminary Test

### 4.2.1 Occlusion Test

The estimation of the pleural pressure through the measurement of the esophageal pressure can be considered accurate only whether the catheter is placed in the correct position to a depth in which $P_{pl}$ changes are well transmitted into the esophagus. The verification is usually done through an occlusion that, though, results to be an invasive procedure in infants with respiratory disease or ventilatory support. Therefore, the length to insert the distal tip into the stomach can be predicted using the NEMU method, that consists in measuring the distance from the nose to the earlobe, to a point midway between the xiphoid process and the umbilicus that can estimate the required insertion length. [31]

In order to verify the satisfactory outcome of this method and the accurate positioning of the esophageal manometry system, a manual airway occlusion test, lasting five respiratory efforts, has been conducted in two of the healthy studied infants. The peak deflections from the esophageal transducer occurring with each inspiratory effort have been identified and related to the simultaneously pressure changes acquired at the airway opening with the pneumotach and used as

reference. Equal changes in esophageal and airway pressures indicate complete transmission of pleural pressure to the measurement site in the esophagus.

During the airway occlusion, the mean peak-to-peak esophageal pressure changes measured from the catheter in the esophagus result to be higher than the mean changes in the airway opening pressure as shown in the Table 4-2:

*Table 4-2: Occlusion test results obtained in the two studied infants*

| **Patient** | **Mean $\Delta P_{es}$** (cmH2O) | **Mean $\Delta P_{ao}$** (cmH2O) | **Ratio $\pm$ SD** | **p-Value** |
|---|---|---|---|---|
| Infant 1 | 16.78 | 16.01 | 1.05 ± 0.09 | 0.391 |
| Infant 2 | 21.30 | 19.31 | 1.10 ± 0.04 | 0.695 |

With appropriate calibration and placement of the esophageal catheter a $\Delta P_{es}/\Delta P_{ao}$ ratio close to unity should be achieved in healthy patients. However, this value is not easy to obtain in preterm infants. In this case, $\Delta P_{es}$ results to be higher than $\Delta P_{ao}$. This may be due to an air leak during occlusion or poor equilibration of $\Delta P_{alv}$ and $\Delta P_{ao}$ caused by airway obstruction or pressure losses because of the compliance of the upper airways. Moreover, failure to achieve a satisfactory $\Delta P_{es}/\Delta P_{ao}$ ratio may be attributed to the fact that $\Delta P_{es}$ doesn't equal $\Delta P_{pl}$.

Finally, it should be remembered that $\Delta P_{pl}$ may not be transmitted accurately to the esophageal manometer in the presence of esophageal spasm or increased tone and marked cardiac artefact. To avoid these problems, during the study, esophageal pressure signal has been checked continuously to adjust the catheter position if necessary and minimize the noise. Furthermore, during the offline analysis of the data, periods of signals in which esophageal spasm were present have been discarded and not considered in the calculation of the mechanical parameters.

## 4.2.2 Tidal Volume Measurements

To determine the accuracy of respiratory inductive plethysmography calibration, the tidal volumes measured from the calibrated sum signal from the bands have been compared with the simultaneously recorded volume obtained from the integrated flow signal acquired with the pneumotach during a period of 30 spontaneous breaths.

The comparison of $V_t$ between RIP and PNT revealed that the values from all the patients were accurate within a range of 10%.

For comparison of $V_t$ between RIP and PNT, the data have been analyzed during consecutive breaths as the mean percentage difference between RIP and PNT volume measurements:

$$difference\ [\%] = ((\overline{V}_{t_{RIP}} - \overline{V}_{t_{PNT}})/\overline{V}_{t_{PNT}}) * 100$$

*Table 4-3: Accuracy of Vt calibration*

| | **All patients** | **No BPD patients** | **BPD patients** |
|---|---|---|---|
| Difference % | -2.40 ± 2.88 | -1.36 ± 2.43 | -3.45 ± 3.13 |

This result shows that our calibration is consistently precise enough for quantitative measurement of lung volumes.

The weight-corrected tidal volumes measured with both the RIP and the PNT are plotted on a X-Y graph in figure 4.1.

The data have been fitted through a linear regression analysis obtaining the results reported in Table 4-4, that demonstrate a significant coincidence between the tidal volumes computed with the two different techniques.

*Table 4-4: Linear regression of tidal volumes measured with RIP and PNT*

| **Rsqr** | **Slope** | **Std error** | **p-Value** |
|---|---|---|---|
| 0.9877 | 1.0075 | 0.0356 | < 0.0001 |

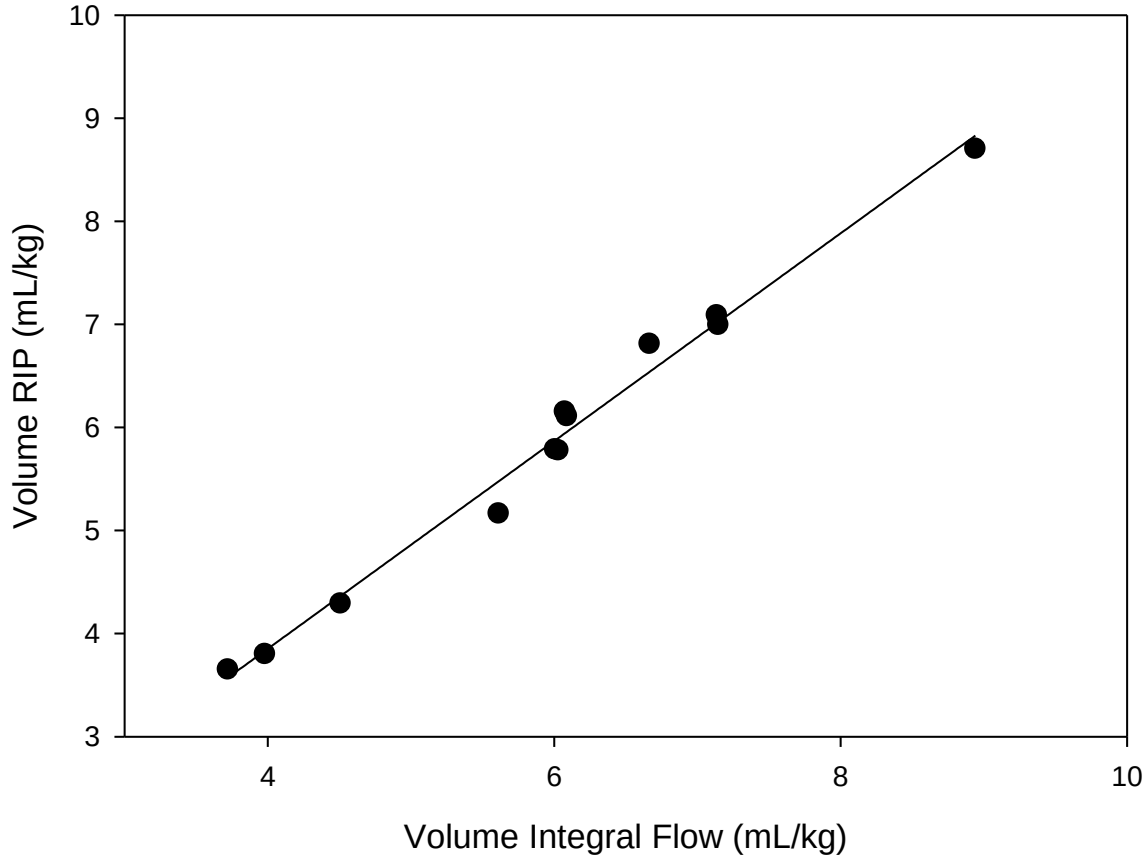


*Figure 4.1: Comparison between volumes obtained with RIP and PNT*

### 4.2.3 Repeatability of the Static Compliance

To test the repeatability property in the measurements of compliance, multiple apnea have been provoked for each level of positive pressure (5-10-15). The compliances of the total respiratory system and chest wall have been computed at each apnoea as the ratio between the change in volume and the applied step in airways opening and esophageal pressure respectively. The compliance of the lung has been calculated using the difference between $P_{ao}$ and $P_{es}$. The resulting compliances have been averaged according to the pressure value at which they were obtained and the coefficient of variation (CV) has been computed for each infant and each level of pressure. The coefficients associated to all the compliances have been then averaged and the outcomes are shown in Table 4-5.

*Table 4-5: Repeatability of respiratory system, chest wall and lung compliance expressed by the coefficient of variation computed at different pressure levels.*

| | **Compliances** (mL/cmH2O) | **Applied pressure step** | | |
|---|---|---|---|---|
| | | **5 cmH2O** | **10 cmH2O** | **15 cmH2O** |
| **CV [%]** | $C_{rs}$ | 22.85 ± 8.33 | 18.33 ± 8.10 | 28.19 ± 13.95 |
| | $C_{cw}$ | 22.15 ± 15.90 | 26.86 ± 18.48 | 36.41 ± 19.84 |
| | $C_l$ | 24.11 ± 19.22 | 30.15 ± 24.34 | 28.29 ± 28.19 |

The coefficients demonstrate that the variation in the computed values of compliance is greater than 20% in almost all the considered cases. The more repeatable is the value of total respiratory system and this result is due to the fact that $P_{ao}$ is the measure that less likely could be affected by noise, differently from the esophageal pressure, required for the measurement of the other two compliances.

# 4.3 Comparison between Healthy and BPD patients

The study of the respiratory system in health or disease as a complex system whose functioning can be determined by different aspects could give a better insight of BPD with intriguing consequences for the clinician. A complete characterization of different subsystems involved in the process of ventilation could improve the understanding of bronchopulmonary dysplasia, as well as, predict the temporal behaviour of the disease state providing clinically useful information for patient management. Moreover, a better phenotyping of such a chronic lung disease is becoming increasingly more necessary since it is realized that, in the future, therapy will be more and more phenotype specific. Analysis of lung function variability has been already shown to be able to distinguish between different variants of asthma and obstructive airway disease. [32]

In this contest, we aimed to identify parameters that can describe alteration in control of breathing and lung mechanics.

Therefore, in the following chapter, we applied the developed methods for comparing the effects of BPD on lung function in term of breathing pattern, static and dynamic compliances, and work of breathing to obtain a more detailed description of this disease. Mechanical parameters are used also to assess changes in lung function according to the severity level of BPD.

## 4.3.1 Tidal Volume

The weight-corrected tidal volumes computed as described in section 4.2.2 have also been plotted highlighting the difference between the value of $V_t$ in healthy subjects and patients with different level of BPD. The results are shown in figure 4.2.

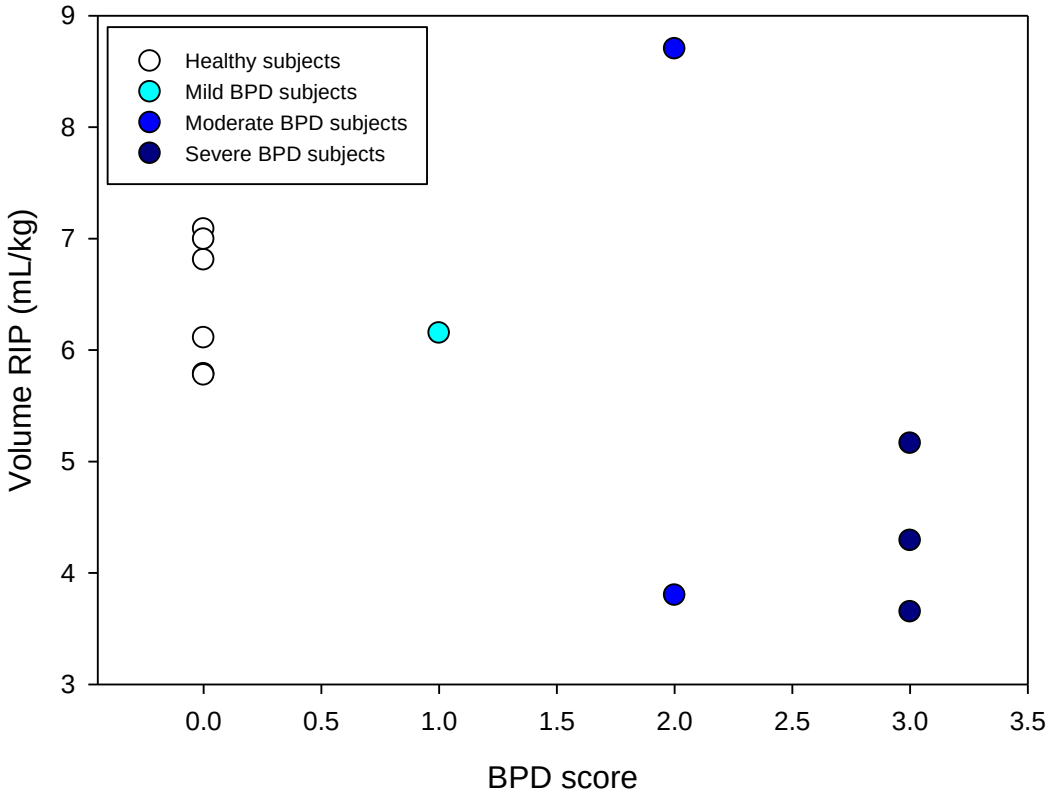


*Figure 4.2: Comparison between volume obtained with RIP according to the level of severity of BPD*

From the data, we can see that BPD patients have lower tidal volume than healthy subjects, except for patient number 12. If we exclude this infant, the mean values of $V_t$ for the two groups are 6.75 ± 1.02 and 4.61 ± 1.04, respectively for without BPD and BPD subjects. The difference between these values is statistically significant (p=0.005). These findings agree with the values obtained by Durand et al. [33], suggesting that infants with BPD have significantly lower values of tidal volumes than healthy infants. $V_t$ decreases with increasing severity of the disease, in parallel with a shorten of the total time and an increase in the respiratory frequency.

## 4.3.2 Breathing Pattern Variability

Breathing pattern and thoraco-abdominal asynchrony indexes have been computed as explained in section 2.2.2. Both volume excursions collected at the rib cage and abdomen have been analysed to detect synchronous or paradoxic motion of one compartment with respect to the other and the

total volume in an effort to distinguish differences between normal subjects and patients with chronic lung disease.

Specifically, the paradox motion indexes IAI and EAI have been computed pairwise for each volume signal and they are presented in order as the index obtained from the signals recorded by the two bands, form the abdominal volume trace with respect to the total one and from the rib cage excursions in relation to the chest wall ones.

Moreover, LBI index has been computed as explained in section 2.2.2 as a relative number because the RIP measurements from the rib cage and the abdomen were uncalibrated. Uncalibrated volumes are arbitrary volumes measured by RIP, which are relative to other breaths differently for each patient.

The obtained BP and TAA parameters are shown in Table 4-6, that distinguishes between the results in patients with and without BPD.

*Table 4-6: Comparison between thoraco-abdominal parameters in healthy and BPD infants*

| | Unit of measure | No BPD patients | BPD patients | p-Value |
|---|---|---|---|---|
| $T_i$ | s | 0.45 ± 0.012 * | 0.40 ± 0.010 * | p=<0.001 |
| $T_e$ | s | 0.61 ± 0.058 * | 0.48 ± 0.060 * | p=0.006 |
| **RR** | (breaths/min) | 63.07 ± 3.457 * | 73.17 ± 3.486 * | p=0.001 |
| **DC** | % | 44.28 ± 1.416 * | 46.70 ± 1.392 * | p=0.023 |
| **%RC** | % | 21.81 ± 15.451 | 24.34 ± 18.895 | p=0.814 |
| **%AB** | % | 78.25 ± 15.415 | 75.52 ± 18.794 | p=0.799 |
| **IAI** | % | 48.14 ± 1.532 | 47.41 ± 1.093 | p=0.426 |
| | | 33.91 ± 8.542 | 39.04 ± 6.820 | p=0.333 |
| | | 44.74 ± 1.570 | 43.07 ± 3.396 | p=0.286 |
| **EAI** | % | 49.00 ± 1.409 | 49.53 ± 0.835 | p=0.518 |
| | | 37.40 ± 6.658 | 33.83 ± 7.120 | p=0.425 |
| | | 45.28 ± 1.158 | 43.29 ± 2.986 | p=0.141 |
| **LBI** | | 1.33 ± 0.048 | 1.34 ± 0.20 | p=0.566 |

**Ti: inspiratory time; Te: expiratory time; RR: respiratory rate; DC: duty cycle; %RC and %AB: percentage contribution of the rib cage and abdomen to tidal volume; IAI and EAI: inspiratory and expiratory asynchrony indices; LBI: labour breathing index. *p<0.05 in t-test.**

The results in Table 4-6 show that all the parameters regarding the inspiratory and expiratory times and the respiratory frequency present a statistically significant difference between the mean values obtained in the two groups of patients.

In particular, BPD infants presents higher respiratory frequency and longer inspiration time as a percentage of breathing period, these results are in line with what found in literature.[33]

On the contrary, the t-test applied to the distributions of all the other thoraco-abdominal indexes return a $p > 0.05$, meaning that the differences between the mean values in the two groups are not great enough to exclude the possibility that the discrepancy is due to random sampling variability.

It would be expected that thoraco-abdominal asynchrony was higher in BPD infants because of a weak respiratory muscle function associated with an abnormal lung and chest wall combination. Furthermore, in presence of a mild-to-moderate respiratory insufficient, infants may be engaging in breathing pattern strategies to balance energy expenditure and gas exchange consisting in switching between thoracic and abdominal contribution to tidal breathing to spare effort rather than fatiguing both the RC and AB muscle groups.

Nevertheless, these results are in line with what stated by Sackner et al. [34], who proved that phase angle and maximal compartment amplitude are not consistent in distinguishing between normal and patients with COPD (a pathology of the adult respiratory system that present several similarities to BPD) during natural and voluntarily controlled breathing pattern. Moreover, according to his study indexes of asynchronous and paradoxic motion in patients with COPD do not correlate well with severity of the airways disease as their values often overlap those obtained in normal subjects and, therefore, the indexes cannot be considered a diagnostic test.

In our research, as well, the values of IAI and EAI differ in a not statistically significant way between the two groups and result to be unnecessary to classify the healthy and sick patients.

However, due to the limited number of subjects, the power of the performed statistical test are below the desired threshold and therefore negative results should be considered carefully.

## 4.3.3 Variability Analysis

For each subject, we have recorded an average of 339 ± 85 breaths to be analysed and we have examined the temporal pattern exhibited by three respiratory related variables: tidal volume, end-expiratory lung volume and inter-breath interval. Patient number 13 has not been included in this part of the study because he was too sick to extend the measurement procedure without a ventilatory support.

The figure 4.3 shows an example of the time course of the total chest wall volume and its pulmonary rip cage and abdominal components for one of the studied infants before volume calibration.

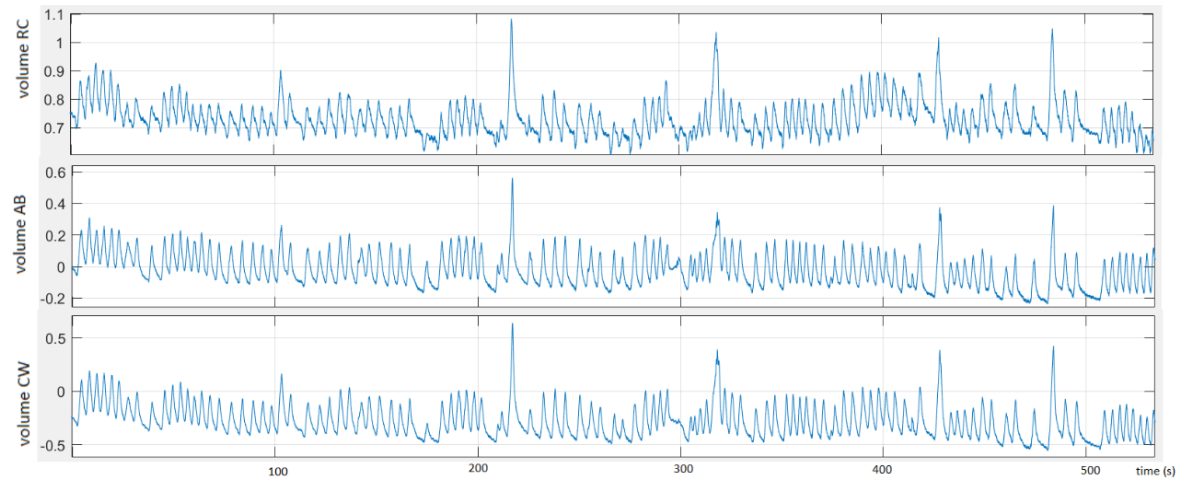


*Figure 4.3: Experimental traces of total and compartmental chest volumes in a representative subject*

The time series of the ventilatory parameters are obtained by detecting EE and EI points and computing the value of each parameter on a breath-by-breath basis. The DFA plots corresponding to the analysed time series are shown in figure 4.4. It can be seen that the fluctuation function of each ventilatory parameter increases linearly on a double logarithmic graph through about three decades of breath numbers.

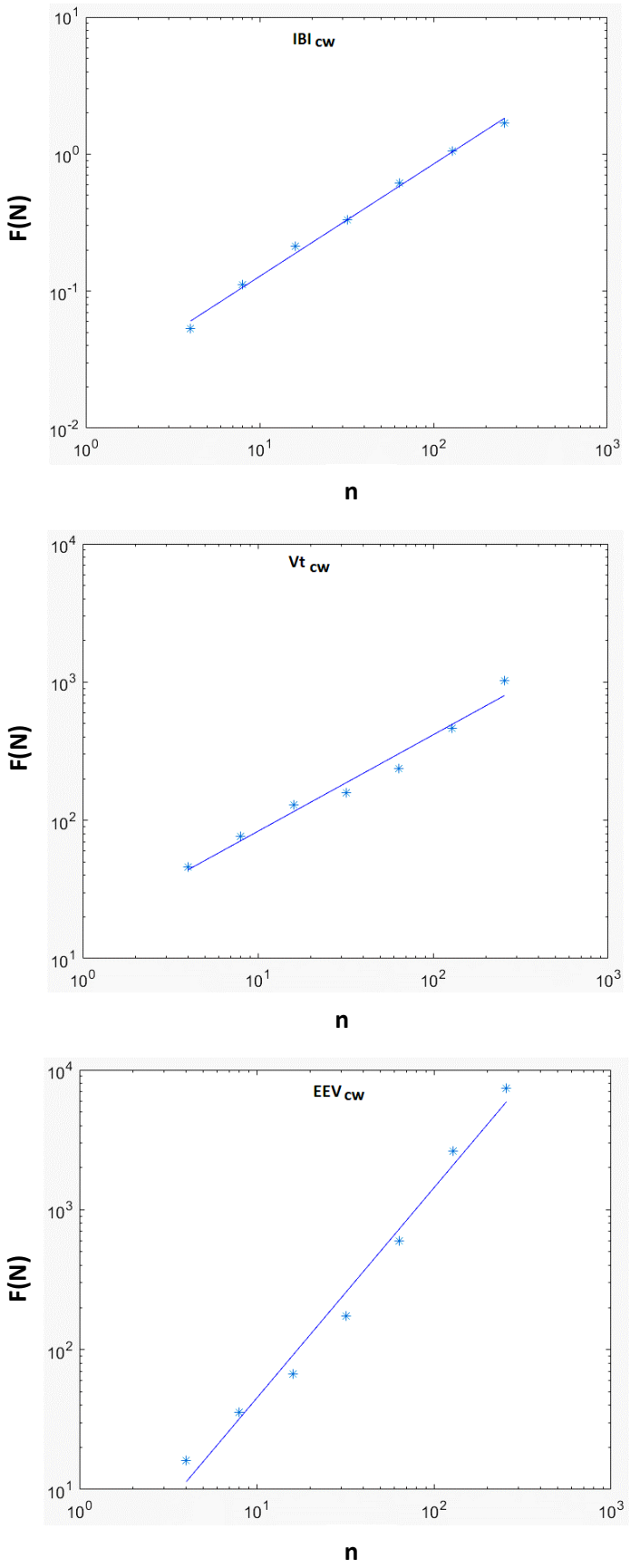


*Figure 4.4: Fluctuation as a function of window size for the time series from volume tracings of a representative subject: each panel refers to a specific variable of the breathing pattern.*

For this representative subject, the value of the exponent $\alpha$ obtained as the slope of the linear regression fits to the data is higher than one for the end-expiratory volume and equal to 0.82 and 0.69 for the IBI and tidal volume respectively, suggesting that EELV is considerably more correlated than the other parameters.

Regarding all the subjects, we have found different values according to the severity of the disease. Table 4-7 compare breathing patter parameters obtained in patients with and without BPD, diagnosed on the basis of the current definition.

*Table 4-7: Comparison between breathing pattern parameters*

| | | No BPD patients | BPD patients |
|---|---|---|---|
| **IBI** | mean (s) | 0.99 ± 0.07 | 0.88 ± 0.13 |
| | CV | 34.23 ± 14.53 | 30.43 ± 12.38 |
| | $\alpha$ | 0.73 ± 0.12 | 0.64 ± 0.03 |
| $\boldsymbol{V_T}$ | mean (mL) | 7.50 ± 3.43 | 5.00 ± 1.45 |
| | CV | 37.83 ± 23.91 | 35.89 ± 15.90 |
| | $\alpha$ | 0.60 ± 0.12 | 0.69 ± 0.06 |
| **EELV** | mean (mL) | 59.40 ± 7.55 | 48.48 ± 4.63 |
| | CV | 4.93 ± 3.03 | 5.69 ± 3.71 |
| | $\alpha$ | 1.23 ± 0.14 | 1.32 ± 0.13 |

The above table summarizes the mean ± standard deviation of the average, the coefficient of variation (CV) and the exponential coefficient $\alpha$ of the ventilatory parameters for the healthy and sick subjects: IBI, $V_T$ and EELV. The end-expiratory volume series exhibits an increased $\alpha$ and decreased CV compared to $V_T$ and EELV, showing a stronger long-range correlation both in healthy and BPD subjects. Moreover, EELV presents stronger correlation properties in BPD than in healthy conditions, presenting larger $\alpha$ and CV. Tidal volume has similar behaviour, while IBI exhibits lower variability in healthy patients and minor correlation in the presence of chronic lung disease.

Figure 4.5 shows the scaling exponent for IBI, $V_T$ and EELV averaged as a function of the assigned BPD score in each patient.

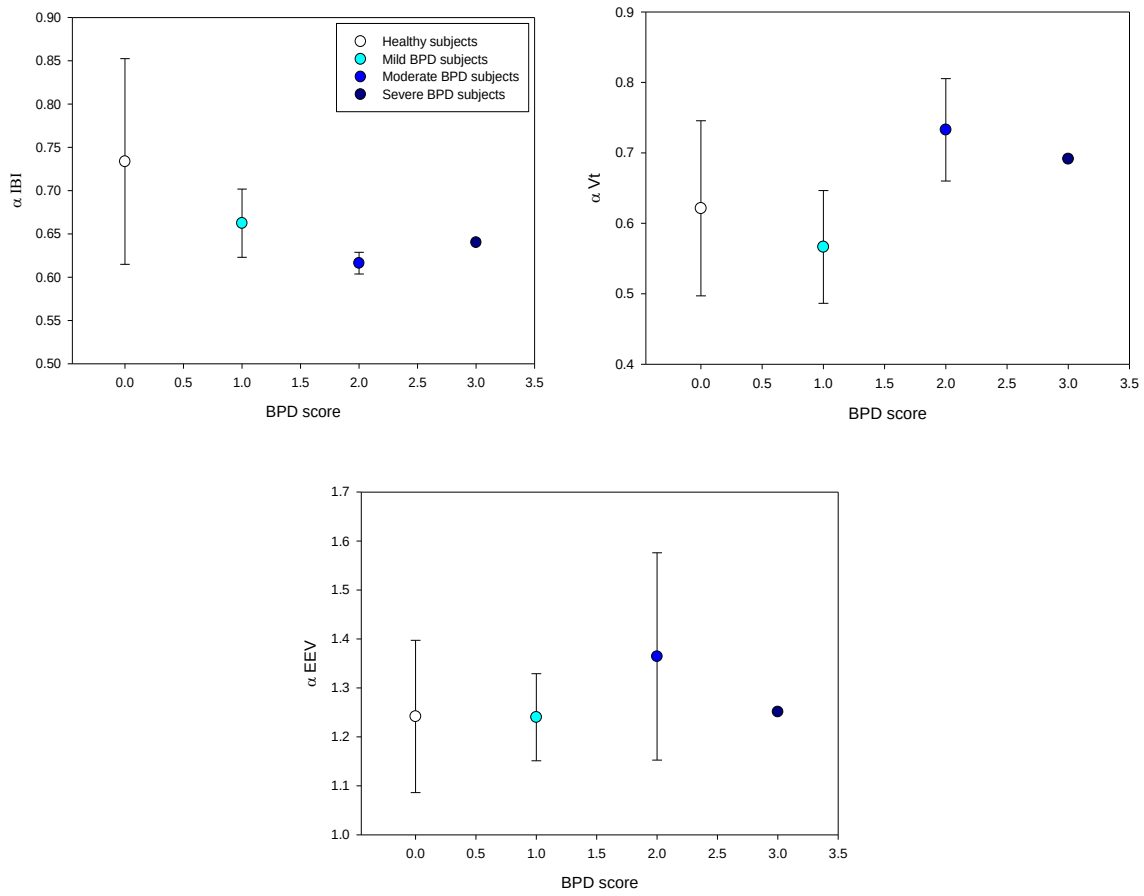


*Figure 4.5: Scaling exponent of each breathing pattern parameter as a function of the BPD score*

To summarize, all ventilatory parameters (IBI, $V_T$, EELV) show significant fluctuations and long-range correlations in these fluctuations defined by a scaling exponent $\alpha$ higher than 0.5. The coefficient $\alpha_{EELV}$ is greater than $\alpha_{EELV}$ and $\alpha_{EELV}$ in both healthy and BPD infants. End-expiratory lung volumes, indeed, have the smallest variability with respect to the average value and the strongest correlation over long time scale regardless of the presence of the disease. This suggests the presence of different mechanisms of control for this parameter. In fact, in newborns, EELV is maintained above the resting volume by active mechanisms, whose presence suggests that a great contribution of EELV variability is determined by the control of breathing and that the variability of EELV could be related in part to variability of the muscles activity and of $T_e$. These long-term correlations are maintained also in presence of chronic lung disease, even if the values of $\alpha$ slightly change.

However, we haven't found a statistically significant difference between the two categories. For all the three parameters, the difference in the mean $\alpha$ of the two groups is not great enough to reject the possibility that the difference is due to random sampling variability (p>0.05). This might be due to the low number of subjects considered in this study that does not allow to discriminate between the two groups and highlight the alterations in the BPD patients. The power of the tests performed was indeed below the desired value (0.80).

## 4.3.4 Static and Dynamic Compliances

The static compliances have been computed for the total respiratory system and for chest wall as the ratio between the volume acquired with the bands and the changes in $P_{ao}$ and $P_{es}$ respectively, during the procedure described in section 2.2.5. The absolute values of the calibrated volume have been corrected based on the total lung capacity reached at each 20cmH2O step before each apnoea. Moreover, the compliance of the lung has been computed inverting the equation (11) in section 1.1.3.2, that expresses its contribution to the compliance of the total respiratory system. The value of the volume and pressures reached during each airway occlusion have been stored and plotted on a X-Y graph as showed in figure 4.6.

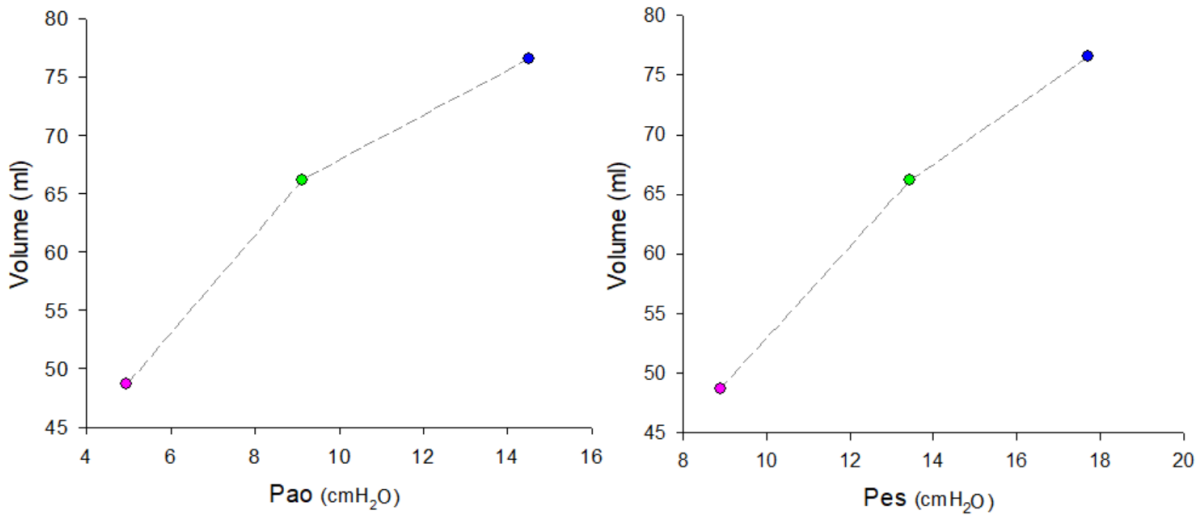


*Figure 4.6: Relaxation curve of the thoraco-abdominal wall in a representative patient. Pink: apnoea at 5 cmH2O. Green: apnoea at 10 cmH2O. Blue: apnoea at 15 cmH2O*

The slope of the line passing by the points corresponding to the apnoea at 5 and 10 cmH2O has been used as a measure of static compliance of the respiratory system and of the chest wall according to the considered pressure.

It must be remembered that lung compliance is a function of lung volume and may differ in a given infant depending on multiple factors. For this reason, compliance comparisons between infants require some sort of normalization for lung volume. We decided to correct the results for the body weight of each infant, since FRC is an approximate linear function of body weight. The $C_{cw}$ of the infant 12 has been considered outlier and, thus, neglected.

A detailed comparison between weight-corrected static compliances in healthy and BPD patients can be found in Table 4-8.

*Table 4-8: Static compliances in healthy vs BPD infants*

| | No BPD | BPD |
|---|---|---|
| $C_{RS_{stat}}$ [ml/cmH2O*kg] | 1.36 ± 0.50 * | 0.47 ± 0.36 * |
| $C_{CW_{stat}}$ [ml/cmH2O*kg] | 1.95 ± 1.29 | 0.93 ± 1.01 |
| $C_{L_{stat}}$ [ml/cmH2O*kg] | 0.97 ± 0.67 | 0.71 ± 0.53 |

***p<0.05 in t-test.**

The results show that both the compliance of the whole respiratory system and the ones of the chest wall and lung decrease with the diagnosis of the disease.

The difference in the mean $C_{RS_{stat}}$ of the two groups is greater than would be expected by chance, stating a statistically significant difference between the healthy and BPD patients (p=0.005).

In contrast, there is not a statistically significant difference between the values of $C_{CW_{stat}}$ and $C_{L_{stat}}$in the two groups (p=0.184 and p=0.486).

The low power of the test performed to the values of chest wall and lung compliance could be due to the distortion of the chest wall, that is a relevant condition in sick or very preterm infants, affects the measurements of the pleural pressure, leading to inaccurate values of compliance.

This condition doesn't reflect on the measurement of the total respiratory system compliance, which does not depend on the measurement of the esophageal pressure and which is likely to be close in value to the lung compliance.

Indeed, the outcomes in the respiratory system compliance presented in Table 4-8 are similar to those obtained by Simbruner in his study on static compliance in infants with respiratory distress syndrome in the first few hours after birth. [35]

These results can be better visualized in figure 4.7, where the values of the weight-corrected static compliances are plotted as a function of the BPD score.

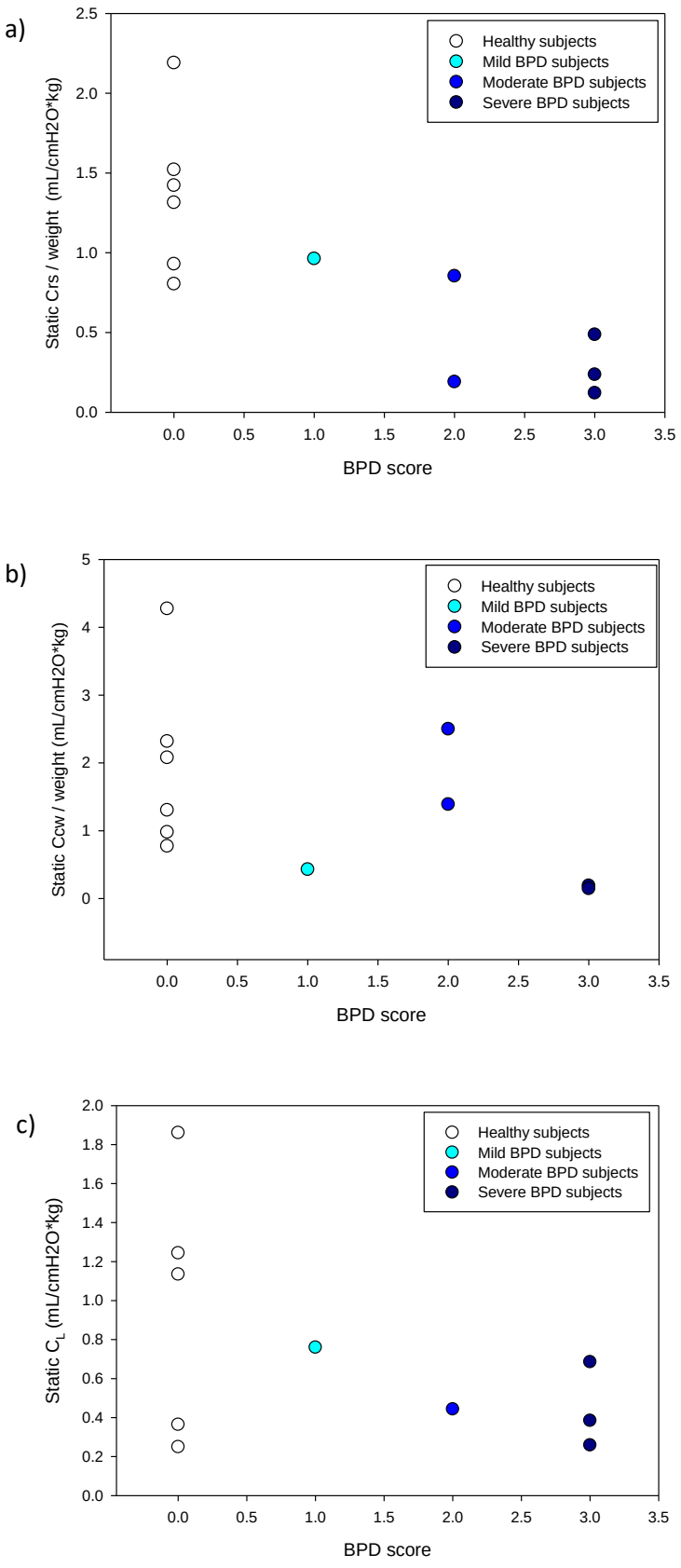


*Figure 4.7: Static compliance of the total respiratory system (a), chest wall (b) and lung (c) as a function of the BPD score.*

Measurements of the total respiratory system compliance result to be more useful to predict the course as well as classify the severity if BPD.

The relaxation curve of the thoraco-abdominal wall is physiologically characterized by a decrease in pendency with increasing pressure and volume. The shape of the P-V curve of total respiratory system and chest wall have been checked and compared for the two groups of patients. The compliances, computed as ratio between changes in volume and changes in $P_{ao}$ or $P_{es}$, have been computed for each apnea in each infant. The values obtained have been then averaged according to the value of pressure at which the occlusions were performed (5-10-15). The compliance at each of these 3 level of pressure corresponds to the slope of the P-V curve in that specific point. The results are presented in Table 4-9.

*Table 4-9: Comparison of the static compliance of the total respiratory system and chest wall obtained at each level of airways occlusion pressure between healthy and BPD subjects*

| | | Airways Occlusion Pressure | | |
|---|---|---|---|---|
| | | **5 cmH2O** | **10 cmH2O** | **15 cmH2O** |
| **All** | $C_{RS_{stat}}$ [ml/cmH2O] | 1.296 | 1.033 | 0.883 |
| | $C_{CW_{stat}}$ [ml/cmH2O] | 2.948 | 2.202 | 2.064 |
| **No BPD** | $C_{RS_{stat}}$ [ml/cmH2O] | 1.677 | 1.219 | 1.010 |
| | $C_{CW_{stat}}$ [ml/cmH2O] | 3.487 | 2.781 | 1.978 |
| **BPD** | $C_{RS_{stat}}$ [ml/cmH2O] | 0.916 | 0.848 | 0.756 |
| | $C_{CW_{stat}}$ [ml/cmH2O] | 2.410 | 2.427 | 1.348 |

These outcomes show that the slope of the P-V curve decreases with the increasing level of pressure for both the total respiratory system and the chest wall. this tendency is maintained also in presence of chronic lung disease even if the absolute values of compliance are lower than those obtained in healthy patients.

Moreover, the dynamic compliance of the lung has been computed for each infant during a period of spontaneous breathing as the mean ratio between volume and trans-pulmonary pressure changes during each considered breathing cycle. The transpulmonary pressure $P_L$ is computed as the difference between the pressure at the airway opening and the esophageal pressure.

The calculation of this parameter has been limited to only ten of the twelve processed infants, indeed, infants 1 and 6 have been excluded when computing $C_{L_{dyn}}$ because of the presence of artefacts in the esophageal pressure signal that compromised the measurements.

The dynamic compliances obtain for each patient are presented in the following table with a comparison between the healthy and BPD patients.

*Table 4-10: Measurement of dynamic compliances in all the studied subjects*

| | $C_{L_{dyn}}$ [ml/cmH2O] | BPD | Mean Dynamic Compliance |
|---|---|---|---|
| Infant 2 | 1.25 ± 0.10 | 0 | 1.63 ± 0.47 |
| Infant 3 | 1.20 ± 0.16 | 0 | |
| Infant 4 | 2.02 ± 0.66 | 0 | |
| Infant 5 | 2.05 ± 0.26 | 0 | |
| Infant 7 | 1.79 ± 0.38 | 1 | 0.93 ± 0.43 |
| Infant 8 | 0.60 ± 0.09 | 2 | |
| Infant 9 | 0.84 ± 0.08 | 2 | |
| Infant 10 | 0.91 ± 0.24 | 3 | |
| Infant 11 | 0.76 ± 0.06 | 3 | |
| Infant 12 | 0.69 ± 0.10 | 3 | |

In parallel with the difference found in the static compliances according to the presence of the chronic lung disease, even the dynamic compliance of the lung turned out to decrease significantly in BPD patients.

The results in Table 4-10 are expressed as volume/pressure in units of mL/cmH2O. However, to obtain a more reliable comparison between the subjects we correct the results for the body weight of each infant. The weight-corrected dynamic lung compliances are shown in Table 4-10 and classified according to the presence or not of BPD.

*Table 4-11: Comparison of dynamic lung compliance between healthy and BPD subjects*

| | No BPD | BPD | p-Value |
|---|---|---|---|
| $C_{L_{dyn}}$ [ml/cmH2O*kg] | 0.63 ± 0.20 * | 0.37 ± 0.13 * | 0.039 |

***p<0.05 in t-test.**

The difference in the mean values of the two groups is greater than would be expected by chance ($p < 0.05$), then, there is a statistically significant difference between healthy and BPD groups.

To visualize the difference among the different levels of severity, the weight-corrected dynamic lung compliances for each patient have been plotted as a function of the BPD score.

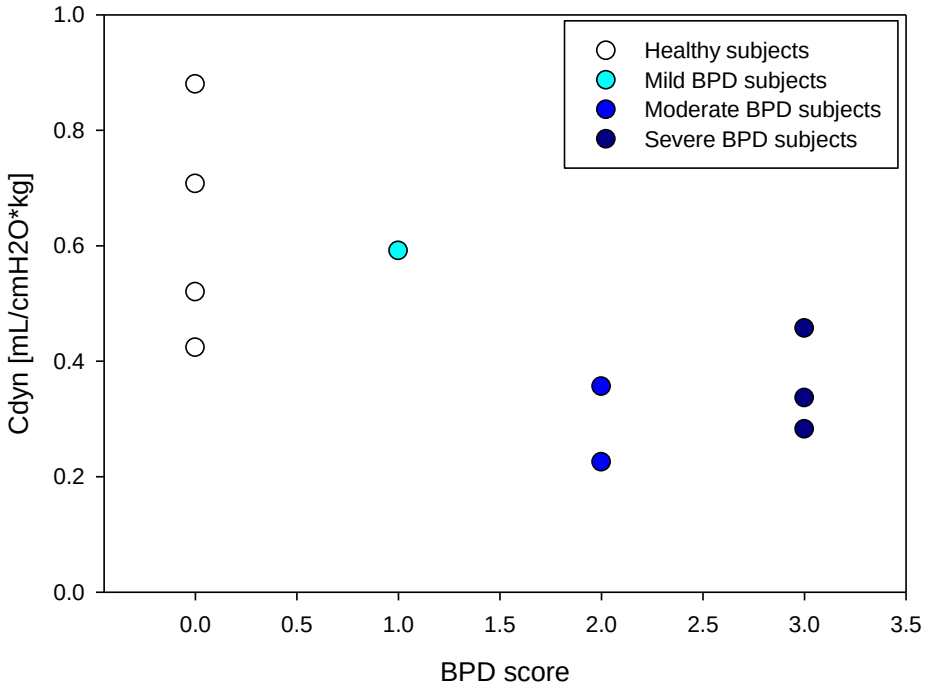


*Figure 4.8: Weight-corrected dynamic lung compliances as a function of the BPD score*

This decrease of lung compliance in infants with BPD are consistent with the results obtained in the thoraco-abdominal synchrony (section 4.3.2). Indeed, a significant TAA, as the one obtained in sick patients, can indicate abnormal lung function with excessive negative intrapleural pressure swings due to decreased lung compliance.

Finally, the obtained values of lung compliance are three times lower than that of the chest wall previously obtained both in healthy and BPD infants, reflecting the low rigidity of chest wall in premature infants, due to the uncompleted ossification of the ribs. Indeed, a high chest wall compliance unable to withstand normal negative intrapleural pressure swing indicates an inefficient system, typical of premature infants, as the respiratory muscle expend energy not only in exchanging tidal volume but also in distorting the rib cage.

## 4.3.5 Work of Breathing

To verify the efficiency of the respiratory function and the effort exerted in healthy and BPD patients, work of breathing (WOB) have been computed and compared between the two groups. As explained in section 2.2.6, the calculation of WOB requires the measurement of esophageal pressure.

For this analysis, about 30 spontaneous breaths have been considered for each subject and all the necessary volume and pressure signals have been normalized with respect to their minimum points to obtain a zero baseline. Infants number 1 and 6 have not been included in this part of the study because of the presence of errors in the esophageal pressure measurements. For each patient, we have obtained the elastic and resistive work of breathing starting from the transpulmonary pressure-volume loop. The resistive WOB has then been divided into the inspiratory and expiratory components, corresponding respectively to the lower and upper portion of the loop. Before the computation of WOB indexes, the P-V loop for each breath has been manually checked and excluded from the measurement process if considered anomalous and fitful. Accepted P-V loops of two representative subjects are shown in figure 4.9.

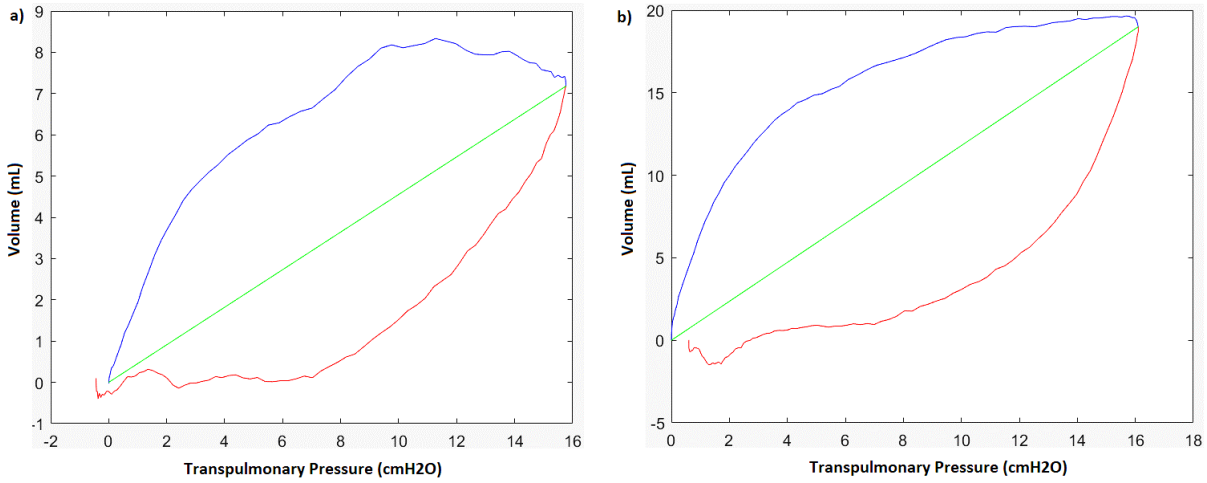


*Figure 4.9: Comparison between the P-V loop in a representative healthy (a) and BPD (b) patient*

The WOB indexes obtained following the procedure and accepting the hypothesis presented in section 2.2.6, have been corrected for the tidal volume to carry out an inter-subject comparison. The resulted are reported in Table 4-12:

*Table 4-12: Comparison between WOB indexes in healthy and BPD patients*

| | No BPD patients | BPD patients | p-Value |
|---|---|---|---|
| $elWOB$ | 4.24 ± 1.15 * | 7.25 ± 2.22 * | p=0.027 |
| $rWOB_{insp}$ | 3.06 ± 0.46 * | 4.50 ± 1.24 * | p=0.040 |
| $rWOB_{esp}$ | 5.42 ± 1.97 * | 9.86 ± 3.01 * | p=0.025 |
| $rWOB$ | 8.37 ± 2.06 * | 13.80 ± 4.22 * | p=0.032 |

**elWOB: elastic work of breathing; rWOBinsp: inspiratory resistive work of breathing; rWOBesp: expiratory resistive work of breathing; rWOB: total resistive work of breathing. *p<0.05 in t-test.**

Both the elastic and resistive work of breathing are considerably lower in healthy patients than in subjects in which bronchopulmonary dysplasia has been diagnosed. The difference in the mean values of the two groups for all the measures is greater than would be expected resulting to be statistically significant in the classification of the patients.

In this study, a consistently difference has been found in terms of elastic and resistive work that could be very useful in the clinical environment. Infants with moderate-to-severe BPD demonstrate a meaningful elevation in WOB due to a parallel decrease in lung and chest wall compliance, that cause a greater fatigue to exchange gas and balance energy expenditure.

The all components of WOB rise significantly with the development of the disease. Even the expiratory resistive work that is often at the expense of the elastic recoil energy stored in the respiratory system during inspiration and it is unlikely affect the respiratory energetics, increases considerably. A partition of the value obtained into the different components of work is present in figure 4.10 and 4.11.

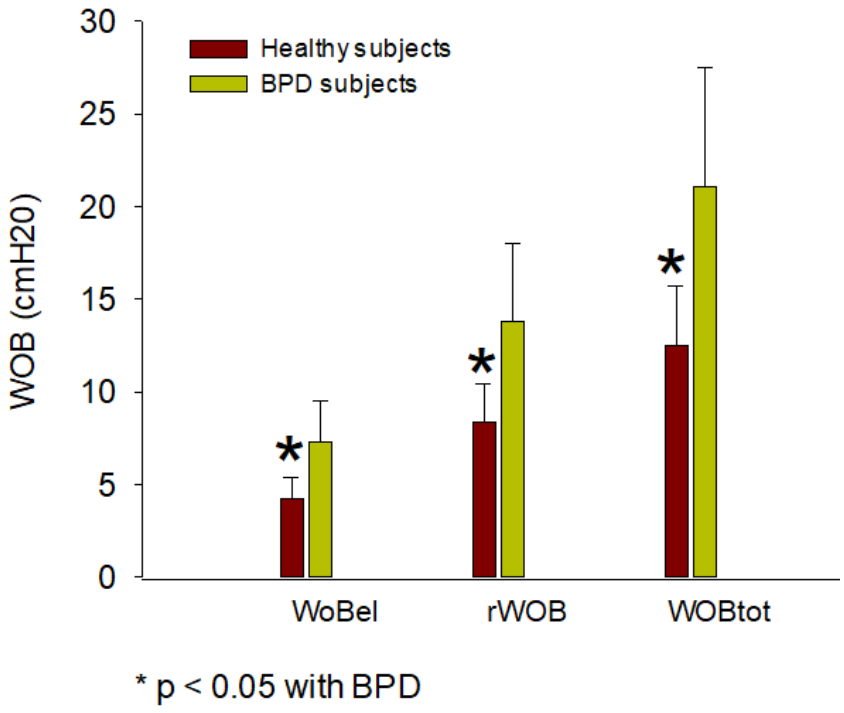


*Figure 4.10: Work of breathing divided into its elastic and resistive components. Data are presented as mean and standard deviation and compared between healthy and BPD subjects.*

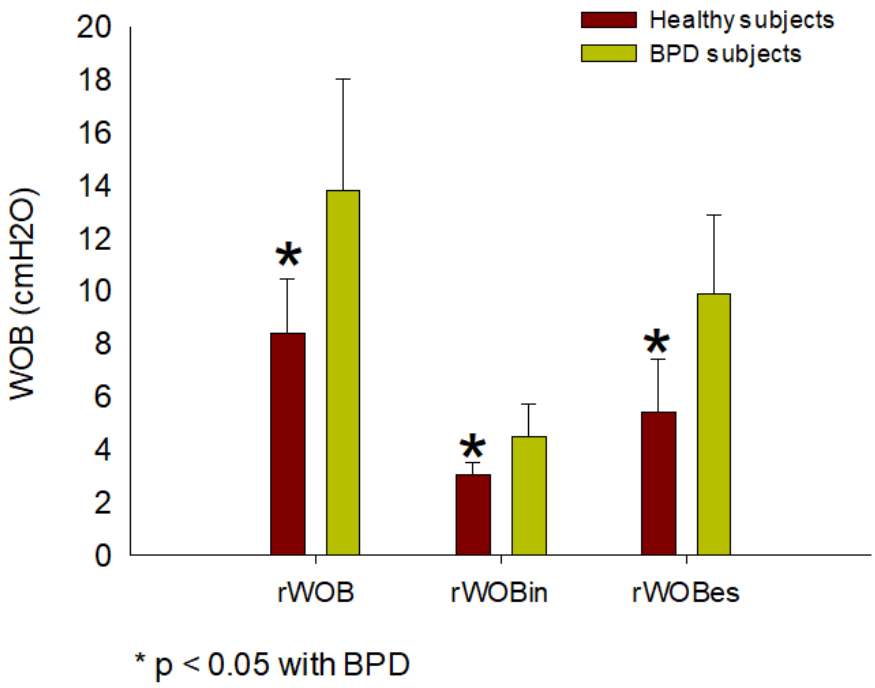


*Figure 4.11: Resistive work of breathing divided into its inspiratory and expiratory components. Data are presented as mean and standard deviation and compared between healthy and BPD subjects.*

As specify in section 2.2.6, WOB has been computed without considering the curves of chest wall and lung elastic recoil that could refine the differentiation. These assumptions, however, are quite common for this kind of studies. [36]

# Chapter 5 Conclusions

Considering the extreme heterogeneity of the clinical conditions of preterm infants who have developed BPD, an objective definition of the disease and, then, a common strategy for the therapy are not feasible. Thus, the understanding of the modifications in the respiratory system in BPD patients can help to tailor the treatment processes. Measuring parameters that detect the functioning of the various systems involved in respiration in each individual patient enhances the prediction of the ventilatory support duration and the neurophysiological consequences in comparison with general clinical variables and standard drivers.

This study aimed to characterize the possible alterations in the development of breathing control, lung and chest wall.

We developed the set up and methods to obtain useful information about the breathing pattern and the respiratory mechanics. In particular, respiratory inductive plethysmography has been used to obtain the breathing pattern parameters and their variability, while, the estimation of the esophageal pressure was required to measure the chest wall and lung compliances and the work of breathing.

Preliminary in-vitro and in-vivo studies have been conducted to verify critical aspects of the developed methods that resulted to be adequate for our aim. The developed set-up, indeed, once tested in-vitro, has been employed in the neonatal intensive care unit at the King Edward Memorial Hospital in Perth (WA) within a clinical study, which is funded by the National Health and Medical Research Council, to understand more about the contribution of different physiological factors to the development and severity of BPD with the aim to identify treatments that reduce the long-term consequences of premature birth. The clinical study is still in progress, but the promising preliminary results are presented in this work.

Tests conducted both in-vitro and in-vivo confirmed the reliability of the measurements.

The RIP resulted to be consistently precise enough for quantitative measurements of volume during brief periods of time. However, the functioning of the *Respitrace* device is sensitive to temperature changes and affected by thermal instability [37], thus, we have found a small drift that could be due to an insufficient acclimation period prior to the beginning of the procedure but it does not significantly affect our measurements. The calibration of the volume signal recorded by the bands was accurate enough to obtain a regression line between data acquired with RIP and PNT having a slope equal to 1.0075. The esophageal catheter produced reliable peak to peak pressure changes during the occlusion test in both the studied infants, giving a ratio between $\Delta P_{es}$ and $\Delta P_{ao}$ equal to 1.05 ± 0.09 and 1.10 ± 0.04 respectively. During quiet tidal breathing, the changes in pleural pressure, generated by the respiratory muscle, are in the order of 6 cmH2O and increase in the presence of lung disease. The magnitude of the changes in $P_{pl}$ results to be 1/6 to 1/4 of the applied $\Delta P_{ao}$, in agreement with what stated in literature [38].

However, in-vivo the measurements of esophageal pressure can be distorted by a periodic increase in esophageal tone (spasm), which impedes pleural pressure transmission to the catheter tip. Moreover, sick preterm infants usually have chest wall distortion and under such conditions esophageal pressure may reflect a local pressure rather than a mean pleural pressure. This problem has been solved by a manual selection of the breaths and points used for the computation of the parameters of interest.

The in-vivo clinical study showed that BPD infants can be distinguished from the healthy ones according to different parameters. Indeed, they are characterized by lower tidal volume (4.61 ± 1.04 mL), lower inspiratory and expiratory times (0.40 ± 0.010 s and 0.48 ± 0.060 s respectively) and higher respiratory rate (73.17 ± 3.49 breaths/min). Regarding respiratory mechanics, BPD is associated with a significant decrease in the static compliance of the respiratory system (0.47 ± 0.36 mL/cmH2O*kg) and in the dynamic compliance of the lung (0.37 ± 0.13 mL/cmH2O*kg).

Finally, the evaluation of the respiratory energetics and the computation of the work of breathing led to the achievement of satisfactory results in the comparison between healthy and BPD subjects, as both elastic and resistive work of breathing consistently increase in sick infants. In case of disease, elastic WOB is equal to 7.25 ± 2.22 and resistive WOB is 13.80 ± 4.22.

A consistently difference between the two classes of patients resulted also from the partition between inspiratory and expiratory resistive work. These outcomes could be very useful in the clinical practice to evaluate the breathing efforts in critically ill patients and to optimize the type of respiratory support for a particular disease condition.

On the other hand, no statistically significant difference has been found between healthy and BPD infants in the values of other parameters that we have analysed. Thoraco-abdominal and paradoxic indexes (IAI, EAI, LBI), the scaling exponent $\alpha$, computed to study breathing pattern variability of IBI, $V_t$ and EELV, and the static compliances of the lung and chest wall show a meaningless difference in the mean values obtained from the two groups of patients.

However, the power of the performed statistical test is below the desired value (0.800), indicating that it's less likely to detect a difference even if it actually exists, thus, the negative results should be interpreted cautiously. Indeed, the high p-value returned by the t-test conducted for these parameters could be due to the low sample size. To determine whether the statistical parameters derived from the breathing pattern in infants are physiologically justifiable and capable of detecting maturational changes in respiratory control, a greater number of preterm newborns need to be included in the study.

Then, the first limit of this study is the small number of patients caused by the difficulty to enrol patients with chronic lung disease because of the reluctance of parents to consent to the study.

However, we are currently studying more newborns to strengthen the results. The limitations of this study also include invasive measurement of the esophageal pressure.

In conclusion, a quantitative analysis of the BP parameters, the static and dynamic compliances, and the work of breathing with the tools described in this work allows to achieve a new insight into the alterations of the respiratory control, mechanics, and energetics, caused by the disease. Moreover, it can help to implement personalized therapies in order to improve the neonatal clinical outcomes. Future perspectives of this study include the implementation of code for real time analysis, the increase of the sample size for the clinical study and the application of these methods for the differentiation between various phenotypes of the pathology.

# Bibliography


[1] S. Beck *et al.*, "The worldwide incidence of preterm birth: A systematic review of maternal mortality and morbidity," *Bull. World Health Organ.*, vol. 88, no. 1, pp. 31–38, 2010.

[2] L. Liu *et al.*, "Global, regional, and national causes of under-5 mortality in 2000–15: an updated systematic analysis with implications for the Sustainable Development Goals," *Lancet*, vol. 388, no. 10063, pp. 3027–3035, 2016.

[3] J. Hammer, E. Ernst, and E. Eber, "The peculiarities of infant respiratory physiology," in *Paedriatric Pulmonary Function Testing*, 2005.

[4] B. B. Poindexter *et al.*, "Comparisons and limitations of current definitions of bronchopulmonary dysplasia for the prematurity and respiratory outcomes program," *Ann. Am. Thorac. Soc.*, vol. 12, no. 12, pp. 1822–1830, 2015.

[5] E. Kirkman, "Respiration: control of ventilation," *Anaesthesia and Intensive Care Medicine*. 2017.

[6] T. Gerhardt and E. Bancalari, "Lung compliance in newborns with patent ductus arteriosus before and after surgical ligation.," *Biol. Neonate*, 1980.

[7] P. Persson, S. Lundin, and O. Stenqvist, "Transpulmonary and pleural pressure in a respiratory system model with an elastic recoiling lung and an expanding chest wall," *Intensive Care Med. Exp.*, 2016.

[8] R. S. Harris, "Pressure-volume curves of the respiratory system.," *Respir. Care*, 2005.

[9] S. N. J. Kazzi, S. Schurch, K. L. McLaughlin, R. Romero, and J. Janisse, "Surfactant phospholipids and surface activity among preterm infants with respiratory distress syndrome who develop bronchopulmonary dysplasia," *Acta Paediatr. Int. J. Paediatr.*, 2000.

[10] M. Vom Hove, F. Prenzel, H. H. Uhlig, and E. Robel-Tillig, "Pulmonary Outcome in Former Preterm, Very Low Birth Weight Children with Bronchopulmonary Dysplasia: A Case-Control Follow-Up at School Age," *J. Pediatr.*, 2014.

[11] C. P. Speer, "Inflammation and bronchopulmonary dysplasia: A continuing story," *Semin. Fetal Neonatal Med.*, 2006.

[12] W. H. Northway, R. C. Rosan, and D. Y. Porter, "Pulmonary Disease Following Respirator Therapy of Hyaline-Membrane Disease," *N. Engl. J. Med.*, 1967.

[13] B. J. Stoll *et al.*, "Neonatal outcomes of extremely preterm infants from the NICHD Neonatal Research Network.," *Pediatrics*, 2010.

[14] E. Baraldi and M. Filippone, "Chronic lung disease after premature birth.," *N. Engl. J. Med.*, 2007.

[15] M. Cuevas Guaman, J. Gien, C. D. Baker, H. Zhang, E. D. Austin, and J. M. Collaco, “Point Prevalence, Clinical Characteristics, and Treatment Variation for Infants with Severe Bronchopulmonary Dysplasia,” *Am. J. Perinatol.*, 2015.

[16] R. Plavka *et al.*, “High-frequency jet ventilation improves gas exchange in extremely immature infants with evolving chronic lung disease,” *Am. J. Perinatol.*, 2006.

[17] W. H. Tooley, “Epidemiology of bronchopulmonary dysplasia,” *J. Pediatr.*, vol. 95, no. 5, pp. 851–855, Nov. 1979.

[18] A. T. Shennan, M. S. Dunn, A. Ohlsson, K. Lennox, and E. M. Hoskins, “Abnormal pulmonary outcomes in premature infants: prediction from oxygen requirement in the neonatal period.,” *Pediatrics*, 1988.

[19] A. H. Jobe and E. Bancalari, “NICHD / NHLBI / ORD Workshop Summary,” *Am. J. Respir. Crit. Care Med.*, 2001.

[20] R. A. Ehrenkranz *et al.*, “Validation of the National Institutes of Health consensus definition of bronchopulmonary dysplasia.,” *Pediatrics*, 2005.

[21] U. Frey, M. Silverman, A. L. Barabási, and B. Suki, “Irregularities and power law distributions in the breathing pattern in preterm and term infants,” *J. Appl. Physiol.*, 1998.

[22] D. N. Baldwin, J. J. Pillow, J. Stocks, and U. Frey, “Lung-function tests in neonates and infants with chronic lung disease: Tidal breathing and respiratory control,” *Pediatric Pulmonology*. 2006.

[23] U. Frey, G. Maksym, and B. Suki, “Temporal complexity in clinical manifestations of lung disease,” *J. Appl. Physiol.*, 2011.

[24] A. J. E. Seely, G. C. Green, and A. Bravi, “Continuous Multiorgan Variability monitoring in critically ill patients — Complexity science at the bedside,” in *Engineering in Medicine and Biology Society,EMBC, 2011 Annual International Conference of the IEEE*, 2011.

[25] H. H. Szeto, P. Y. Cheng, J. A. Decena, Y. Cheng, D. L. Wu, and G. Dwyer, “Fractal properties in fetal breathing dynamics.,” *Am. J. Physiol.*, 1992.

[26] K. Konno and J. Mead, “Measurement of the separate volume changes of rib cage and abdomen during breathing.,” *J. Appl. Physiol.*, 1967.

[27] G. S. Neto, T. O. Gerhardt, N. Claure, S. Duara, and E. Bancalari, “Influence of chest wall distortion and esophageal catheter position on esophageal manometry in preterm infants,” *Pediatr. Res.*, 1995.

[28] M. a Sackner *et al.*, “Calibration of respiratory inductive plethysmograph during natural breathing.,” *J. Appl. Physiol.*, 1989.

[29] C. K. Peng, S. Havlin, H. E. Stanley, and A. L. Goldberger, “Quantification of scaling exponents and crossover phenomena in nonstationary heartbeat time series,” *Chaos*, vol. 5, no. 1, pp. 82–87, 1995.

[30] E. Akoumianaki *et al.*, “The application of esophageal pressure measurement in patients with respiratory failure,” *American Journal of Respiratory and Critical Care Medicine*. 2014.

[31] A. E. Klasner, D. A. Luke, and A. J. Scalzo, “Pediatric orogastric and nasogastric tubes: A new formula evaluated,” *Ann. Emerg. Med.*, 2002.

[32] M. Muskulus, A. M. Slats, P. J. Sterk, and S. Verduyn-Lunel, “Fluctuations and determinism of respiratory impedance in asthma and chronic obstructive pulmonary disease,” *J. Appl.*

*Physiol.*, 2010.

[33] M. Durand and H. Rigatto, “Tidal volume and respiratory frequency in infants with bronchopulmonary dysplasia (BPD),” *Early Hum. Dev.*, 1981.

[34] M. A. Sackner, H. Gonzalez, M. Rodriquez, A. Belsito, D. R. Sackner, and S. Grenvik, “Assessment of asynchronous and paradoxic motion between rib cage and abdomen in normal subjects and in patients with chronic obstructive pulmonary disease,” *Am. Rev. Respir. Dis.*, 1984.

[35] G. Simbruner, H. Coradello, G. Lubec, A. Pollak, and H. Salzer, “Respiratory compliance of newborns after birth and its prognostic value for the course and outcome of respiratory disease,” *Respiration*, 1982.

[36] J. G. Saslow *et al.*, “Work of breathing using high-flow nasal cannula in preterm infants.,” *J. Perinatol.*, 2006.

[37] K. Leino, S. Nunes, P. Valta, and J. Takala, “Validation of a new respiratory inductive plethysmograph,” *Acta Anaesthesiol. Scand.*, 2001.

[38] A. Coates, J. Stocks, T. Gerhardt, Esophageal Manometry in: J. Stocks, P.D. Sly, R.S.Tepper, W.J.Morgan, “Infant Respiratory Function testing,” *Wiley-Liss, Inc.*, 1996.